**AGROCAMPUS OUEST**

☐ **CFR Angers**

☑ **CFR Rennes**

Année universitaire : 2015 - 2016

Spécialité : Agronomie

Spécialisation :

Sciences halieutiques et aquacoles

Dominante : Ressources et Ecosystèmes Aquatiques (REA)

## Mémoire de fin d’études

☑ d’Ingénieur de l’Institut Supérieur des Sciences agronomiques, agroalimentaires, horticoles et du paysage

☐ de Master de l’Institut Supérieur des Sciences agronomiques, agroalimentaires, horticoles et du paysage

☐ d'un autre établissement (étudiant arrivé en M2)

# Developing an integrated Bayesian life cycle model to infer connectivity of the Sole population in the Eastern Channel from mark-recapture data

Par : Matthieu VERON

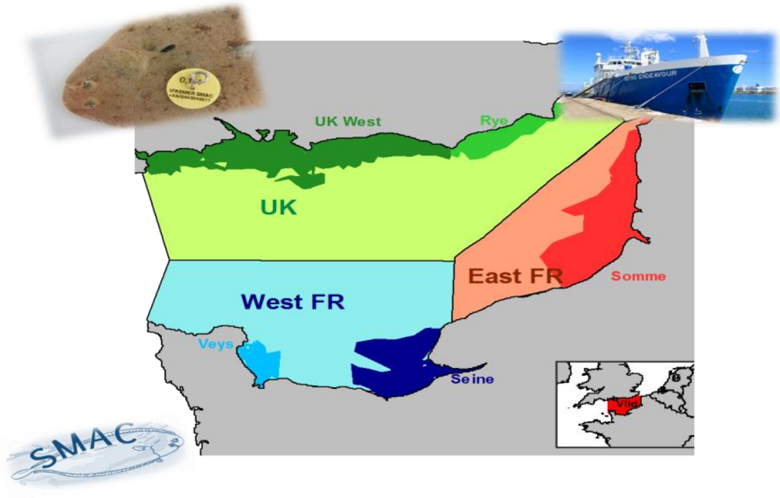

Sole population in the Eastern Channel (Photo Credit: Ifremer)

***Soutenu à Rennes le 14 Septembre 2016***

***Devant le jury composé de :***

Président : GASCUEL Didier, Agrocampus Ouest

Maître de stage : RIVOT Etienne, Agrocampus Ouest

Enseignant référent : GASCUEL Didier, Agrocampus Ouest

Evaluateurs extérieurs :

SAVINA- ROLLAND Marie

TRENKEL Verena

# Fiche de confidentialité et de diffusion du mémoire

## Confidentialité

☑ Non ☐ Oui si oui : ☐ 1 an ☐ 5 ans ☐ 10 ans

Pendant toute la durée de confidentialité, aucune diffusion du mémoire n'est possible (1).
Date et signature du maître de stage (2) :
**A la fin de la période de confidentialité,** sa diffusion est soumise aux règles ci-dessous (droits d'auteur et autorisation de diffusion par l'enseignant à renseigner).

## Droits d'auteur

L'auteur(3) **VERON Matthieu**
autorise la diffusion de son travail (immédiatement ou à la fin de la période de confidentialité)

☑ Oui ☐ Non

Si oui, il autorise

☐ la diffusion papier du mémoire uniquement(4)

☐ la diffusion papier du mémoire et la diffusion électronique du résumé

☑ la diffusion papier et électronique du mémoire (joindre dans ce cas la fiche de conformité du mémoire numérique et le contrat de diffusion)

Date et signature de l'auteur :

## Autorisation de diffusion par le responsable de spécialisation ou son représentant

L'enseignant juge le mémoire de qualité suffisante pour être diffusé (immédiatement ou à la fin de la période de confidentialité)

☐ Oui ☐ Non

Si non, seul le titre du mémoire apparaîtra dans les bases de données.
Si oui, il autorise

☐ la diffusion papier du mémoire uniquement(4)

☐ la diffusion papier du mémoire et la diffusion électronique du résumé

☐ la diffusion papier et électronique du mémoire

Date et signature de l'enseignant :

(1) L'administration, les enseignants et les différents services de documentation d'AGROCAMPUS OUEST s'engagent à respecter cette confidentialité.
(2) Signature et cachet de l'organisme
(3).Auteur = étudiant qui réalise son mémoire de fin d'études
(4) La référence bibliographique (= Nom de l'auteur, titre du mémoire, année de soutenance, diplôme, spécialité et spécialisation/Option)) sera signalée dans les bases de données documentaires sans le résumé

## ***Remerciements***

Avant tout, je tiens à remercier très sincèrement Etienne Rivot de m'avoir suivi, épaulé et conseillé au cours de ce stage de fin d'études. Merci Etienne pour ta patience indéniable, ton écoute et ta grande disponibilité, tes conseils toujours aussi avisés et ta motivation, surtout quand cela ne marchait pas (de mon côté en tous cas). J'ai beaucoup appris à tes côtés tout au long de ces 6 mois, que ce soit au niveau humain, scientifique ou encore sur moi-même. J'ai vraiment apprécié l'ensemble de nos échanges au cours desquels tu as toujours su écouter jusqu'au bout mes idées et ma perception des choses. Ce sont 6 mois de stage que j'aurais eu plaisir à prolonger pour quelques années et j'espère que l'on sera amené à travailler de nouveau ensemble.  Enfin je tiens à te remercier de me donner l'opportunité de continuer mon travail pour un petit bout de temps, ce qui comme tu le sais, me tiens à cœur.

Merci également à Elodie et Olivier qui ont co-encadré ce stage. Merci pour vos conseils et vos différents points de vue qui m'ont souvent permis de prendre de la hauteur sur ce que je faisais. J'ai vraiment apprécié de travailler avec ce « trio » que vous formez avec Etienne et qui permet un mélange de compétences scientifiques amenant toujours des remarques pertinentes et des avis d'experts sur diverses thématiques.

Je tiens également à remercier Jérôme qui a toujours su m'aider face aux difficultés conceptuelles informatiques. Merci beaucoup pour ton écoute, ta disponibilité et surtout ta grande capacité et ingéniosité à régler un certain nombre de caprices informatiques qui j'avoue, m'ont souvent dépassé.

Je tiens également à dire merci à l'ensemble de l'équipe du Pôle Halieutique : Catherine, Sophie, Elodie, Marie, Hervé, Didier, Olivier, Jérôme et Etienne pour leur bonne humeur, leur accueil au sein de cette équipe et leur grande disponibilité. J'ai passé de très bons moments parmi vous qui ont tous été aussi entrainant et motivant les uns que les autres pour travailler.

Merci au copains stagiaires, contractuels (de passage ou « résidents »), thésard et post-docs présents au labo, avec notamment les gens de ma promo, Aurore, Alexis et Pierre Yves mais aussi Mathieu, Shani, Morgane, « Dble J », Erwan, Maxime, Martin et Emilie pour leur bonne humeur et leur entrain au travail. Merci particulièrement à Max que j'ai souvent été questionné pendant mon stage et à qui j'ai aussi « piqué » des cœurs pour faire tourner mes beaux modèles, ce dont je m'excuse.

Enfin merci aux copains de l'extérieur, à mon Papa pour son soutien continu ainsi qu'à Coline qui m'a bien aidé mais aussi supporté.

## *RESUME ETENDU EN FRANÇAIS*

# Développement d’un modèle Bayesien de cycle de vie intégré pour estimer les mouvements de la Sole en Manche Est à partir de données de marquage-recapture

## Contexte

La Sole commune en Manche Est (*Solea solea*), espèce nourricerie-dépendante, fait aujourd’hui l’objet d’une attention particulière au niveau national d’une part et international d’autre part. Ce stock, d’intérêt commercial majeur au niveau de cette région, est à ce jour évalué par le Conseil International pour l’Exploration de la Mer (CIEM, division VIId) comme étant surexploitée. Cette exploitation intervient à la suite de nombreuses pressions impactant en particulier les individus au niveau des jeunes stades du cycle de vie. En effet, au cours de la vie pélagique (stades œufs et larves), la Sole est soumise à un contrôle hydro-climatique induisant une répartition spatiale « spécifique » des larves au niveau de zones de nourricerie. L’ensemble des juvéniles en résultant sont par la suite soumis à un ensemble de pressions anthropiques impactant alors la population globale à l’échelle de la Manche Est.

Une forte structuration spatiale induite par une faible dispersion au cours de la phase larvaire ainsi qu’une forte rétention des juvéniles au niveau de leur zone de nourricerie est alors observée au niveau de ce stock (Rochette et al., 2012). Les répercussions de cette structuration spatiale au niveau du stock global de la Manche Est sont diverses et variées. Dans un contexte d’exploitation durable, le maintien d’une telle structuration au niveau de la population adulte avec une faible dispersion des individus entre les zones pourrait alors nécessiter une spatialisation de la gestion de ce stock. Pourtant, l’évaluation de ce stock actuellement fournie par le CIEM est effectuée sous l’hypothèse d’un stock homogène, isolé des stocks de Manche Ouest et du Mer du Nord laissant ainsi en suspens la question de l’existence d’une métapopulation.

## Objectif

C’est dans ce contexte qu’émergent l’importance et le but du projet SMAC (Sole en Manche Est : amélioration des connaissances pour une meilleure gestion du stock). L’objectif de ce programme est en effet d’accroître les connaissances sur la dynamique du stock de Sole en Manche Est en vue de les intégrer au sein d’un modèle d’évaluation. En amont de l’acquisition de données de marquage recapture, cette étude propose de préparer le cadre méthodologique nécessaire à l’intégration de telles données au sein d’un modèle de cycle de vie spatialisé. Il s’agit dans un premier d’étudier l’impact du niveau de connectivité sur l’établissement des points de référence biologique utilisés par la suite dans le cadre de l’évaluation de stock. Dans un deuxième temps, ce travail s’intéresse à la faisabilité de l’estimation de paramètres de migration à partir de données de marquage-recapture intégrée au sein d’un modèle de cycle de vie. On cherche donc ici à quantifier la sensibilité des estimations au protocole de marquage d’une part mais également la sensibilité des estimations à notre connaissance à priori sur un paramètre clé des programmes de marquage-recapture qu’est le taux de déclaration des marques.

## Matériels et Méthodes

- ✓ Développement du modèle

Cette étude intervient à la suite de divers travaux scientifiques ayant permis le développement au préalable, d’une approche de modélisation hiérarchique Bayésienne de la dynamique de la Sole en Manche Est (Rochette et al., 2013, Archambault et al., 2016).

A travers cette approche il est possible de prendre en compte des processus démographiques complexes tout en les séparant des processus d'observation. Nous proposons donc de développer la spatialisation de ce modèle au niveau de la population adulte afin de permettre la mobilité de ces individus entre les zones préalablement définies (West FR, UK et East FR). La dynamique de population est ici modélisée sur 30 ans, de 1982 à 2011. Dans le cadre de cette modélisation nous disposons :

- Des sorties d'un modèle individu centré caractérisant la dérive larvaire (1982 – 2007)
- Des indices d'abondance de juvéniles au niveau des cinq nourriceries identifiées (Solent, Rye, Somme, Seine et Veys) fournis pour chacune des années modélisées
- Des données de captures aux âges (de 2 à 15 ans) disponibles à partir des évaluations de stock fournies par le CIEM à l'échelle de la Manche Est
- Des indices d'abondance pour les individus adultes (deux séries temporelles disponibles à l'échelle de la Manche Est (UKCBT, BEBCT) et une serie temporelle d'indices d'abondance au niveau de chacune des sous populations (UKBTS)).

✓ Une approche semi-empirique : Estimation - Simulation – Estimation

Situé en amont de l'obtention de données de marquage recapture, ce travail se base sur l'exploitation d'un jeu de données fictif. Du fait d'une contrainte temporelle, cette étude se place dans une approche semi empirique par laquelle nous estimons dans un premier temps les paramètres clés de la dynamique de population. Ces paramètres sont ensuite utilisés comme inputs au sein d'un modèle de simulation de dynamique de population permettant l'obtention d'un jeu de données de marquage recapture. Ces données sont ensuite utilisées comme « données réelles » de marquage recapture au sein d'un modèle intégré de cycle de vie afin d'estimer les mouvements de la Sole en Manche EST.

✓ Différents scénarios pour quantifier la sensibilité des estimations au protocole de marquage et à notre connaissance à priori

Dans le but de fournir des pistes de protocoles optimaux dans le cadre des opérations de marquage-recapture prévues dans SMAC, trois scénarios sont alors étudiés : un scénario tenant compte d'un nombre optimal de marques, un scénario tenant compte d'un nombre réaliste de marques (i.e. prenant en compte le nombre de marques prévues dans SMAC) ainsi qu'un scénario dit minimaliste (tenant compte d'un faible nombre de marques).

D'autre part, cette étude s'intéresse également à sensibilité des estimations quant à l'effet de notre connaissance à priori sur la valeur et la spatialisation du taux de déclaration au niveau de la Manche Est.

## Résultats

Les résultats mettent en lumière la nécessité de prendre en compte le rôle joué par les adultes dans la structuration spatiale de la population de Sole en Manche Est et par conséquent la nécessité d'avoir recours à des approches de modélisation intégrée permettant l'assimilation de données de marquage-recapture.

Notre étude révèle une forte sensibilité des paramètres clé de la dynamique de population aux différentes hypothèses de connectivité. Cette sensibilité se répercute finalement sur la productivité de chacune des sous population induisant alors une réévaluation des points de références biologiques de ce stock et donc une modification en profondeur de l'évaluation de stock.

D'autre part, nos résultats permettent de valider le protocole de marquage prévu dans le cadre du projet SMAC. Nos analyses portées sur le nombre de marques prévues nous permettent de supposer l’obtention d’informations adéquates afin d’estimer les mouvements des soles au sein de la Manche Est.

Enfin, cette étude a porté une attention particulière au taux de déclaration des marques. Nos analyses mettent en lumière l’importance de connaitre ce taux de déclaration. En effet, une mauvaise spécification de ce taux, que ce soit au niveau de sa valeur ou au niveau de sa distribution spatiale, implique d’une part une incertitude plus élevée dans les estimations des paramètres de mouvement et d’autre part, la présence d’un biais systématique dans ces estimations.

Cependant, nos résultats démontrent que l’utilisation d’un Prior informatif sur ce taux de déclaration permet une estimation fiable des paramètres de mouvement. Ainsi, l’utilisation d’une telle information *à priori* maintiendrait à l’écart le risque d’introduire une erreur dans la spécification du taux de déclaration (valeur et distribution spatiale) et favoriserait donc la fiabilité des estimations.

## Conclusion

Cette étude démontre l’importance de prendre en compte le rôle joué par l’ensemble des stades du cycle de vie dans la structuration spatiale de la population de Sole en Manche Est : des stades pélagiques (œufs et larves) aux stades adultes.
Les expériences de marquages prévues dans SMAC devraient permettre l’amélioration des connaissances sur le rôle joué par les adultes dans cette structuration spatiale grâce à l’intégration de ces données au sein d’un modèle intégré de cycle de vie. L’utilisation d’un nombre maximal de marques ainsi que la promotion de ce projet auprès de la pêcherie commerciale afin de favoriser la déclaration de ces marques constituent la clé de réussite de cette partie du projet.

# CONTENT

## LIST OF ILLUSTRATIONS

### *Figures*

## *Tables*

## List of APPENDIX

# 1 Introduction

## 1.1. Developing life cycle models to go beyond classical stock assessment models

Marine fish populations are exposed to various environmental (Bakun, 1996) and anthropogenic (Halpern et al., 2008) pressures that impact populations at various life stages throughout their life cycle and at various associated spatial scales.

The direct impact of fishing on fish populations and ecosystems has received considerable attention (Myers and Worm, 2003). Intense harvesting decreases in both number and size of age group, what increases recruitment volatility and impedes the resilience of populations (Jackson, 2001).

Environmental variations also impact populations and ecosystems with effects at multiple biological (from individual to ecosystems) and spatial (from local to global) scales. For instance global change has a direct impact on physical conditions such as sea level rising, temperature increase, changes in ocean circulation and, vertical stratification or increasing ocean acidification (Sarmiento et al., 2004). Consequences on marine populations can be observed through modifications of biology (physiology, growth, mortality, fecundity) or areas distribution, and highly depend upon the characteristics of the life cycles. In particular, hydroclimate conditions have a huge repercussion on the dispersion and survival of early life stages (eggs and larvae) of many fish species (Petitgas et al., 2013).

The effect of habitat loss or degradation on fish populations and ecosystems due to the increasing concentration of human activities along inshore waters, but equally due to fishing activities is also of considerable concern. Loss or degradation of habitat those are essential for some key life stages may disrupt fish life cycle and impedes population renewal. Pressures on habitats mainly occur onshore even if it extends to the ocean. Indeed, through pollution and physical destruction, human pressures on coastal ecosystems deteriorate a set of essential fish habitats like coastal nurseries (Le Pape et al., 2007; Lotze et al., 2006; Peterson et al., 2003; Rochette et al., 2010). Moreover, fishing is also likely to directly alter habitat structures that are key to accomplish their life cycle (Hutchings, 2000; Pauly et al., 2005).

One of the main challenges of fisheries ecology is therefore to develop integrated life cycle models to go beyond classical stock assessment models that are usually designed to only account for the direct impact of fishing mortality on fish populations and that keep away the whole spatial structure of marine fish populations. Numerous demographic and ecological processes interact at various spatio-temporal stages, it is therefore critical to develop models that explicitly account for the spatial dimension of marine populations and explotation.
Integrated life cycle models can help to address those challenges and have received considerable attention in the recent literature (Maunder and Deriso, 2011; Maunder and Punt, 2013). They can allow us to consider complexity of marine population dynamics while quantifying the influence of different pressures impacting on fish life cycle and their interactions. Various sources of information can be integrated and uncertainty is propagated among the model and is quantified.

## 1.2. A need to account for the spatial dimension in fish population dynamics

A good understanding of the way the various demographic and ecological processes interact through various spatial scales over the life cycle is not only critical for a good understanding of the population dynamics, but also for an accurate assessment of stock status and to design spatially explicit management measures (Goethel et al., 2011; Grimm et al., 2003; Maunder, 2005). Metapopulation concept is appealing for a better understanding of marine ecosystems dynamics. It has been largely applied to model and to understand the persistence and productivity of interconnected subpopulations (Frisk et al., 2014; Smedbol et al., 2002). The degree to which subpopulations are connected to or isolated from adjacent population through movements of fish has important implications to determine appropriate management stock units, and to correctly align stock delineation with ecological reality (Begg et al., 1999; C. L. Cunningham et al., 2007; Grimm et al., 2003; Tuck and Possingham, 1994).

Several examples have shown that failure to properly account for the spatial structure of populations can lead to bias stock assessment and ultimately lead to set up inappropriate management measures. Based on simulations, Punt et al. (2005) have shown that models that consider connectivity between subpopulations can outperform simpler models that ignore metapopulation structure.

Estimates of stock size, fishing mortality and recruitment can be substantially biased (Hart and Cadrin, 2004; Porch et al., 2001; Punt and Butterworth, 1995)by ignoring movements between components of populations. A fair assessment of the spatial structure of populations is particularly critical when different subpopulations have highly contrasted productivity. This is the case of source-sink dynamics, when the dynamics of the metapopulation as a whole are formed by interaction of multiple subpopulations with contrasted productivity, some of them (the sink) being substantively replenished by others of bigger size and/or of higher productivity (the source) (Cooper and Mangel, 1999; Hastings and Harrison, 1994; Kritzer and Sale, 2004). When it exists, ignoring the heterogeneity of productivity among subpopulations may lead to serious overfishing and depletion of the less productive component (Begg et al., 1999).

## 1.3. Attempt to consider spatial structure in fish population models

### a) *The role of the early stages in spatial structure and population dynamics*

The critical influence of the marine currents on the dispersion of the early life stages (eggs and larvae) and on the resulting spatial structure of populations has received considerable attention over the last two decades (Frisk et al., 2014; Petitgas et al., 2013; Rochette et al., 2010). Most of the work has concerned the development of framework allowing the coupling of physical and biological processes to understand recruitment processes according oceanography conditions. Those models are useful to explore how the recruitment success is influenced by the patterns of connectivity occurring during larval stages with changes in retention or dispersion from spawning grounds to areas suitable or not for survival (Fässler et al., 2011; Gallego et al., 2012; Hinrichsen et al., 2011; Rochette et al., 2012).

### b) *The importance of adult mediated connectivity within population dynamics*

However, dispersion of eggs and larvae with currents is not the only factor of the spatial structure of populations. Missing and exchange between subpopulations can occur at different life history stages along the life cycle, in particular through juveniles and adult movements (Frisk et al., 2014). The role of adult movements can be especially important when larval and juvenile retention occurs (Grosberg and Levitan, 1992). For instance, C. Cunningham et al., 2007 pointed out different patterns in migration between juvenile and adult stages of the Atlantic mackerel. These latter (adults) realize annual spawning-feeding-overwintering migrations that modify stock abundance whereas fishing effort remains the same. Salmonids that reproduce in very confine freshwater habitat but that, realize some reproductive migrations over great distances to reach optimal foraging conditions are another example for the key role of adult mediated connectivity.

Over the last decades, progresses have been achieved to develop integrated stock assessment models that can extract information about biological and fishery processes from multiple data sources and markers (Maunder and Punt, 2013) to build spatially structured stock assessment models. The combination of natural genetic markers with otolith chemistry revealed successful to determine stock structure and fish movement (Ashford et al., 2008; Campana et al., 2000). Artificial markers such as tags are also more and more used (Tanner et al., 2016). Conventional passive tags coupled with mark-recapture models remain widely used, but can provide only loose information on fish movement because of low or unknown tag recapture declaration rates. Recent technological progresses have encouraged the development of electronic tags that can provide fishery-independent data on fish movement and other biological variables.

### 1.4. Towards holistic approaches to quantify connectivity at various life stages along the life cycle: integrated life cycle models

In order to improve fisheries management and our understanding of the underlying processes in ecosystems, a holistic approach is needed to quantify connectivity at all life cycle stages within cycle models for stock assessment. Integrated models provide a framework to combine several sources of data and information into a single analysis to integrate various sources of data in order to take maximum benefit from all the available information (Maunder and Punt, 2013).

Integrated life cycle models are mostly based on the state-space modelling framework. State-Space models are a wide class of models that explicitly consider two sets of equations, the process equations that depict the dynamics of the hidden process of interest (including process errors), and the observation equations that mimic the relationships between the hidden states of the system and the data (including observation errors). When applied to population dynamics models, the process equations are formed from the population model that takes into account all demographic processes in the life cycle (e.g., cohort dynamics, movements …). Observation equations relate the different sources of data (e.g. survey, counts …) to the hidden population processes. A joint likelihood equation allows to simultaneously estimate all parameters and hidden states of the model by synthetizing all available data, while propagating the different sources of uncertainty in the model and in the data (Buckland et al., 2007; King et al., 2010; Newman et al., 2014; Parent and Rivot, 2013).

Bayesian analysis of integrated models has received considerable attention during the last three decades. The Bayesian framework has two main advantages. First, it allows to include prior information into models (Hilborn and Liermann, 1998; Punt and Hilborn, 1997). Second, it provides inferences on all unknowns in a full probabilistic framework, and is therefore adapted to fully propagate uncertainty in all estimates and outputs of model simulations and to assess the probability of the different outcomes of various management options (McAllister and Kirkwood, 1998; Patterson et al., 2001; Punt and Hilborn, 1997; Sippel et al., 2015).

One of the biggest breakthroughs in stock assessments modeling in recent years has been the development of state-space models for tag-integrated assessment models, which fully integrates population dynamics and tag-recapture models to simultaneously estimate the population dynamics and the movement and connectivity between different subpopulations (Goethel et al., 2011)Those integrated models allow to simultaneously estimate important parameters for stock assessment such as stock size, natural mortality, age-specific selectivity and movement (Maunder and Punt, 2013). They can ultimately reduce bias and uncertainty of parameters estimates and stock assessment (Goethel et al., 2011; Maunder, 2001b). A seminal example is the full-assessment models including movement developed by Quinn et al. (1990) through the Migratory catch-at-age analysis. Within this model, tagging studies have been used and analyzed to obtain movement rates that are then used as input in a second step.

Even if movement parameters can be estimated from an external analysis of the tag-recapture data and then plugged into a spatial stock assessment model, integrating the estimation of movement directly into the model appears as a more rigorous method. For example, it is easy to understand that within a tag-integrated life cycle model, estimation of movement rates is directly dependent on the probability of tag recovery. But because it is usually assumed that tag population follows the same dynamics as untagged population the probabilities of tag recovery are closely tied up with estimates of fishing pressure. As this fishing pressure is dependent on population dynamics which depend on movement rates, trying to estimate these two quantities independently can surely lead to bias in estimates.

Tag integrated assessment models appeared later with inter alia one emblematic example developed by Maunder (1998, 2001b), the integrated tagging catch-at-age analysis (ITCAAN). It explicitly includes movements and fits to both age-structured tagging and catch-at-age data. Porch et al., 2001 developed one of the first tag-integrated models for Bluefin tuna based on equations developed by Hilborn (1990) for predicting recovered tags. The model can accommodate two types of population structures determined by the level of natal homing displayed. In this model, mixing occurs at the adult life stage. Mature fish only contribute to the spawning biomass of its natal population.

## 1.5. Case study: The Eastern Channel Sole population

### 1.5.1) Life cycle

The common sole (Solea solea) is a coastal and estuarine nursery-dependent flatfish species (Le Pape et al., 2003). Eggs are spawned in early spring in offshore habitats. Eggs and larvae then derive passively with currents during several weeks and settle in suitable nursery grounds where they metamorphose. Five nursery sectors along French and English coasts have been identified (Solent, Rye, Veys, Seine and Somme) (Rochette et al., 2010) (***Fig. 1***). Juvenile spend the first two years on these habitats. Recruitment success therefore depends on both survival of the pelagic stages and the juvenile stages. Then they migrate towards deeper areas, where they reproduce and are harvested (Riou et al., 2001).

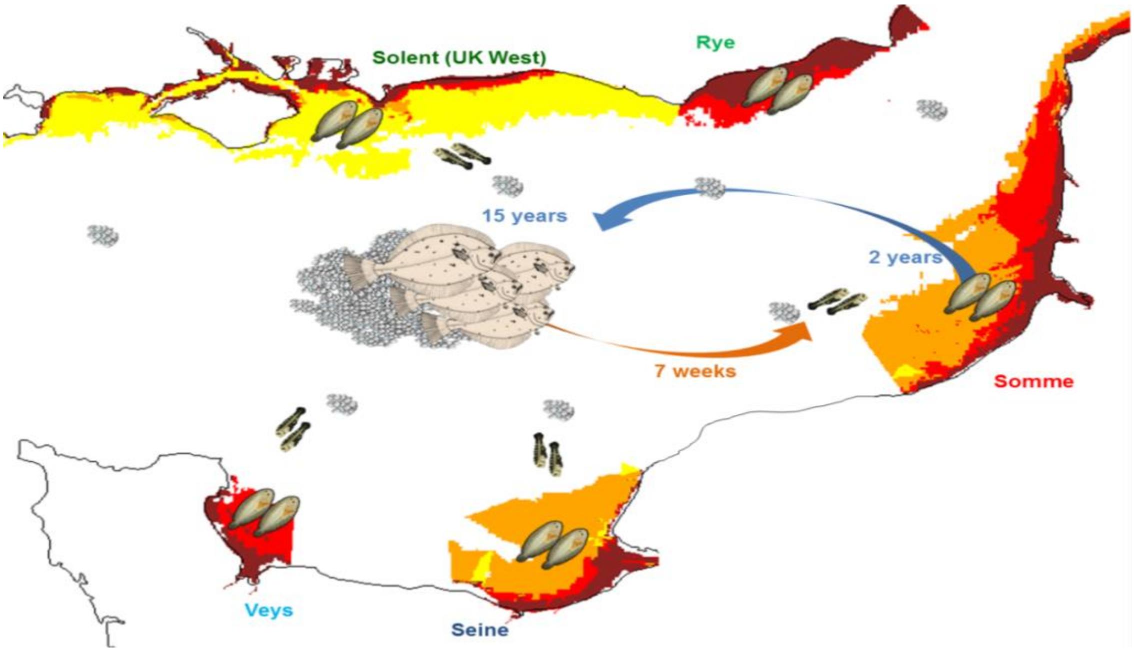

**Figure 1.** Life cycle of the Eastern Channel Sole population (Adapted from Rochette (2010) and Archambault (2014)).

As many other nursery-dependent fish species, this population suffers from various environmental and anthropogenic pressures. Because of this specific life cycle **(*Fig. 1*)**, these stressors appear at specific stages and impact fish populations at different spatial scales. The first eggs/larvae stages depend upon hydro-climate conditions which control larval transport and larval supply (Rochette et al., 2012) and involve high variability in recruitment (Le Pape et al., 2003a,b). Juvenile growth and survival are conditioned by the habitat sustainability and quality of coastal and estuarine nurseries. Ultimately, adult population (from age -2 to age -15) is targeted by fishing with a high exploitation.

### 1.5.2) Stock assessment

The sole in the Eastern English Channel (International Council for the Exploitation of the Seas, area VIId; hereafter denoted EC) is one of the most harvested flatfish populations and constitutes an important commercial flatfish resource. This population is exploited with annual landings of about 4,000 t (ICES, 2015) (***Fig. 2d***). Three countries are mainly involved in landings: France in large proportions with total landings fluctuating around 60%, Belgium and Britain. This population is currently managed as a homogeneous single stock, well-mixed, without spatial segregation inside the EC. Moreover, the current assessment considers a population separated from the North Sea stock and the Western Channel stock. Applying the $MSY$ (Maximal Sustainable Yield) approach, ICES advised that catches in 2016 should be no more than 2,685 tons (ICES, 2015). Over the time series, the Spawning Stock Biomass ($SSB$) (***Fig. 2a***) shows fluctuations without any trend and remains above $MSY\ B_{trigger}$ since 2002.

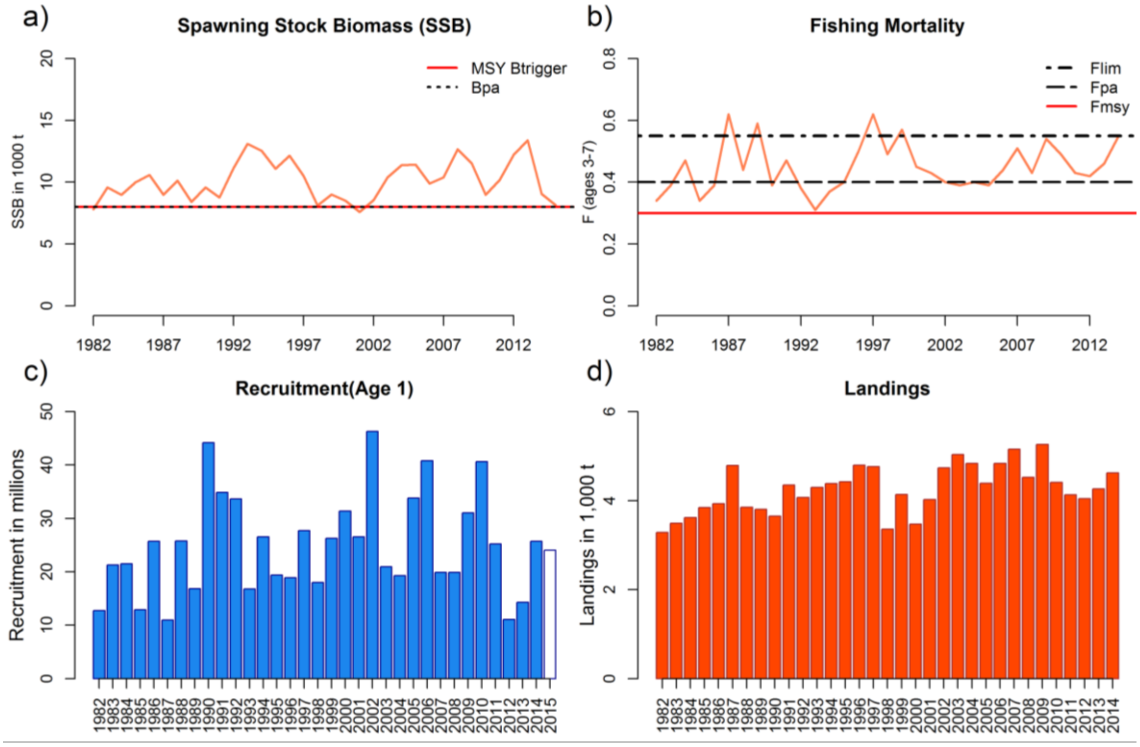

**Figure 2.** Summary of stock assessment: a) Spawning Biomass (1000's t), b) Fishing Mortality (average over age 3-8), c) Recruitment (in millions) and d) landings over the period between 1982 and 2015 (1000's t). Predictions appear as white bars. (Adapted from ICES, 2015)

However, due to a really low recruitment in 2012 (the lowest within the time series; ***Fig. 2c***), we observe a decrease in $SSB$ which appears in 2015 close to the $MSY\ B_{trigger}$ but still above. It is critical to point out that recruitment predictions are fully based on a unique scientific estimation campaign performed over the Somme nursery ground whereas it is known that five nursery grounds contribute to the whole recruitment of the EC Sole population. If the different nurseries show various productivities asynchronous in time, such an assumption would bias recruitment predictions.

Fishing mortality has always been above the $\mathrm{F}_{\mathrm{MSY}}$ (***Fig. 2b***) and is increasing since 2012. Since 2013, the stock assessment produced by the working group of ICES indicates an exploitation far above $\mathrm{MSY}$ with current $\mathrm{F}/\mathrm{F}_{\mathrm{MSY}} = 1.8$ (ICES, 2015). This assessment drove decision-makers to suggest successive cuts of the TAC during the last 3 years.

### 1.5.3) Spatial structure of the population and consequences for stock assessment

Getting a better understanding of the spatial structure is still the objective of current research. Some ecological clues indicate that the existence of a metapopulation structure formed by set of three subpopulations with low connectivity cannot be ruled out.

Tagging experiments have been carried out by the Center for Environment Fisheries and Aquaculture Science (Cefas) in the North Sea and the EC between 1955 and 2004 in order to improve knowledge on the movement of juvenile and mature sole. 91 tagging operations allowed to tag 30,000 fish within these areas with a majority of tags on juvenile sole (66%). Fish were tagged using “Petersen” discs that individually identify each tagged fish. Once tagged, fish were released close to the capture position and tagging characteristics were recorded for each tag release (geographic coordinates, tagging date, and individual size). During this experiment, a reward system has been established in order to encourage the declaration rate. Finally, Burt and Millner (2008) emphasized a spatial heterogeneity of the declaration rate which varies from 8 to 40% according to the recapture area. It appears to be around 42% for the UK coasts and around 16% along the west French coast in the EC. The mean time at liberty appears to be around 600 days but 20% of recaptures have been realized with a time at liberty below 90 days. Results emphasized seasonal pattern of movement (mainly in autumn and winter) with a movement mainly being westward in the EC (from the ICES management area IVb to the area VIIe). Around 70% of sole remain within the Eastern Channel (ICES area VIId) with movement mainly southward within this area. It also appears that sole return to the same release area to spawn in spring.
Otherwise, other scientific works demonstrated a high larval retention within spawning regions (Rochette et al., 2012) (***Fig. 3b***) and a very low connectivity between separated nursery grounds during juvenile stages (Riou et al., 2001) resulting in a spatial segregation during early life stages. Then in the hypothesis where few movements occur at adult stages (Burt and Millner, 2008), a strong metapopualtion structure may result (***Fig. 3a***) due to low adult-mediated connectivity (Archambault et al., 2016; Frisk et al., 2014).

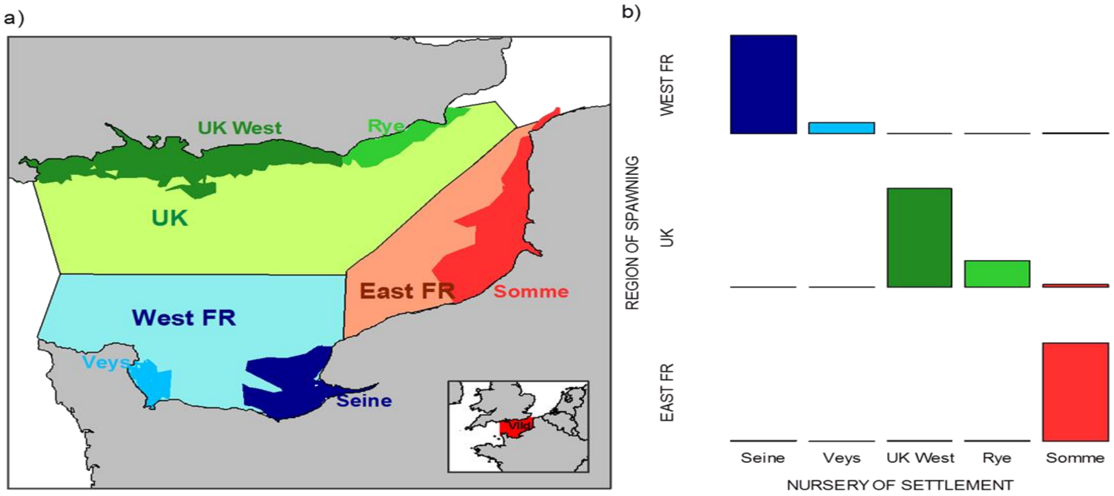

**Figure 3.** a) Eastern Channel area (corresponding to the ICES management area VIId) with the three subpopulations (West-FR, UK and East-FR) based on larval retention and a low adult-mediated connectivity. b) Probability to reach and settle successfully in one of the five nursery grounds (Seine, Veys, UK West, Rye and Somme) given the eggs origin subpopulation. (Adapted from Archambault et al (2016))

Also, spatio-temporal dynamics of the fishery indicate that the catches are not uniformly spread over the EC, with more than 50% of the total catches (in weight) that occur in the East-FR area (Archambault et al., 2016). Therefore, a spatial heterogeneity of both the population dynamics and the fishery dynamics could be considered.
Within this perspective, recent modelling work has explored the influence of considering such a metapopulation on stock assessment (Archambault et al., 2016). The authors have compared inferences on population dynamics and stock assessment obtained under two contrasted hypotheses: the first one (based on Rochette et al., 2013) assumes a single population, well-mixed and spatially homogeneous such as this stock is currently assessed. The other one assumes existence of three subpopulations with a full spatial segregation. (Both configurations are presented in ***Appendix I***).

Results show that key estimates of population dynamics parameters, stock assessment and management reference points are highly sensitive to the hypotheses made on the spatial structure. Overexploitation of the full population appears when a single population is assumed. On the contrary, when a three subpopulation structure is considered, inferences revealed very high contrast levels of exploitation among subpopulations (West FR subpopulation is at full exploitation while East FR and UK subpopulations are overexploited) (***Fig. 4***).This modelling work is a pavement that highlights the need to investigate adult-mediated connectivity for the Sole population in EC.

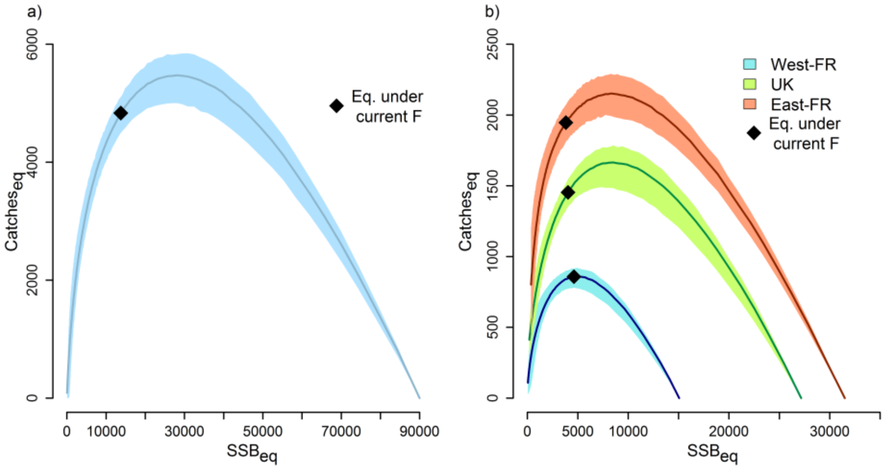

**Figure 4.** Relation between the SSB and catches at equilibrium for the model considering a) a single population and b) three isolated subpopulations. Shared area: 50% credibility interval obtained from the Monte Carlo simulation. Solid lines: posterior medians. Black diamond: Eq. under current F represents the position on the equilibrium curve obtained with the current fishing mortalities (average over the 4 most recent years). (Adapted from Archambault et al. (2016))

## 1.6. SMAC project

### 1.6.1) Overview

This work stands within the framework of the **SMAC** research project ("***S****ole en* ***M****anche Est:* ***A****mélioration des* ***C****onnaissances pour une meilleure gestion*"; http://wwz.ifremer.fr/smac/Le-Projet-Smac). The SMAC project is funded by ***F****rance* ***F****ilière* ***P****êche* (**FFP**) and the ***D****irection des* ***P****êches* ***M****aritimes et de l'****A****quaculture* (**DPMA**) and involves collaborations with IFREMER (project lead) and several stakeholders. The main objective of this project is to improve understanding of the population dynamics of the Sole population in the Eastern Channel and its interactions with the spatio-temporal dynamics of the fishery, for a better management of this stock. The SMAC project addresses three main questions: the connectivity and spatial structure of the Sole population in the EC, the spatio-temporal variability of the recruitment and

the selectivity applied on this population (see details of each question addressed by the SMAC project in ***Appendix II***).
This present study stands in the 1st axis “Connectivity and spatial structure of the Sole population” which aims at improving understanding on the spatial structure of the Sole population in the Eastern Channel. As demonstrated by previous studies (Archambault et al., 2016), quantifying the adults movements within the EC is critical for a correct understanding of the population dynamics and stock assessment. In this work we explore how new data that are planned to be gathered during the SMAC project could be used as an additional source of information to improve population dynamics and stock assessment models.

### 1.6.2) Outline of the capture-mark-recapture protocol planned in SMAC

Within the SMAC project, tagging experiments will be undertaken throughout 2016 and 2017 within the ICES division VIId.

- **Tagging**

Individual but passive tags (Petersen discs; ***Fig. 5a***) will be used to track fish over the Eastern Channel. This kind of tags has been largely used in tagging experiments and has particularly been proved efficient for flatfish (Burt and Millner, 2008). Each disc will be individually numbered so as to inquire on individual movements. Mark-recapture data will provide two spatial data points for each tagged individual (release and capture).

The first tagging tests were performed throughout the scientific survey IBT (from January 19th to February 19th 2016) aboard the N/O Thalassa. This scientific survey allows stock assessment for fish in the EC and the North Sea thanks to a vertical cut trawl. Tagging campaigns are planned during two type trips: onboard with professionals including two working days per year and per zones (as previously defined; ***Fig. 3a***) and during scientific surveys (UKBTS, NOURSOM, COMOR). Tagging with professionals will be done over spawning grounds (ideally in the three zones identified in ***Fig. 3a***) during winter. Finally, 6 days per year have been planned, and should allow to tag 200 to 400 fish per trip. As a result, it should be possible to tag 5,000 fish per year spread over the three zones (West-FR, UK, and East-FR) so has eventual anisotropy in movements among zones could be explored. According to catches composition most of tagged fish should range between 2 and 7/8 years old. Tagged fish will be released close to the catch position and real time at liberty will depend on the fishing pressure and natural mortality.

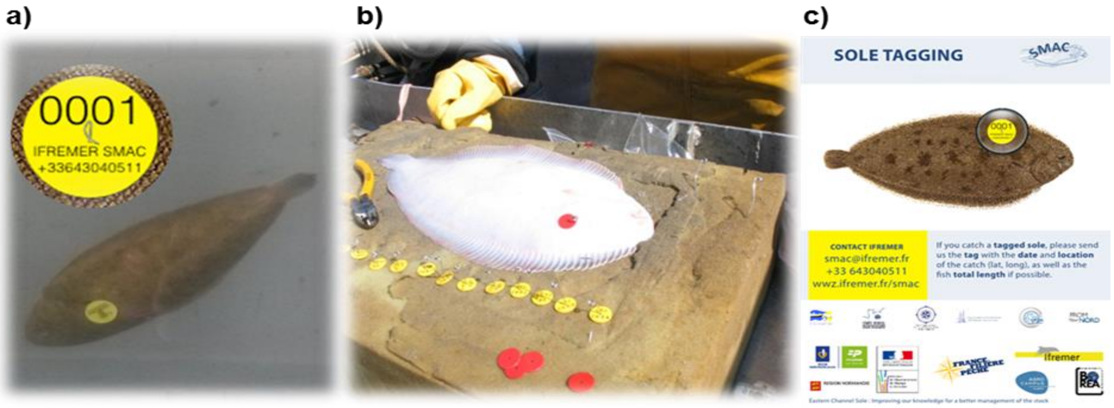

If you catch a **tagged sole**, please send us the **tag** with the **date** and **location** of the catch (lat, long), as well as the fish **total length** if possible.

Eastern Channel Sole : Improving our knowledge for a better management of the stock

**Figure 5.** Tagging experiment: a) A “Petersen” disc with the individually number, Ifremer phone number and the name Project “SMAC”. b) Placement of a Petersen disc on the dorsal side and secured by a piece of stainless steel wire through a hole, and anchored to a disc on the under body. c) The tagging poster warning for this current project (Photo credit: Ifremer)

- **Recapture**

Recapture will exclusively be carried out by commercial fisheries. Therefore during this project, dedicated and triggered promotion activity towards fishermen will be performed so as to maximize the return rate from these major actors to avoid possible bias in the forthcoming analysis. To that end, posters warning have been distributed all along the Eastern Channel coasts (both English and French), in Belgium and in Netherlands (http://wwz.ifremer.fr/smac/Marquage and http://wwz.ifremer.fr/smac_eng/Tagging ) (***Fig. 5c***; ***Appendix III***). Recapture rate is of course unknown. It depends upon the fishing mortality (estimated with the stock assessment model) and the tag recapture declaration rate. The former is unknown, but, based on previous mark-recapture experiments in the EC, a recapture rate of about 40% over the EC could be expected.

### 1.7) Challenges of the modelling approach and objectives

The challenge of this present work was to set the foundations of the modelling framework that could serve as a basis to embed tag-recapture data into an integrated hierarchical life cycle model to infer connectivity in the Sole life cycle in Eastern Channel.

Conventional tagging data have proven to be particularly useful with regard to estimate mortality rates and abundances using Bayesian modelling framework. However, this success has been mixed by using these data to inform connectivity parameters in spatially structured models.

Indeed, the success of tagging data in integrated stock assessment models could be mixed by a low number of tag returns, and also a bad knowledge of the value and of the spatio-temporal distribution of tags recapture and declaration rates. Even if the number of tag released is large, very loose information will be obtained from the tagging data if the tag returns rate is low. Hence, before planning a tag-recapture experiment, a critical step is to explore *a priori* how much tagging data would be needed to get sufficient and reliable information on fish movements.

Second, a high degree of confounding can occur between estimates of movement and the spatial heterogeneity of the tag-recapture declaration rate. Indeed, the tag return rate depends on both the tag-recapture rate (that depend on $F$, hence the need to embed the tag-recapture model with the stock assessment model) and on the tag recapture declaration rate which remains unknown and potentially heterogeneous in space and time. Therefore it is critical to investigate how spatio-temporal hypotheses on the tag-recapture declaration rate can impact estimations of movements and as well as the risk of bias if this rate is a priori under/overestimated.

To address this challenge, we used the following methodology:

- We first extended the hierarchical life cycle of Archambault et al. (2016) by including movement within the older life stages. As an improvement to the two extreme hypotheses tested in Archambault et al. (2016) (three isolated subpopulations / one single homogeneous population), this model extension open up the possibility to parametrize connectivity levels and to test how connectivity level affects inferences on population dynamics and stock assessment.

- Secondly we developed an integrated life cycle model that integrates a tag-recapture component within this spatially life cycle model to simultaneously estimate population dynamics and movements.

- Thirdly we analyzed how tagging dataset quality may affect inferences on connectivity parameters and population dynamics. To that end, a Simulation-Estimation approach was built to assess the influence of the number of tags released and of an unprecise knowledge of the tag recapture declaration rate.

# 2 Materials and Methods

## 2.1) Outline of the approach

### 2.1.1) Using the integrated life cycle model of Archambault et al (2016) as a baseline

Below, we provide the outline of the model we developed and of the approach we used (***Fig. 6***). As the model largely relies on the one fully detailed in Archambault et al. 2016 (fully available in ***Appendix IV***), we only detail how the model has been modified to introduce movement between the three subpopulations and the integration of the mark-recapture sub-model. All other model components that are not changed from Archambault et al. (2016) are not detailed.

The population dynamics is age and stage structured, and modeled during 30 years from 1982 to 2011. The adult population consists of 14 ages classes between age -3 and age -15 (subscript a) and all remaining fish were assumed to die at age -15.The life cycle model was written in a hierarchical (state-space) Bayesian framework (Archambault et al., 2016; Parent and Rivot, 2013; Rivot et al., 2004; Rochette et al., 2013) that accommodate both the stochasticity in the population dynamics and observation errors. Bayesian estimates of all unknown quantities of the model (abundance at age, key parameters, …) are obtained using MCMC methods (described in ***Appendix V***). The spatial structure of the model is not modified from Archambault et al. (2016). Five coastal nursery grounds (Veys, Seine, UK West (solent), Rye and Somme) where fish live up to age -2 are considered and the spatial structure of the "adult population" (fish older than -2) considers the three subpopulations (West FR, UK, and East FR).

The model assimilates an extensive dataset which is composed by: (i) the outputs of an individual-based model (biophysical larval drift model), (ii) the juvenile abundance indices (hereafter denoted AIs) over the five nursery grounds provided for each year of the period modelled but with missing data, (iii) catches-at-age data (age 2-15) are available from stock assessment reports only at the scale of the EC (not available separately for the three subpopulations), supplemented by ancillary data for the catch weight ratio per subpopulation (total weight; no age structure) showing that higher proportions of catches are regularly realized in the East-FR area, (iv) Two time series of AIs for adults (age 2-15) were available at the scale of the EC: the UK (UKCBT) and the Belgium (BEBCT) commercial fleet catch-per-unit effort. The scientific UK Bottom Trawl Survey (UKBTS) provided AIs at the adult stage for each of the three subpopulations.

### 2.1.2) Parametrizing the movement among zones as a connectivity matrix

Movement was modelled using the "Box-transfer" method initially developed by Beverton and Holt (1957) and already used by several authors like Hampton (1991) to model population dynamics of the southern Bluefin tuna off of Australia, Heifetz and Fujioka (1991) to incorporate tag shedding and tag reporting to model movement of sablefish. This method consists in parameterizing movements among "box" (box represents subpopulations) through a connectivity matrix that allows to a proportion of fish to move from a subpopulation $i$ towards another one $j$ or to stay into the subpopulation $i$ on a discrete time step. It is a discrete Markovian movement model (Goethel et al., 2011)where movement is assumed to be a random process for which the probability to move from a subpopulation $i$ to $j$ at time step $t$

only depends upon the subpopulation $i$ where individuals are at time step $t$ and is completely independent of the past trajectory.

### 2.1.3) Assessing the influence of various level of connectivity on the population dynamics and stock assessment

We then rely on the continuous parameterization of the connectivity among subpopulations to assess how connectivity assumptions affect estimates of key population dynamics parameters and stock assessment. As already highlighted by Archambault et al. (2016), parameters that drive the productivity in each nursery sectors (e.g. the carrying capacity and the maximum survival rate) are key for the population dynamics. Hence, we assessed how estimates of the productivity parameters of each nursery sectors and of their relative contribution to total recruitment are sensitive to change in connectivity level among the three subpopulations. We also assessed how posterior estimates of the Spawning Stock Biomass ($SSB$), the recruitment ($R$), and the fishing mortality ($F$) are sensitive to the connectivity structure among the three subpopulations. Ultimately, we assessed the sensitivity of management reference points, $MSY$, $F_{MSY}$ and $SSB_{MSY}$.

### 2.1.4) Integrating capture-mark-recapture data within the Bayesian stock assessment model to simultaneously estimate parameters and movements

We developed a tag-recapture sub-model to integrate tagging data into the stock assessment model. This sub-model keeps track of tagged fish among time. The fully mix assumption was made (Goethel et al., 2011; Hilborn, 1990) that assumes that tagged fish have the same dynamics and parameters as untagged fish. Each cohort of tagged fish was defined as a fish tagged group released in a given region a given year. Recapture of tagged fish occurred during commercial fishing (with the same fishing mortality that untagged fish) but the observation model of tagged fish additionally support a "declaration rate" of marked fish caught and returned for scientific interpretation (declaration rate is typically not 100%).

### 2.1.5) Simulation-estimation approaches and scenarios to assess the accuracy (bias) and precision of connectivity parameters estimates from capture-mark-recapture data

We used pseudo mark-recapture datasets simulated by a population dynamics model with known parameters (including movement, recapture and declaration rates) to assess how the integrated Bayesian estimation procedure can accurately and precisely estimate connectivity parameters. Then we explored various scenarios to quantify impacts of the number of tags and the spatial tag-recapture declaration rate distribution on the accuracy and precision of Bayesian estimates of connectivity parameters.

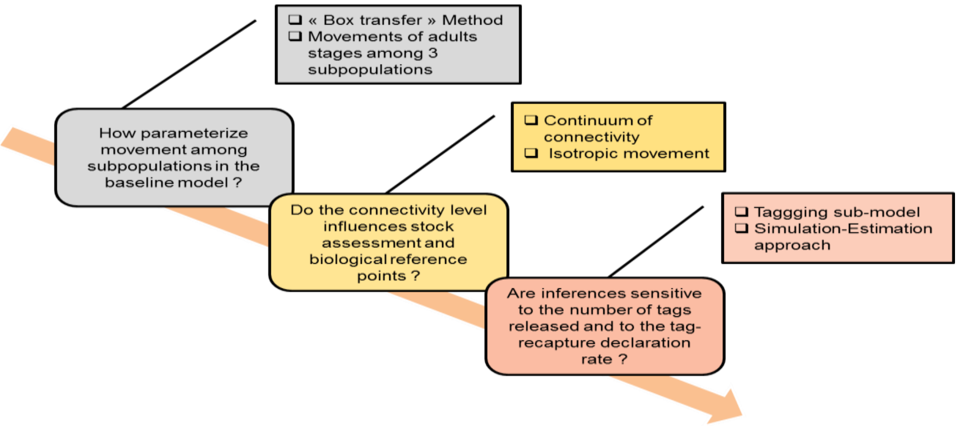

**Figure 6.** Chart flow of the modelling approach used in this study. Boxes correspond to the methods and hypotheses used to address questions.

### 2.2) Parametrizing movement among zones in the Eastern Channel

As in Archambault et al. (2016), fish leave nursery grounds to reach offshore habitats at age -2. A strong assumption is that movement among the three subpopulations only concern fish aged over 2 years (age -2 and more). The model assumed an age-structured dynamics with a yearly time step but account for connectivity among the three subpopulations at each stage of the life cycle. Movement was modelled through the "Box transfer" method using a 3 x 3 connectivity matrix $T$ (1). $T_{i,j}$ represented the proportion of fish in subpopulation $i$ that moved to the subpopulation j. $T_{i,i}$ corresponded to the connectivity parameter of residency. The model assumed that 100% of the fish moved or stayed, so as the sum of the $T_{i,j}$ over all arrival zones $j$ is equal to 1 for all departure subpopulation $i$.

$$(1) \qquad \boldsymbol{T} = \begin{bmatrix} & \cdots & \\ \vdots & \boldsymbol{T_{i,j}} & \vdots \\ & \cdots & \end{bmatrix}$$

An important assumption of the model is that movement occurred at the end of the year after natural and fishing mortality. A second important assumption was that once a fish moved between subpopulations, it is immediately integrated in the demographic rates of the "new" subpopulation. Once an individual crossed a boundary, population of origin is lost and it is mixed with the "new" subpopulation. Therefore, movement rates of any fish at any time are considered as a property of all fish of one subpopulation at this time (Goethel et al., 2014). Therefore, for fish older than age 3, cohort dynamics including movement are modelled as:

$$(2) \qquad \boldsymbol{N_{a+1,y+1,j}} = \left( \sum_{i=1}^{3} \boldsymbol{N_{a,y,i}} \times \boldsymbol{e}^{-(\boldsymbol{M_a} + \boldsymbol{F_{a,y,i}})} \times \boldsymbol{T_{i,j}} \right) \times \boldsymbol{e}^{\boldsymbol{\varepsilon_{a,y,j}}} , \qquad \boldsymbol{2 < a < 15}$$

where $M_a$ is the natural mortality, $F_{a,y,i}$ is the fishing mortality rate, $T_{i,j}$ is the connectivity matrix and $\boldsymbol{e}^{\boldsymbol{\varepsilon_{a,y,j}}}$ is a normal random noise with a variance $\sigma_p^2$ arbitrarily fixed to a very low value (Archambault et al., 2016). The abundance at a given age $\boldsymbol{a}$ in stock $\boldsymbol{j}$ is the sum of the number of fish in the previous age class that survived natural and fishing mortality over the precedent year and moved into the stock $\boldsymbol{j}$ or remained resident if $\boldsymbol{i} = \boldsymbol{j}$. The sequence of events within each year included: natural and fishing mortality, movement among sub-populations and spawning period (***Fig. 7***).

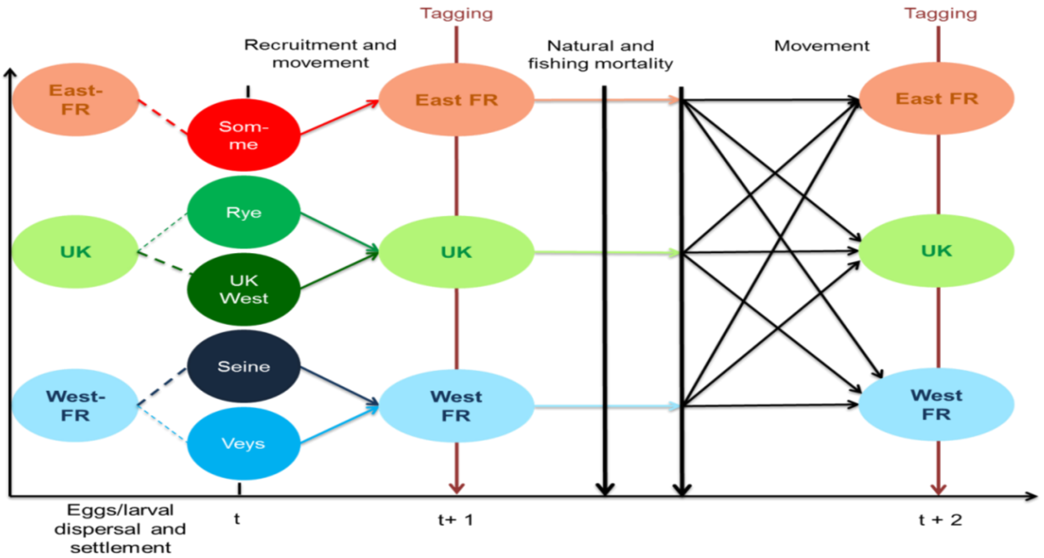

**Figure 7**. Schematic representation of the temporal and spatial stock dynamics assumed within the tag-integrated model. Then, dynamics are the same with spawning period and the same cycle. It assumed that once fish moves between zones, it instantaneously integrated on the demographic characteristics of the new subpopulation.

### 2.3) Different connectivity levels and influences on the stock assessment

Our model proposes a continuous parametrization of the connectivity between the three subpopulations that provides the possibility to test for a continuum of connectivity levels between the two extreme hypotheses of Archambault et al. (2016) (three isolated subpopulations / one single homogeneous population).

Eight scenarios of connectivity levels among subpopulations have been performed: 5, 10, 20, 30, 40, 50, 60, and 70% of connectivity. Movement is modelled as isotropic (***Table 1***), and thus assuming that the x% of fish leaving the subpopulation $\boldsymbol{i}$ were evenly dispersed among the two others subpopulations. The maximum connectivity level in our simulations was 70% and roughly corresponds to an homogeneous mixing between the three subpopulations (at each time step, 30% of fish remain in their subpopulation and 70% move to the two other ones with 35% in each of the two). Then, this scenario intuitively looks like a scenario considering a homogeneous single stock at the scale of the EC.

**Table 1.** Movement matrix used in estimations of reference management points. Various connectivity levels (5%, 10%, 20%, 30%, 40%, 50%, 60%, and 70%) with an isotropic dispersion. p corresponds to the probability of moving towards an adjacent subpopulation.

$$\begin{array}{c|c}
 & \begin{matrix} \text{West-FR} & \text{UK} & \text{East-FR} \end{matrix} \\
\hline
\begin{matrix} \text{West-FR} \\ \text{UK} \\ \text{East-FR} \end{matrix} & \begin{pmatrix} (\mathbf{1}-\boldsymbol{p}) & \left(\frac{\boldsymbol{p}}{\mathbf{2}}\right) & \left(\frac{\boldsymbol{p}}{\mathbf{2}}\right) \\ \left(\frac{\boldsymbol{p}}{\mathbf{2}}\right) & (\mathbf{1}-\boldsymbol{p}) & \left(\frac{\boldsymbol{p}}{\mathbf{2}}\right) \\ \left(\frac{\boldsymbol{p}}{\mathbf{2}}\right) & \left(\frac{\boldsymbol{p}}{\mathbf{2}}\right) & (\mathbf{1}-\boldsymbol{p}) \end{pmatrix}
\end{array}$$

The spawning stock biomass ($SSB$), recruitment ($R$), fishing mortality ($F$) and Maximum Sustainable Yield ($MSY$), the associated fishing mortality ($F_{MSY}$) and spawning stock biomass ($B_{MSY}$) were therefore estimated for each of these scenarios. As outlined in Archambault et al (2016), simulations are stochastic and results can not be derived analytically. In particular, the evaluation of quantities at $MSY$ can not be realized analytically due to the nature of the population dynamics model that results from a combination of stochastic Beverton-Holt relationships fitted on each nursery sector. Because the three subpopulations are connected together, local $MSY$ do not exist anymore, and the local fishing mortalities (eventually different among subpopulation) leading to the $MSY$ equilibrium point at the scale of the EC are found by simulations. All the simulation methods used to estimate quantities at the $MSY$ are fully described in the ***Appendix VI***.

The $AICM$ criterion (Akaike Information Criterion through Monte-Carlo; Eq. 3) was used to compare the performance of different models. The $AICM$ corresponds to an extension of $AIC$ (Akaike Information Criterion) to Monte-Carlo inference and which is based on the Bayes Factor (Raftery et al., 2007). This criterion deals with model explicative power and is based on the use of the log-likelihood (which can be obtained from the deviance parameter). This criterion is defined as :

$$\text{(3)} \qquad \boldsymbol{Deviance} = -\mathbf{2} \times \boldsymbol{l}$$

$$\boldsymbol{AICM} = \mathbf{2} \times (\bar{\boldsymbol{l}} - \boldsymbol{s}_{\boldsymbol{l}}^{\mathbf{2}})$$

where $\bar{\boldsymbol{l}}$ and $\boldsymbol{s}_{\boldsymbol{l}}^{\mathbf{2}}$ are the mean and variance of the log-likelihood along the chain. Note that following the definition (3), the preferred model is the one with the highest $AICM$.

## 2.4) Integrating a tagging model within the integrated life cycle model

### 2.4.1. Population dynamics of tagged fish

A tagging sub-model was developed to keep track of tagged fish among time. The tagging model concerned only the sub-adults and adults (i.e. cohort with ages between age -2 and -15) and described movement and survival dynamics of fish from each tagging cohort (***Fig. 8***). The only difference with the untagged population was that the recruitment of marked fish corresponds to tag-release operations and can potentially happen at any age, and that is independent from the natural recruitment dynamics of untagged fish (Maunder, 2001b).

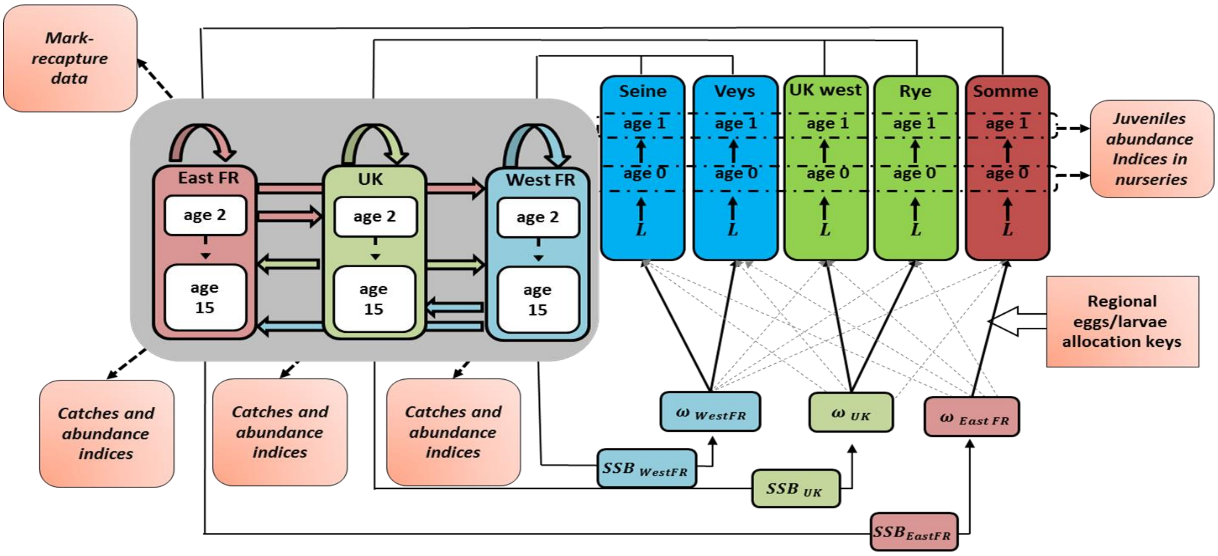

**Figure 8.** Tag-integrated life cycle model developed in our study. The tagging sub-model is represented by the grey box. Data or external model outputs considered as data are represented by the orange boxes. (Adapted from Archambault et al. (2016)).

Initial tag abundance $N^{release}_{Am,Zm,Ym,a,z,y,}$ was given by the observed number of releases. After release, mixing of tagged fish with untagged population was assumed to occur instantaneously, and tagged fish were assumed to have the same behavior as untagged fish. Tagging was supposed to occur at the beginning of the year allowing released fish to move to another subpopulation after suffering natural and fishing mortality. Therefore 6 indices are needed to track the dynamics of tagged fish denoted $N^{release}_{Am,Zm,Ym,a,y,z}$: the first three indices are needed to characterize the tag release cohort ($Ym, Am$ and $Zm$, for the Year, Age and subpopulation of tag release) and the three other ones characterize the age, year and subpopulation within the population once fish are fully mixed within the entire population. Note that $Am = a$ and $Ym = y$ for the year of release.

During time at liberty (defined as the time between tagging and recapture) tagged fish shared the same population parameters as the untagged fish, such as movement, natural and fishing mortality. Tag shedding and both vulnerability and mortality induced by the tag were ignored. An important assumption was made concerning fishing pressure on tagged population the first year as the model assumed that tagged fish undergo a fully year of fishing pressure, independently of the month when tagging occurs within the year.
The dynamics of the tagged population $\boldsymbol{N^{*}_{Ym,Zm,Am,a+1,y+1,j}}$ are thus given by:

$$\boldsymbol{N^{*}_{Ym=1,Zm,Am,a,y,i=Zm} = N^{release}_{Ym=1,Zm,Am,a,y,i=Zm} \quad , \quad y = Ym,, N * \geq 2} \tag{4}$$

$$\boldsymbol{N^{*}_{Ym,Zm,Am,a+1,y+1,j} = \left(\sum_{i=1}^{3} N^{*}_{Ym,Zm,Am,a,y,i} \times e^{-(M_a + F_{a,y,i})} \times T_{i,j}\right) \times e^{\varepsilon_{a,y,j}} \quad , \qquad \geq Ym + 1}$$

where $e^{\varepsilon_{a,y,j}}$ are independent and identically distributed Normal random noise.
Following Archambault et al. (2016) process noise variance σ²p was arbitrarily fixed to a very low value. This provides a demographic transition to be stochastic, while limiting variability around the obtained value and allow to speed up the MCM sampling process.

Recaptures of tagged fish (which occurs through the commercial fishery; $\boldsymbol{R^{*}_{Ym,Zm,Am,a,y,i}}$) were modelled with Baranov's catch equations modelled in each subpopulation using the current abundance of tagged fish in the subpopulation $\boldsymbol{i}$ and a fishing mortality specific to subpopulation $\boldsymbol{i}$.

$$\boldsymbol{R^{*}_{Ym,Zm,Am,a,y,i} = N^{*}_{Ym,Zm,Am,a,y,i} \times F_{a,y,i} \times \frac{\left(1 - e^{-(M_a + F_{a,y,i})}\right)}{M_a + F_{a,y,i}} \times e^{\varepsilon_{a,y,j}}} \tag{5}$$

### 2.4.2. Observation equations (likelihood)

The observation model for tagged fish (likelihood) assumed that tag recovery was a stochastic process where the number of tags recovered from each release cohort $Am$ at each region $Zm$ and time step $Ym$ was conditional on fish available for the annual harvest, natural mortality rate and the tag-recapture declaration rate $\boldsymbol{\beta_{y,i}}$, parametrized as time and region specific. An example of tag-recapture data obtained after recapture is presented in the ***Table 2***. This Table highlights the connectivity matrix and shows the impact of different fishery mortality among subpopulation through the number of tag recovered. Tag recoveries were modelled using a binomial distribution (4):

$$\boldsymbol{R^{obs}_{Ym,Zm,Am,a,y,i} \sim Bin\,(\,\beta_{y,i}\,, R^{*}_{Ym,Zm,Am,a,y,i})} \tag{6}$$

where $\boldsymbol{R^{obs}_{Ym,Zm,Am,a,y,i}}$ is the number of sole tags recovered at age $a$, a year $y$ in a region $i$ and coming from a fish released the year $Ym$ in the region $Zm$ at the age A$m$.

**Table 2.** Example of ag-recapture data obtained after 2 years, for each subpopulation. The total of tags released the first year is identical in all subpopulation for each cohort released. The recapture rate depends on the fishing mortality of each subpopulation.

| | | Recapture | | | | | |
|---|---|---|---|---|---|---|---|
| | | First year | | | Second year | | |
| | | West-FR | UK | East-FR | West-FR | UK | East-FR |
| 135 Released in each of three subpopulations for fish age 3 | West-FR | **11** | 1 | 1 | **6** | 1 | 1 |
| | UK | 1 | **19** | 3 | 1 | **10** | 3 |
| | East-FR | 5 | 4 | **22** | 5 | 4 | **7** |
| 105 Released in each of three subpopulations for fish age 4 | West-FR | **7** | 2 | 4 | **5** | 2 | 4 |
| | UK | 1 | **15** | 3 | 1 | **7** | 3 |
| | East-FR | 0 | 1 | **17** | 0 | 1 | **5** |
| 30 Released in each of three subpopulations for fish age 5 | West-FR | **2** | 1 | 1 | **1** | 1 | 1 |
| | UK | 0 | **4** | 1 | 0 | **2** | 1 |
| | East-FR | 0 | 0 | **4** | 0 | 0 | **2** |
| 15 Released in each of three subpopulations for fish age 6 | West-FR | **1** | 0 | 1 | **1** | 0 | 1 |
| | UK | 0 | **2** | 0 | 0 | **1** | 0 |
| | East-FR | 0 | 0 | **2** | 0 | 0 | **1** |
| 15 Released in each of three subpopulations for fish age 7 | West-FR | **1** | 0 | 1 | **1** | 0 | 1 |
| | UK | 0 | **2** | 0 | 0 | **1** | 0 |
| | East-FR | 0 | 0 | **2** | 0 | 0 | **1** |

### 2.4.3. Which parameters can be identified by the tag-Integrated model?

Because of the complex interactions between process and observations equations in state-space models, and because of the information brought by prior distribution, parameters identifiability is difficult to gauge in such complex integrated state-space models. As in most stock assessment models (although exception exists), the total mortality ($Z = M + F$) can be estimated but natural and fishing mortality can not generally be identified separately.

The tag return rate depends upon both the total mortality rate (natural and fishing mortality) and the tag-recapture declaration rate. When natural mortality and tag-declaration rate are considered known, both fishing mortality (specific for the three subpopulations) and connectivity parameters among the three subpopulations can be estimated simultaneously.
But simultaneously estimating all those parameters is difficult (Sippel et al., 2015) as those parameters are partially confounded. Hoenig et al. (1998) emphasized that estimates of tag-declaration rate and both estimates of fishing and natural mortalities are strongly negatively correlated. Furthermore, estimates of $F$ and $M$ are often biased when the tag declaration rate is mis-specified. In particular, any unknown spatial heterogeneity (e.g. difference among subpopulation) of the tag-declaration rate will be confounded with estimates of $F$ and of connectivity parameters.

Because the catch-at-age model should provide enough information to estimate fishing mortality, the tag-recapture declaration rate should be estimable within the integrated model provided that it is considered homogeneous among subpopulations (to avoid any confusion with movement) and that the natural mortality is known.

## 2.5) The Simulation Estimation approach

A simulation-Estimation approach (Hilborn and Mangel, 1997; Ono et al., 2012; Robert et al., 2010) was used to explore the performance of the Bayesian estimation procedure, i.e, its ability to reliably (bias) and precisely (uncertainty) estimate parameters.

### 2.5.1. Simulations of tag-recapture data with fixed parameters

For all scenarios, the population dynamics of the tagged population was modelled using equations (4), with known level of connectivity. We did the assumption that tagging experiments did not begin at the first year of the model and were performed for two consecutive years. An initial separate time subscript, $yeartag$, was used to represent the first tagging year. This could particularly prove useful later in order to use a database whose tagging experiments could not be consistent with model schedule. Population dynamics were freely simulated until the last year of the model.
When fitted to all available data except any tag-recapture data, results of model comparison show that the model with a connectivity level of 20% provides the best $AICM$ criteria (see section 3.1.1). Hence, the dynamics of the tagged population in all scenarios was simulated with an isotropic 20% connectivity level.

For all scenarios, the tag distribution at age was assumed to be known and arose from the catch composition provided by ICES. According to the range of selectivity, fishes aged from 3 to 7 years were tagged. The percentage at age of the total number of tags were distributing as following:

**Table 3.** Distribution at age of tags (in %) of fishes aged from 3 to 7 years (according to ICES data).

| Ages | 3 | 4 | 5 | 6 | 7 |
|---|---|---|---|---|---|
| % of total number of tags | 45 | 35 | 10 | 5 | 5 |

### 2.5.2. Questions addressed and corresponding scenarios

Simulated tag-recapture data were then used as “real” data in the integrated Bayesian life cycle model to test the ability of the estimation method to reliably and precisely estimate parameters.

Various scenarios S1 → S3 (summarized in ***Table 4***) were performed to investigate the following questions:

(i) What are the effects of the tagging protocol (tag number) on the performance of the estimation method?

(ii) What is the sensitivity of inferences to the value of the tag recapture declaration rate (thereafter denoted $BETA$ $(\beta)$)? How does the quality of inferences degrade when hypotheses on the spatial heterogeneity of this parameter are mis-specified? Finally, can this parameter be estimated provided that prior information is available?

(iii) Would it be possible to estimate the natural mortality, provided that enough prior information is available on the tag recapture declaration rate?

- ***Scenarios S1: Sensitivity to the tagging protocol***

Increasing the tag number of tagging data can improve parameter estimates by reducing uncertainty (Hulson et al., 2011). Scenarios S1 aim at analyzing impacts of tag number on connectivity parameter estimates through three simulated datasets that consider a high number of tagged fish per region and per year (S1a), a more realistic number (provided the resource available in SMAC project, S1b), and a low number of tagged fish (S1c) (***Table 3***).

In those scenarios, no mis-specification of the values of the tag-recapture declaration rate was introduced between simulations and estimations. It was considered known and fixed to $\beta = 0.90$, homogeneous among subpopulations and constant over time, for both simulations and estimations.

**Table 4.** Tagging protocol used for each scenario (high, realistic, and low number of tags) with both the number of tags per age and the number of years of tagging experiments.

| | | Ages | | | | |
|---|---|---|---|---|---|---|
| | | 3 | 4 | 5 | 6 | 7 |
| Scenarios | High **(S1a)** | 270 | 210 | 60 | 30 | 30 |
| | Realistic **(S1b)** | 135 | 105 | 30 | 15 | 15 |
| | Low **(S1c)** | 68 | 52 | 15 | 8 | 7 |

In the Bayesian estimation procedure, almost all of estimated parameters were given weakly informative *a priori* distributions to let the data speak while excluding unrealistic values (as defined by Gelman (2004) and as already used in previous work of Archambault et al., 2016). In particular, we used diffuse prior for all $T_{i,j}$ parameters. Movement is considered *a priori* as anisotropic, that is for any subpopulation of origin $i$, the movement from $i$ to $j$ is not considered *a priori* equal to the movement from $i$ to $j$'. Within this movement matrix, two sets of constraints have been met: (1) movement rates away from a region have to be bound in the interval [0, 1], and (2) all movement rates leaving one subpopulation have to sum to one (residency include). For each movement rates between one subpopulation to another or in the case of residency, we used a Dirichlet prior distribution. This distribution corresponds to a multivariate generalization of the Beta distribution that fulfills the necessary set of parameter constraints. Movement was therefore parametrized as following:

$$\forall i: \qquad (T_{i,j=1}, T_{i,j=2}, T_{i,j=3}) \sim \boldsymbol{Dirichlet}(\alpha_1, \alpha_2, \alpha_3) \tag{7}$$

where $\alpha_j = 3$ for all subpopulations receiving fishes from subpopulation $i$.

Note that in this baseline scenarios, the movement is a priori considered as anisotropic, that is that different values of the connectivity parameters $T_{i,j}$ can be estimated for all $(i, j)$, with the only constraint that $\sum_j T_{i,j} = 1$.

## Scenarios S2: Sensitivity of inferences to a mis-specification of the tag declaration rate

Those scenarios aim at investigating how bias and uncertainty about estimates of connectivity parameters increase when a bad specification of the value and the spatial distribution of the tag-recapture declaration rate are supposed in the Bayesian estimation procedure.

### S2a - Sensitivity to the declaration rate value

We simulated a dataset with a declaration rate fixed to $\beta = 0.45$ and parametrized as being constant over time and between subpopulations. Estimations were conducted firstly with a declaration rate fixed to $\beta = 0.45$ (scenario S2a1 – no mis-specification between simulation and estimation) and secondly fixed to $\beta = 0.90$ (scenario S2a2 – the declaration rate used in the estimation procedure is therefore believed to be greater than in the reality). In both cases, no spatial mis-specification of the declaration rate is introduced, and declaration rate is considered as constant in time and homogeneous among subpopulations.

### S2b - Sensitivity to the declaration rate parametrization

Scenario S2b aim at quantifying how inferences on connectivity parameters are impacted by a mis-specification of the spatial distribution of the declaration rate. Because information on the declaration rate is quite difficult to get from observations, data were simulated with a spatial heterogeneity of the tag-recapture declaration rate but this declaration rate was considered as spatially homogeneous among subpopulations in the estimations procedure to mimic the absence of information when analyzing data. Because SMAC is a French project, data were simulated under the assumption of a lower declaration rate in the UK region (that could result from a less efficient promotion activity towards English fishermen).
Two datasets were simulated with (i) a spatial mis-specification of the declaration rate exclusively in the UK region ( $\beta = 0.45$; scenario S2b1), (ii) a spatial mis-specification of the declaration rate in the both UK and West FR regions with the same declaration rate ( $\beta = 0.45$ ; scenario S2b2). Estimations were performed by fixing the tag declaration rate to $\beta = 0.90$ over the EC.

### S2c – Using an informative prior distribution on the recapture declaration rate

We also evaluated the potential of using an informative prior for the tag recapture declaration rate. The tagging dataset was simulated with a declaration rate fixed to $\beta = 0.90$ and parametrized as being constant over time and space. Instead of fixing the value of the declaration rate in the estimation procedure, a Beta prior distribution was set on the tag recapture declaration rate. Two estimations were performed using (i) an informative prior with a medium variability around 0.90 ($\mu = 0.91$, $\sigma^2 = 7.45.10^{-4}$) (scenario S2c1) and (ii) a less informative prior with a higher variability around 0.90 ($\mu = 4.5$, $\sigma^2 = 0.013$) (scenario S2c2).

$$\boldsymbol{\beta_z \sim beta\,(a, b)} \tag{8}$$

## Scenario S3: Ability to estimate natural mortality

As previously mentioned, it would be possible to estimate natural mortality from the tag-integrated model, provided that tag recapture declaration rate was known and fixed. To assess this possibility, a prior distribution was set on the natural mortality at age, Ma, but that is conservative for the ratio of natural mortality between the different ages modelled in Archambault et al. (2016).

We used the weighting function with a uniform prior distribution (bounded on the interval [0,3]) on the maximal natural mortality (Eq 6).

(9)
$$\boldsymbol{Mmax \sim Unif(0,3)}$$
$$\boldsymbol{M = \alpha_a \times Mmax}$$

where $Mmax$ corresponds to the maximal natural mortality and $\alpha_a$ is a weighting coefficient at age $a$ known from Archambault et al. (2016) (***Appendix IV***) .

### 2.5.3. Quantifying bias and uncertainty of Bayesian estimates

The estimation model was applied for each scenario and error and precision were assessed for each of them. The performance of the estimation concerning movement parameters was therefore quantified by analyzing the marginal posterior distribution of these parameters (with a focus on movement parameters).

The relative bais was used to quantify the difference between the parameter estimate from a given run and the true value used to simulate dataset. The relative bias was calculated as the bias divided by the true parameter value:

(10)
$$\boldsymbol{Relative\ bias = 100 \times \left(\frac{\bar{\theta} - \theta_{True}}{\theta_{True}}\right)}$$

where $\bar{\theta}$ corresponds to the expected posterior mean of parameter $\theta$ and $\theta_{\mathrm{True}}$ the true parameter value used for the simulated dataset.

The precision of the Bayesian estimation was measured by calculating the standard deviation of the posterior distribution of each parameter:

(11)
$$\boldsymbol{SD = \sqrt{Var(\theta)}}$$

**Table 5.** Summary of all scenarios performed in the Simulation-Estimation.

| Simulation scenario | | | | Simulation setting (Two years of tagging experiments) | Estimation model |
|---|---|---|---|---|---|
| **Tagging protocol** (Scenario S1) | | | | | |
| | | S1a | High number | Reporting rate (β) = 90 %<br>Isotropic movement parametrization | Reporting rate (β) =90 %<br>Anisotropic movement parametrization |
| | | S1b | Realistic number | | |
| | | S1c | Low number | | |
| **Influence of the tag declaration rate** (scenario S2) | Sensitivity to : | | | | |
| | **the value** | S2a1 | | Reporting rate (β) = 45 %<br>Isotropic movement parametrization | Reporting rate (β) = 45 %<br>Anisotropic movement parametrization |
| | | S2a2 | | Reporting rate (β) = 45 %<br>Isotropic movement parametrization | Reporting rate (β) = 90 %<br>Anisotropic movement parametrization |
| | **the spatial heterogeneity** | S2b1 | | | |
| | | | UK subpop. | Reporting rate (β) = 45 % | Reporting rate (β) = 90 % |
| | | | West and East FR subpop. | Reporting rate (β) = 90 % | |
| | | | | Isotropic movement parametrization | Anisotropic movement parametrization |
| | | S2b2 | | | |
| | | | UK and West FR subpop. | Reporting rate (β) = 45 % | Reporting rate (β) = 90 % |
| | | | East-FR subpop. | Reporting rate (β) = 90 % | |
| | | | | Isotropic movement parametrization | Anisotropic movement parametrization |
| | **A prior information** | | | Reporting rate (β) = 90 % | |
| | | S2c1 | | | Medium variance of the Beta distribution |
| | | S2c2 | | | High variance of the Beta distribution |
| | | | | Isotropic movement parametrization | Anisotropic movement parametrization |
| **Estimation of the natural mortality (M)** (Scenario S3) | | S3 | | Reporting rate (β) = 90 %<br>Isotropic movement parametrization | Reporting rate (β) = 90 %<br>Anisotropic movement parametrization<br>Uniforme distribution of M - weighting function |

# 3 Results

## 3.1 Sensitivity of posterior estimates to different levels of connectivity among the three sub-populations

### 3.1.1. Model evaluation

Eight different models were fit using the same data sources as in Archambault et al. (2016), but without any tag-recapture data, to evaluate impacts of various connectivity levels on stock assessment and management reference points.
Analysis of the goodness of fit of each of these models through the Akaike Information Criterion through Monte Carlo ($\mathrm{AICM}$) revealed that the model configuration with a connectivity level of 20% (each year, 10% of fish present in a particular subpopulation for a particular year will move to each of the two others sub-populations) best support the data ($\mathrm{AICM} = -26{,}958$ ) (***Table 5***).

**Table 6.** $\boldsymbol{AICM}$ for all configurations of connectivity levels, $\bar{l}$ and $s_l^2$ represent the mean and variance of the log-likelihood along the chain.

| Connectivity level | $\bar{l}$ | $s_l^2$ | $AICM$ |
|---:|---:|---:|---:|
| 5 | -5,022 | 10,357 | -30,758 |
| 10 | -5,041 | 8,948 | -27,979 |
| 20 | -5,035 | 8,444 | -26,958 |
| 30 | -5,014 | 9,260 | -28,546 |
| 40 | -4,984 | 10,047 | -30,062 |
| 60 | -4,953 | 10,603 | -31,111 |
| 70 | -4,950 | 10,880 | -31,663 |

This first result is consistent with previous studies that suggested a low connectivity level between subpopulations in the Eastern Channel (Burt and Millner, 2008). Therefore, in absence of any tagging data, results suggest to use a model with 20% connectivity level among the three subpopulations. Therefore, a connectivity level of 20% was used in baseline model configuration used to simulate tag-recapture data (see below).

### 3.1.2. Sensitivity of parameter estimates and stock assessment to connectivity levels

- **Parameters ($\alpha, K$) and contribution to the recruitment of each nursery sector**

Results revealed that parameters estimates are sensitive to changes in the values of connectivity levels between 0 and 70%. When the connectivity level increases, estimates of parameters show an overall consistent trend towards the same values as the model considering one single population.

Across this continuum, increasing connectivity level directly affects estimates of the carrying capacity per unit of surface ($\mathrm{K}$) (***Fig. 9***), with a balance across nursery sectors: estimates of $\mathrm{K}$ for the Seine, Veys and Rye nursery sectors increase, balanced by a significant decrease in estimates of $\mathrm{K}$ for the Somme nursery sector (-58%) (Mean, Median, Standard deviation and quantiles are provided in ***Appendix VII***). The change in estimates is particularly significant for the Veys nursery sector with an increase of 245% but with a high level of uncertainty. However, the collapse of the estimates of $\mathrm{K}$ and $\mathrm{Alpha}$ ($\alpha$) observed in the Veys nursery sector in the single population configuration (denoted “Pan” in the Figure 10) can not be explained and probably results from a MCMC simulation error.

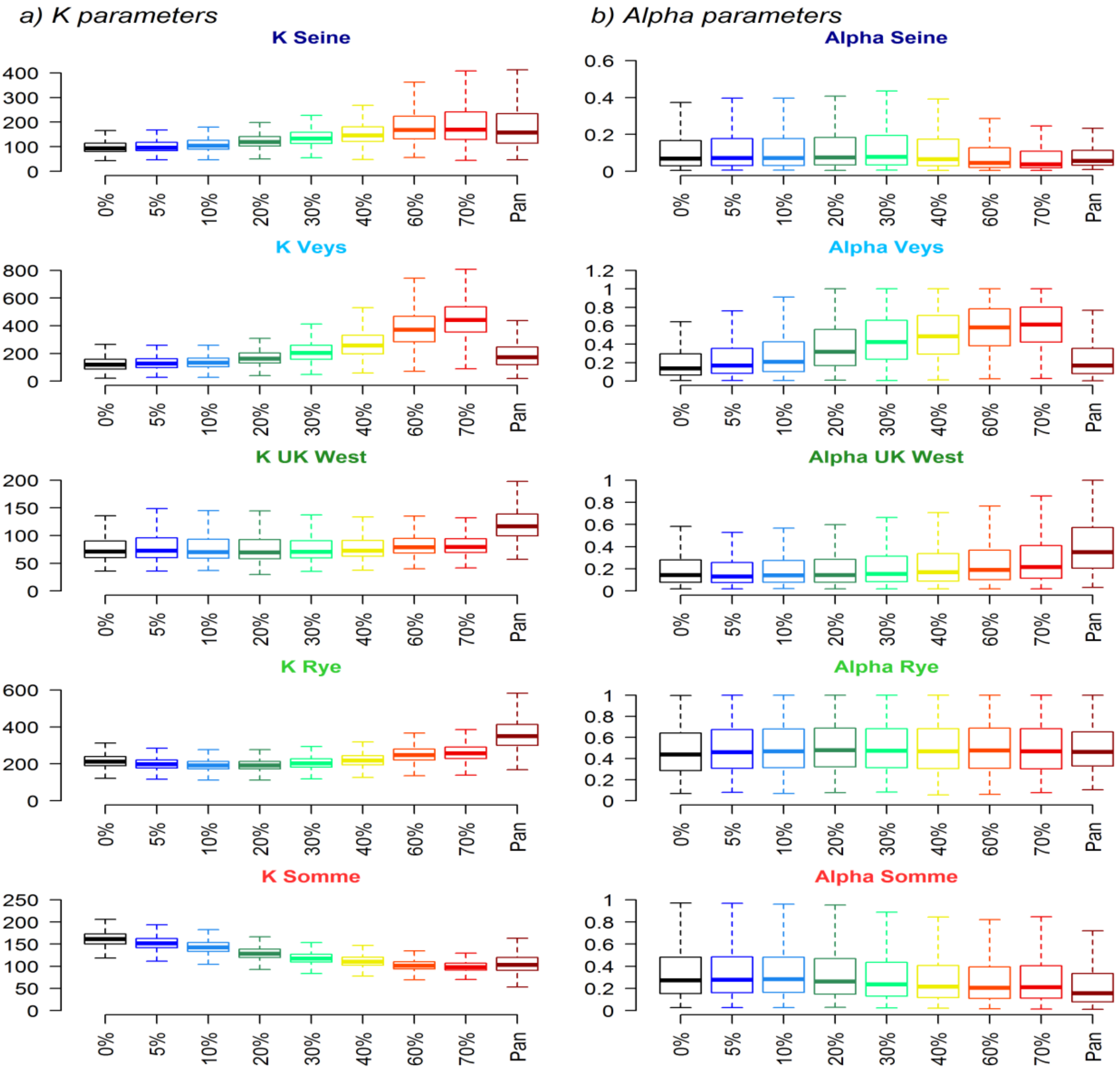

**Figure 9.** Marginal posterior distributions of the nursery-specific Berverton-Holt parameters $\boldsymbol{K}$ and Alpha($\boldsymbol{\alpha}$) obtained for various connectivity levels. The “regional” scenario (“0%”) corresponds to three isolated subpopulations structure (0 connectivity). At the other extreme, scenario « Pan » corresponds to a single population structure. K is in thousands of fish per Km², $\boldsymbol{\alpha}$ is a maximum survival rate.

Estimates for the UK West nursery sector remain broadly unchanged by increasing connectivity level. Regarding the maximal survival rate (***Fig. 9b***), only estimate for the Veys nursery sector is really impacted but still with a high uncertainty around this parameter.
Although all of the parameters are obtained with low uncertainty, increasing connectivity level leads to increase uncertainty about parameter estimates of the density-dependent recruitment process in each sector. That is particularly true for estimates of the carrying capacity (K) (***Fig. 9a***) and especially for the Rye and Veys nursery sectors. Uncertainty about the maximal survival rate (α) is higher for the Somme and Veys sectors when connectivity among subpopulations increases.

Sensitivity of parameter estimates logically induces a sensitivity of the contribution of each nursery sector to the total recruitment in the EC. Increasing connectivity among subpopulations leads to rebalancing of the contribution of nursery sectors to the total recruitment (***Fig. 10***).

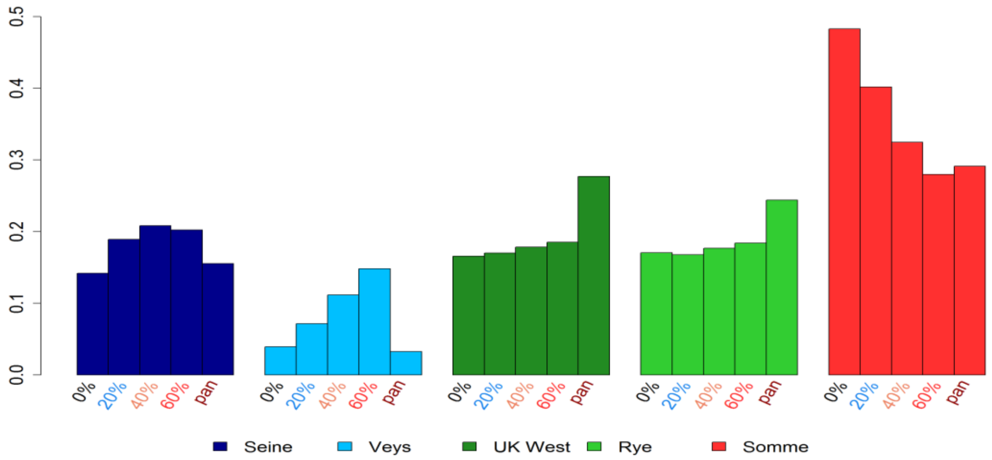

**Figure 10.** Posterior estimates of the contribution of the five nursery sectors to the total recruitment in the Eastern Channel (average over the entire time series) obtained for each connectivity level (three isolated sup-populations (0%), connectivity levels of 20%, 40%, 60%, and a single homogeneous population (« Pan »)).

When considering three isolated subpopulations, the Somme nursery sector contributes to ~48% of the total recruitment (average over the entire time series), the contribution of the Veys nursery sector is very low (~4%) and UK West, Rye and Seine nursery sectors contribute to 17,17 and 14% respectively (***Fig. 10***; see detailed number in ***Appendix VIII***). When, considering a connectivity level of 60%, these contributions are more homogeneous among sectors. Indeed, the Seine, Veys, UK West, Rye and Somme sectors contribute an average of 20, 15, 19, 18 and 28%, respectively, with relatively low variability among years (***Appendix VIII***).

### ○ Spawning stock biomass, recruitment and fishing mortality

Estimates of the Spawning-Biomass ($SSB$), Recruitment ($R$) and Fishing mortality ($F$) are also sensitive to the connectivity. For the East-FR subpopulation (note that only the Somme nursery sector contribute to recruitment of the East-FR subpopulation), logically with the sensitivity of the contribution to the recruitment, increasing connectivity level induces a decrease of $SSB$ and $R$, balanced by an increase in $F_{3-8}$ (***Fig. 11***). The balance between variables that reflect abundance (decrease in $SSB$ and $R$) and fishing mortality (increase in $F_{3-8}$) is explained by the high weight of the catches in the likelihood function with half of the catches observed in the East-FR subpopulation whatever the level of connectivity. Furthermore, the sensitivity to the connectivity level also decreases along the time series. The West-FR and UK subpopulations exhibit opposite sensitivity patterns, with increasing connectivity level that leads to an increase of $SSB$ and $R$ balanced by a decrease in $F_{3-8}$ (***Appendix IX***).

Average $SSB$ and $F_{3-8}$ over the past four years are presented in the ***Table 7***. For each configuration of the connectivity level, sum over the three subpopulations of the estimates of $SSB$ remains consistent with the sum of the estimates $SSB$ obtained in the model considering three subpopulations ($\sim 13{,}290$ t) and obtained with the model considering a single population ($\sim 12{,}950$ t). The impact of connectivity levels on the average $\mathrm{SSB}$ over the four last year leads generally to a similar pattern between subpopulations with a slight decline of total $\mathrm{SSB}$ when connectivity increases from 0 to 20% connectivity, followed by an increase of total $\mathrm{SSB}$. At the same time, the average fishing mortality $\mathrm{F}_{3-8}$ tends to increase until 20% of connectivity and then decreases.

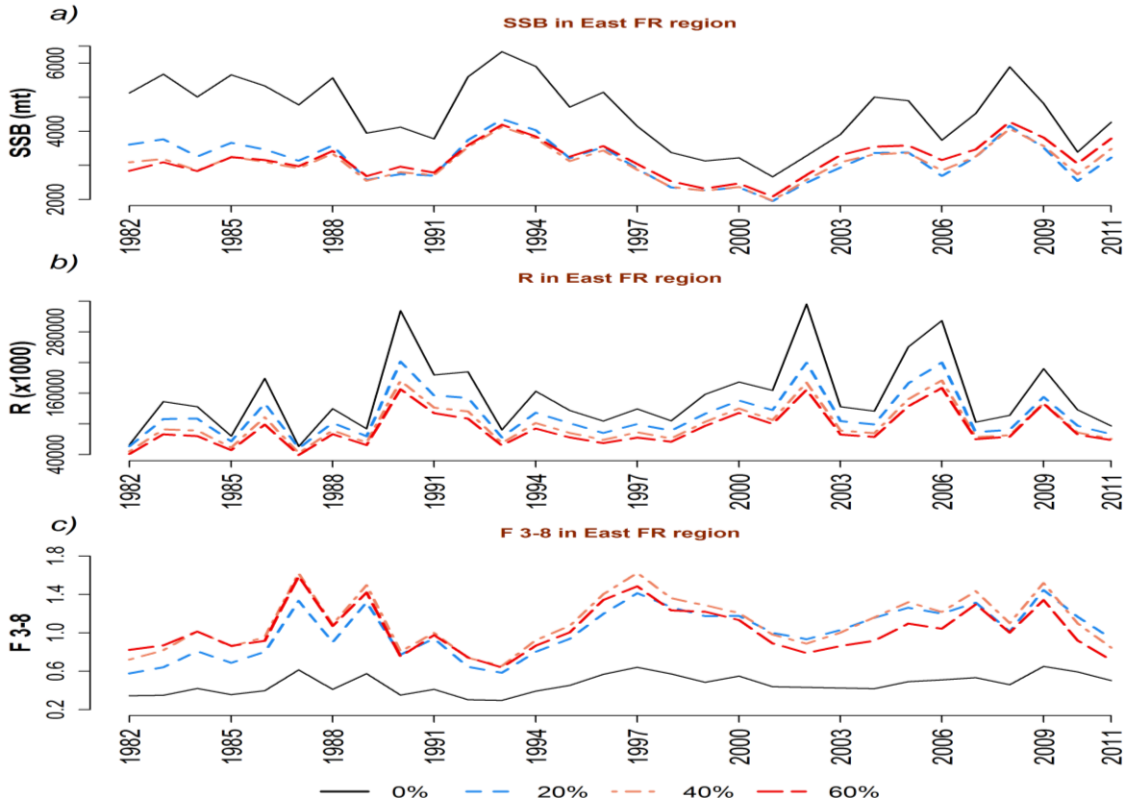

**Figure 11.** Comparison of posterior median estimates of SSB (a), R (b) and $F_{3-8}$ (c) obtained for models considering three isolated sub-populations, and connectivity levels of 20, 40, and 60% for the East-FR subpopulation.

**Table 7.** Summary of the average estimates of SSB and $F_{3-8}$ over the last four years in the models considering three isolated sub-populations for various connectivity levels.

| Reference points | | Different connectivity | | | | One single population |
|---|---|---|---|---|---|---|
| | | 0% | 20% | 40% | 60% | |
| $Average$ $SSB$ | West FR | 4,570 | 4,230 | 4,346 | 4,502 | 12,950 |
| | UK | 4,130 | 3,750 | 4,185 | 4,555 | |
| | East FR | 4,590 | 3,365 | 3,467 | 3,735 | |
| $Average$ $F$ | West FR | 0.2 | 0.20 | 0.18 | 0.17 | 0.38 |
| | UK | 0.39 | 0.45 | 0.37 | 0.32 | |
| | East FR | 0.55 | 1.14 | 1.14 | 0.99 | |

### Management reference points

Finally management reference points, $SSB_{MSY}$, $C_{MSY}$ and $F_{MSY}$ are also sensitive to the level of connectivity (***Table 8***). When the connectivity level increases, $SSB_{MSY}$ and $C_{MSY}$ increase and converge towards values estimated in the model considering one single homogeneous population. However connectivity level of 60% presents higher $C_{MSY}$ than the single population. Changes in estimates of $F_{MSY}$, depend on the subpopulation concerned. Increasing connectivity level leads to an increase of $F_{MSY}$ in the UK and East-FR subpopulations, when $F_{MSY}$ decreases until very low values (0.13) for the West-FR subpopulation.

Finally, results revealed that the assessment of current state of exploitation (evaluated by the ratio between the current local $F$ (average over the last four years) and local $F_{MSY}$) is highly sensitive to the level of connectivity considered (***Table 9***). Results revealed that the level of exploitation in the East-FR subpopulation is always higher than the one at $MSY$, (ratio $F/F_{MSY}$ much greater than 1) whatever the level of connectivity considered. The level of exploitation in the UK subpopulation is also higher than the one at $MSY$ except for a high level of connectivity ($\geq 60\%$). Diagnostics of the current state of exploitation for the West-FR subpopulation are more complex: it is considered as lower than $MSY$ $(0.71 < \mathrm{F/F_{MSY}} < 0.75)$ for low levels of connectivity (< 40%), and then considered as slightly higher than $MSY$ for greater connectivity levels.

**Table 8.** Summary of point estimates of the management reference points $SSB_{MSY}$, $C_{MSY}$, and $F_{MSY}$ obtained in the models considering three isolated sub-populations, 20%,40, and 60% connectivity and a single population.

| Reference points | | Different connectivity | | | | One single population |
|---|---|---|---|---|---|---|
| | | 0% | 20% | 40% | 60% | |
| $SSB_{MSY}$ | West FR | 4,880 | 20,086 | 20,53 | 23,465 | 28,090 |
| | UK | 8,540 | | | | |
| | East FR | 8,300 | | | | |
| $C_{MSY}$ | West FR | 870 | 4,870 | 5,252 | 5,722 | 5,470 |
| | UK | 1,670 | | | | |
| | East FR | 2,150 | | | | |
| $F_{MSY}$ | West FR | 0.19 | 0.29 | 0.16 | 0.13 | 0.21 |
| | UK | 0.21 | 0.23 | 0.33 | 0.35 | |
| | East FR | 0.28 | 0.28 | 0.37 | 0.33 | |

**Table 9.** Summary of the ratio reflecting the current state of exploitation in for all population connectivity structure (in the models considering three isolated sub-populations, various connectivity levels and a single population).

| Ratio | | Different connectivity | | | | One single population |
|---|---|---|---|---|---|---|
| | | 0% | 20% | 40% | 60% | |
| $F/F_{MSY}$ | West FR | 1.05 | 0.69 | 1.13 | 1.31 | 1.81 |
| | UK | 1.86 | 1.96 | 1.12 | 0.91 | |
| | East FR | 1.96 | 4.07 | 3.08 | 3.00 | |

## 3.2 Performance of the estimation method evaluated by the Simulation-Estimation approach

Previous results aforementioned shown that the level of connectivity that is best supported by the available data (no tag-recapture data available yet) should be about 20%. In the simulation-estimation method, pseudo tag-recapture data used to infer the dispersion were then simulated using an isotropic 20% connectivity level, meaning that each year, 10% of fish in any particular sub-population move to each of the two other sub-populations. Performance of the estimation method will be high if the posterior estimates of movement parameters are precisely estimated about 10% (about 80% for the diagonal terms in the matrix $T$). All posterior distributions of connectivity parameters which are presented below are graphically available as boxplot in the section Appendix (***Appendix X***). Uncertainty and relative bias for each scenario are also presented in the ***Appendix X***.

### 3.2.1. Inferences are sensitive to the number of tags released

Overall, results show that any of our three scenarios considering a high (S1a), realistic (S1b) or low number of tags (S1c) would allow us to estimate the movement parameters with rather low bias and uncertainty (***Fig. 12***). However, increasing, the number of tags would logically improve the estimation performance. Indeed, using a realistic (S1b) and high (S1b) number of tags produce much less bias and more precise estimates than using a low number of tags (S1c). When considering a high tag number, bias is estimated between -10.32 and 2.48% whereas bias fluctuates between – 44.7 and 49.76% when a low tag number is considered.

Because the parameters in one line of the connectivity matrix $T$ will always sum to one, estimates of those parameters are correlated. For instance, as shown in the ***Fig. 13*** for the parameters concerning movement from the West-FR sup-population, posterior estimates of the diagonal parameter (probability to stay in the West-FR sub-population) is negatively correlated with the probability to move to the UK sub-population.

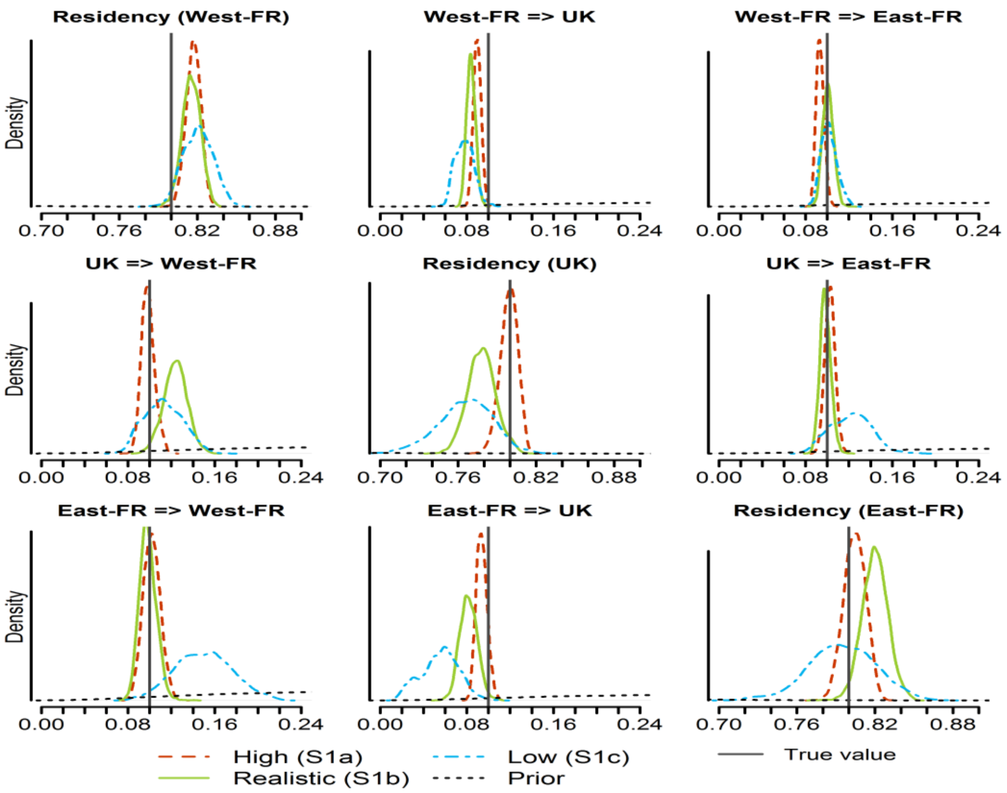

**Figure 12.** Marginal posterior distributions of connectivity parameters obtained for each tag number scenario (high, realistic, and low number of tags). The solid line represents the true value of the connectivity parameter (10% and 80% for diagonal parameters) used for simulating the tag-recapture data.

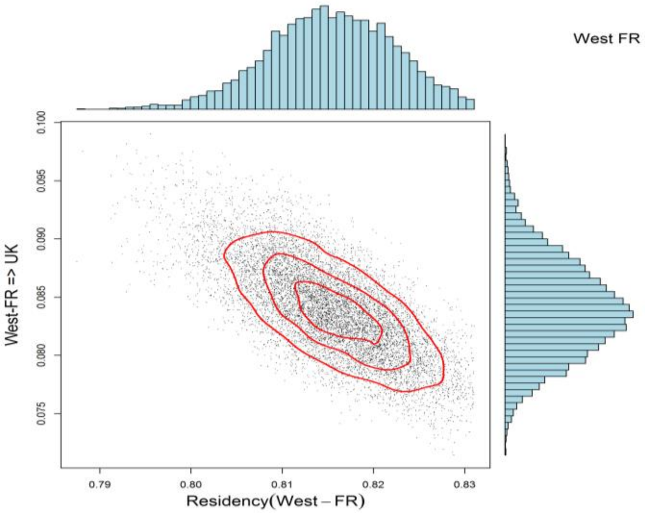

**Figure 13.** Joint posterior distributions of connectivity parameters drawn for the probability to stay in the West-FR region (Residency West-FR) and the probability to move from West-FR to the UK subpopulation (West-FR -> UK). The posterior distribution is obtained with the realistic tags number scenario (S1b).

The three scenarios were built using a range of tag number that remains consistent with what has been planned in the SMAC project. Because the contrast between our three scenarios is rather low, we complete the analysis by investigating the estimation performance with a much wide range of tags number, from 25 (very low number) to 600 (very high number) tags released during two years and in each sub-population. Because of the high computational time needed to run MCMC simulations in the integrated model, those additional scenarios were run with a non-integrated model that only considers the population dynamics of tagged fish. As for other scenarios, tag-recapture data were also simulated with 20% connectivity and with values of $F$ fixed to their median posterior estimates.

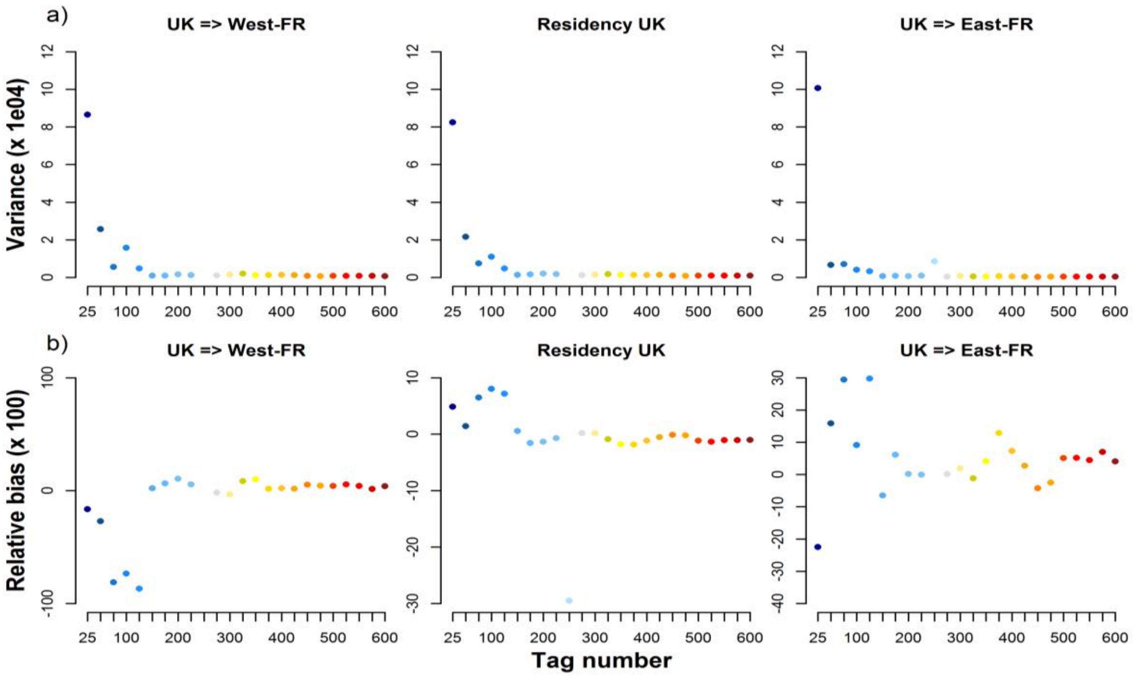

**Figure 14.** Sensitivity of the estimation procedure to the tag number: analysis of (a) the variance and (b) the relative bias obtained by increasing the tag number in the case of a movement from the UK subpopulation towards both the West-FR (UK  West-FR) and East-FR (Uk -> East-FR) subpopulations.

Results show a higher contrast in the estimation performance. Relative bias and uncertainty in posterior estimates are very high when the number of tags released is lower than 150 (***Fig. 14*** and see ***Appendix X*** for all parameters). Interestingly, the variance and bias in posterior estimates quickly decline for a number of tags released greater than 150 to reach a “plateau” after 200 tags released.

### 3.2.2. Sensitivity to the declaration rate

- **Inferences are sensitive to the value of the declaration rate**

We first assess the consequences of a lower tag-recapture declaration rate on the performance of the estimation method by comparing the baseline scenario (declaration rate fixed to $\beta = 0.90$ in both the simulation and the estimation procedure) with scenario S2a1 that use a lower declaration rate $\beta = 0.45$.

In the scenario S2a1, tag-recapture dataset was simulated with a declaration rate fixed to $\beta = 0.45$ and the true value of $\beta = 0.45$ was also considered in the Bayesian estimation procedure. Logically, scenario S2a1 results in lower number of tag returns, and then in a lower informative tag-recapture dataset (***Fig. 15***). As a consequence, estimates of movement parameters in S2a1 are more uncertain than in the baseline scenario. However, decreasing the quantity of information brought by the mark-recapture dataset does not increase the relative bias compared to the baseline scenario.

By contrast, introducing a misspecification in the value of the declaration rate between the reality (data simulation) and the estimation procedure drastically increases bias in posterior estimates. In scenario S2a2, data were simulated with a declaration rate fixed to $\beta = 0.45$, but the estimation procedure has been performed with a declaration rate fixed to $\beta = 0.90$ (i.e. with a declaration rate that was believed greater than it was in the reality.

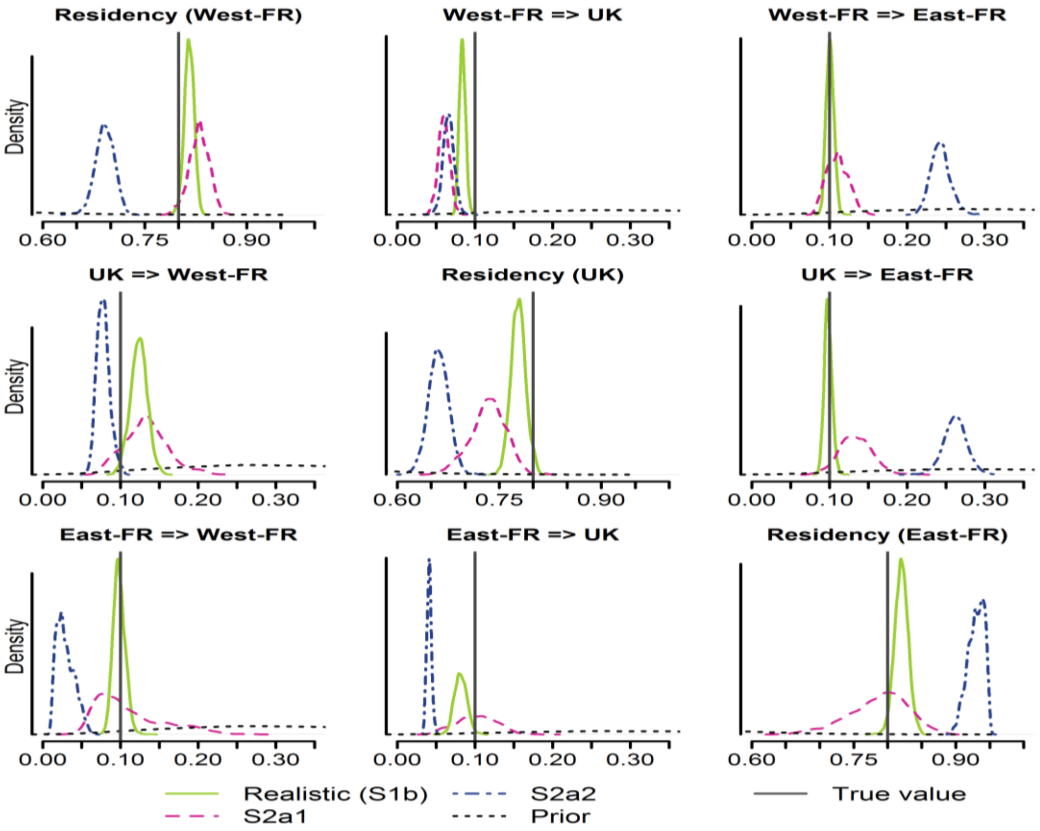

**Figure 15.** Marginal posterior distributions of connectivity parameters obtained with the baseline realistic scenario (S1b), the scenario considering a declaration rate fixed to β=0.45 for both the simulation and estimation procedures (S2a1), and the scenario considering a declaration rate fixed to β=0.45 for simulation and fixed to β=0.90 in the estimation procedure (S2a2). The solid line represents the true value of connectivity parameters (10% and 80% of residency).

In a simple case, interpreting the tag-recapture data by assuming a higher recapture declaration rate than in reality would lead to negatively bias connectivity parameters (positively bias residency parameter), as low number of tag recaptured and declared would be falsely interpreted as low movement tag. However, in our case study, the number of fish available in the tag-recapture dataset depends upon both the recapture rate $F$ and the declaration rate ($\beta$), and $F$ is highly heterogeneous among sub-populations. This certainly creates complex interactions in the estimation procedure, resulting in either positive or negative bias in connectivity parameter estimates.

Finally, our results emphasize that introducing a mis-specification in the value of the declaration rate leads to a significant bias in connectivity parameter estimates. As previously see in the first part of our results, change in movement parameters highly impacts populations dynamics parameter estimates ($SSB$, $F$ and $R$) and then inevitably, change the stock assessment.

### ○ Inferences are sensitive to a spatial mis-specification of the declaration rate

We firstly assess the consequences of a spatial mis-specification in the value of the declaration rate between reality and the Bayesian estimation procedure by comparing the baseline realistic scenario (declaration rate fixed to $\beta = 0.90$ for all sub-populations in both the simulation and estimation) with the scenario S2b1 where the data were simulated with lower declaration rate in the UK sub-population ($\beta = 0.45$) (but the declaration rate is still considered high ($\beta = 0.90$) and homogeneous in space in the estimation procedure).

The mis-specification introduced in the value of the declaration rate of the UK sub-population also generates bias in posterior estimates of connectivity parameters. Because the declaration rate has been fixed to $\beta = 0.90$ in the Bayesian estimation procedure, the low recapture of tags is falsely interpreted as low movements towards the UK sub-population, thus explaining the negative bias observed for connectivity parameters West-FR → UK (bias = -44%) and East-FR → UK (bias = -22%). Because the parameters in one line of the matrix $T$ must be summed to one, negative bias in some parameter estimates induce a positive bias for others. For instance, negative bias in connectivity parameters West-FR → UK and East-FR → UK are balanced by positive bias in residency parameters of those two sub-populations and also by a positive bias of connectivity parameters between those two sub-populations (***Fig. 16***). Uncertainty in posterior estimates is substantially the same as those observed in the baseline realistic scenario (S1b).

Considering a spatial mis-specification of the tag recapture declaration rate in both the West-FR and the UK sub-populations increases again the bias and uncertainty in parameters estimates compared to the baseline realistic scenarios (S1b) (***Fig.16***). Uncertainty in posterior estimates is particularly high for parameter estimates of residency (for all cases of residency) and connectivity parameters towards the West-FR sub-population.

Again, considering higher declaration rate in both West-FR and UK sub-populations in estimation procedure (higher than it is in reality) would logically lead to a negative bias in all movement parameters towards those sub-populations. However, as already pointed out in section (1, scenario S2a2) because of complex interactions between estimates of all sub-populations, and because of constraints in the matrix $T$, a complex balance occurs in bias of all parameter estimates (***Fig.16***).

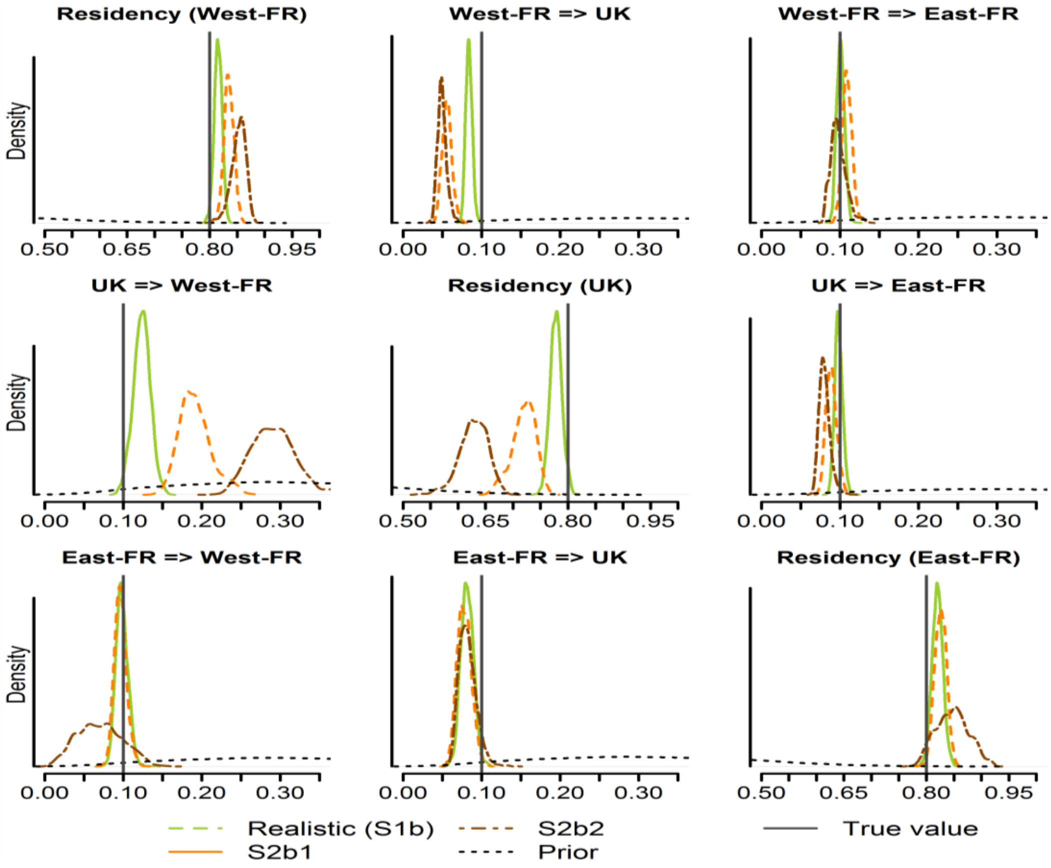

**Figure 16.** Marginal posterior distributions of movement parameters obtained with the baseline scenario (denoted Realistic), the scenario considering a declaration rate fixed to β=0.45 for the UK sub-population in simulation (denoted S2b1), and the scenario considering a declaration rate fixed to $\boldsymbol{\beta} = \mathbf{0.45}$ in simulation for the both West-FR and UK sub-populations denoted S2b2). For all these scenarios estimation procedure was performed with a declaration rate fixed to $\boldsymbol{\beta} = \mathbf{0.90}$ for all sub-populations. The solid line represents the true value of connectivity (i.e. the value at which tagging datasets have been simulated).

Finally, complex interactions between of all sub-populations occur when a spatial mis-specification of the tag recapture declaration is made. Again, this scenario points out the fact that more the declaration rate is spatially unknown more both the bias and uncertainty in parameter estimates are significant.

### Using an informative prior on the declaration rate is workable

Overall, results show that the use of an informative prior on the declaration rate (i.e. without fixing it to $\beta = 0.90$ in the Bayesian estimation procedure) instead of fixing the value in the estimation procedure can also allow us to estimate connectivity parameters with rather low bias and uncertainty.

Bias in estimates of the declaration rate is rather low when using an informative prior with a medium uncertainty about the mean (Scenario S2c1) or using a less informative prior with higher uncertainty about the mean in the Bayesian estimation procedure (***Fig. 17***). Logically, a higher bias in posterior estimates of the declaration rate is obtained in the scenario (S2c2) where an informative prior with higher uncertainty about the mean is set in the estimation procedure. In this case bias varies between 1.1 and 6.1% among sub-populations, whereas bias was estimated between 1.6 and 3.4% with a more informative prior (***Appendix X – Table A 5***).

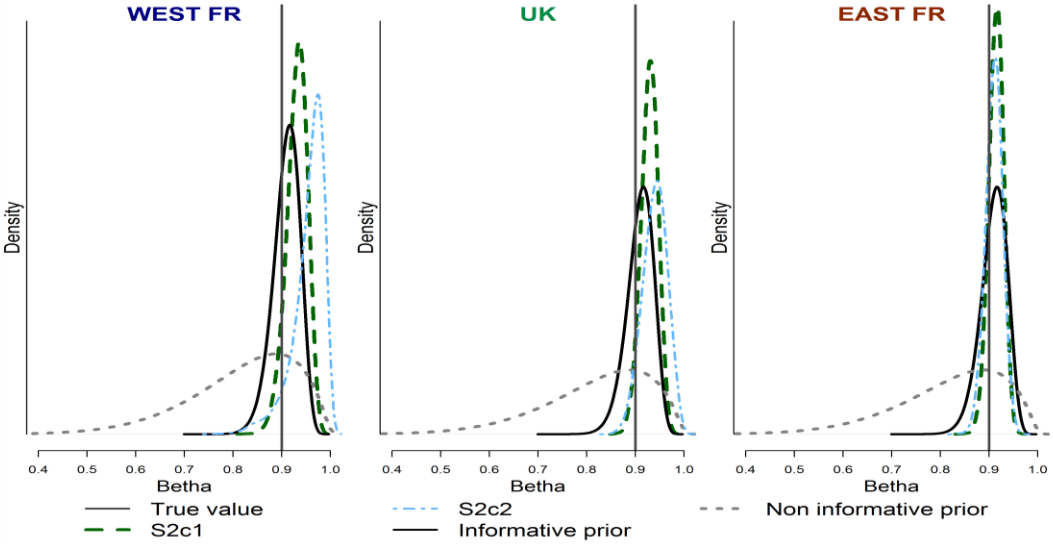

**Figure 17.** Marginal posterior distribution of the declaration rate obtained from models considering an informative prior with medium variability around the true value (S2c1) and an informative prior with higher variability around the true value (S2c2). The solid line represents the true value used for simulating the tag-recapture data.

Interestingly, using an informative prior for the declaration rate instead of a fixed value do not increase bias in posterior estimates of connectivity parameters. The two scenarios (S2c1 & S2c2) allow estimation of connectivity parameters with similar bias and uncertainty as estimates from baseline realistic scenario (S1b) (***Figure 18***). When considering an informative prior with medium variability, bias is estimated between -15.24 and 25.3%. In the case where an informative prior with higher variability is set in the estimation procedure, bias in estimates fluctuates between -15.2 and 29.9%. We recall that bias in estimates, when a realistic scenario is considered, is estimated between -18.36 and 23.66%.

Finally, this scenario is greatly encouraging for the SMAC project. It points out the fact that even if the value of the declaration rate is unknown, the tag-integrated model allows both the estimation of the declaration rate and the connectivity parameters with rather low bias and uncertainty. Therefore, using an informative prior on the declaration rate in the Bayesian estimation procedure is much less risky than fixed it.

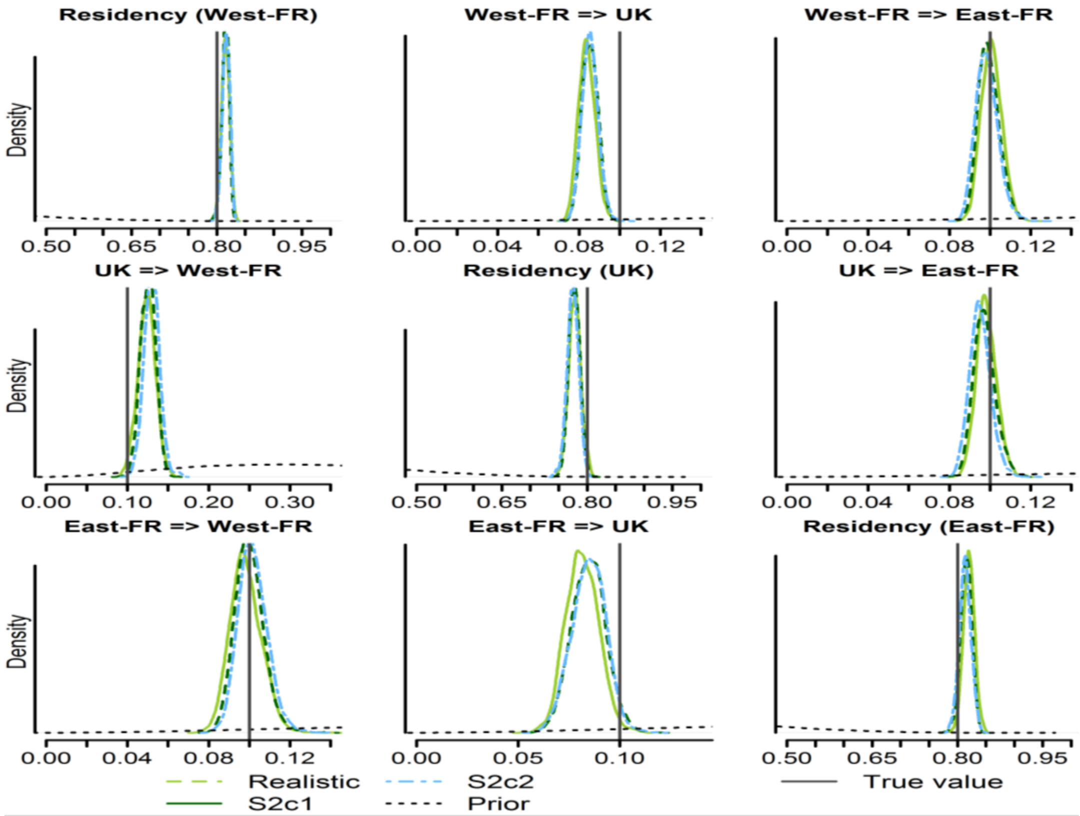

**Figure 18.** Marginal posterior distribution of connectivity parameters obtained from the two scenarios introducing an informative prior on the declaration rate with a medium variability (S2c1) and a higher variability (S2c2). The solid line represents the true value used for simulating the tag-recapture data.

### 3.2.3. Ability to estimate natural mortality

In previous version of the model developed by Archambault et al. (2016), the maximal natural mortality is considered known and fixed to 2.6 year$^{-1}$. The scenario S3 allows us to analyze the ability of the tag-integrated model to estimate natural mortality. In this scenario, tag-recapture dataset is simulated using the realistic baseline scenario, and with a declaration rate fixed to $\boldsymbol{\beta} = \mathbf{0.90}$ for the both simulation and Bayesian estimation procedure. The natural mortality is modelled in the Bayesian estimation procedure on the basis of Archambault et al. (2016) using a weighting function, the maximal natural mortality being estimated from the data (***Fig. 19***).

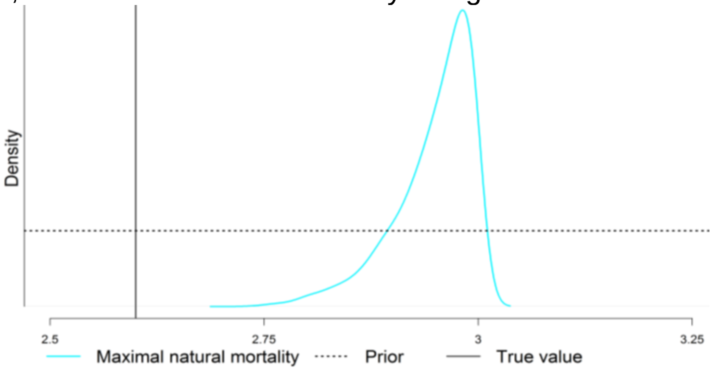

**Figure 19.** Marginal posterior distribution of the Maximal natural mortality obtained with the model considering the realistic baseline scenario with a weighting function for the natural mortality.

Results show that data provide information to estimate the natural mortality. Indeed, natural mortality can be estimated with uncertainty and bias but which remain relatively low with respect to the prior distribution set in the Bayesian estimation procedure (Uniform distribution bounded between 0 and 3). The maximal natural mortality is estimated with a bias of 13.4%

and presents a median around 2.96. Interestingly again, simultaneously estimating the natural mortality and movement parameters do not increase bias in parameters estimates of connectivity parameters (***Figure 20***). Simulations show that using mark-recapture data open the perspective to simultaneously estimate movement parameters and natural mortality. That gives the possibility to incorporate more flexibility around the natural mortality in stock assessment. Furthermore, thanks to the Bayesian modelling framework, this perspective would allow to let speak the data about this quantity which in most of the cases is fixed despite the uncertainty around its value.

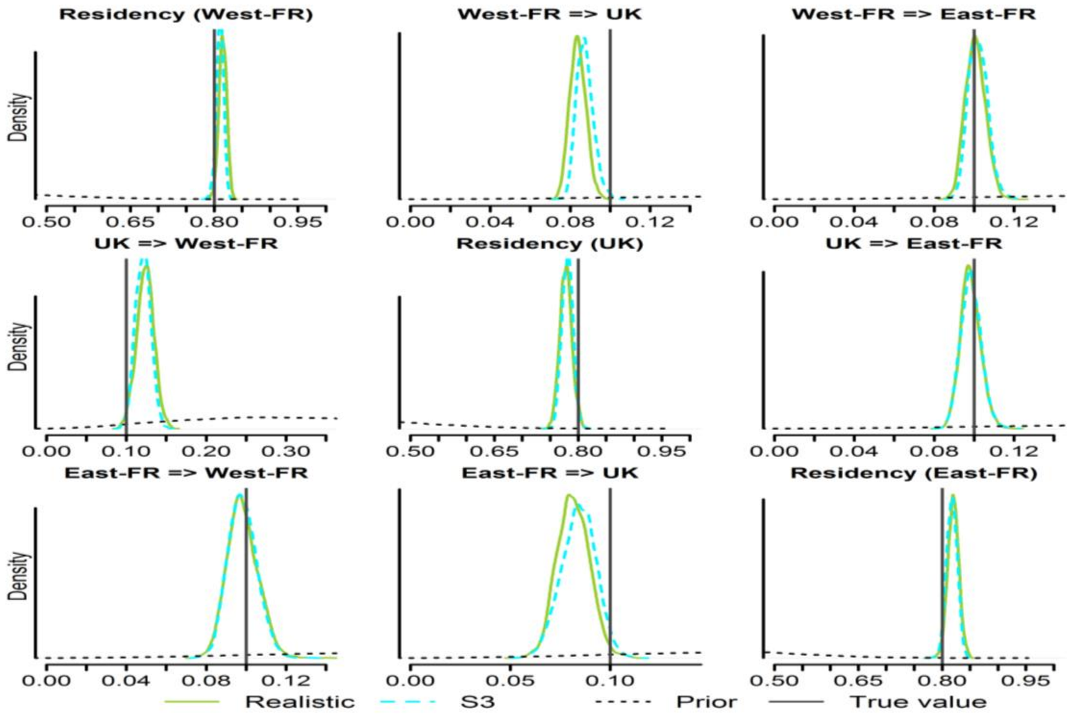

**Figure 20.** Marginal posterior distribution of connectivity parameters obtained from the model considering the realistic baseline scenario to evaluate the ability to estimates the natural mortality.

# 4 Discussion

## 4.1. Contributions of our modelling approach

Although the need to include spatial dimension in fish stock assessment has received considerable attention, still only few stock assessment models and subsequent management decisions explicitly consider spatial structure of marine populations (Goethel et al., 2011; Quinn and Deriso, 1999). One of the main reasons is the paucity of data available to reliably parameterize connectivity between subpopulations. However, as many studies (Hulson et al., 2011; Goethel et al., 2014; Goethel et al., 2015), our results show that a misspecification of adult movements can result in biased estimates of key parameters of the dynamics and abundances of local subpopulations, what may finally result in a misalignment between local stock productivity and stock assessment and management decisions (Frank and Brickman, 2000; Frisk et al., 2014; Goethel et al., 2014).

The tag-integrated modelling framework developed in this study is a substantial methodological contribution that paves the way towards a better understanding and a better management of the Sole population in the Eastern Channel. Based on the hierarchical life cycle model developed in Archambault et al. (2016), we brought two substantial contributions. First we introduced the possibility to parameterize the connectivity between the three subpopulations. Second, we developed the tag-integrated modelling framework that would allow to assimilate capture-mark-recapture data to infer connectivity parameters.

### 4.1.1) Parameterizing movement of fish (>3) among the three subpopulations within the life cycle model

First, our population dynamics model brought a substantial contribution to the models already developed in Archambault et al. (2016). Indeed, those authors developed and compare inferences obtained under two alternative population structures, one that considers a single homogeneous population in the EC, and an other one considering three isolated subpopulations, but with no possibility to explore continuity between those two contrasted structures. In our model, movements of fish older than age -3 between the three subpopulations are introduced in the form of a matrix of connectivity parameters that allow to explore any movement configurations between those two extremes.

Results show that inferences on key population dynamics parameters are highly sensitive to the assumptions made on the connectivity. In particular, estimates of the productivity parameters of each nursery sectors and their relative contribution to the total recruitment are highly sensitive to the connectivity level among the three subpopulations. This sensitivity is also found in posterior estimate of the recruitment, the Stock Spawning Biomass and the fishing mortality which drive the stock assessment and finally management decisions. A key result, as the recruitment at the scale of the EC is currently estimated from the survey in the Somme estuary, is the Somme nursery sector which sees his contribution to the total recruitment moving from 48% (when considering three isolated subpopulations) to 28% (when considering a connectivity level of 60%). This decrease is largely followed by a large decrease in both recruitment and SSB of the East-FR subpopulation.

Overall, those results show that an accurate estimation of movement parameters is essential for a good understanding of the population dynamics and proper stock assessment and management of the Sole population in the EC.

Also, an other key result is that even when no tagging data are introduced in the model, Bayesian model selection criteria ($AICM$) indicate that a connectivity level of 20% appears as the most consistent with the data (except any tagging data). This result is consistent with the body of ecological knowledge which indicates a low but non null connectivity level among the three subpopulations. Interestingly, it is also consistent with rough estimates of movements of fish obtained from the CEFAS tagging data base reported in Burt and Milner (2008). Those values of connectivity are also consistent with estimates for others stocks. Ulrich et al., (2012) emphasized a high level of residency in the case of the plaice stock complex between the North Sea and the Baltic Sea.

Finally, according our results on the connectivity level for the Sole population in the EC, management reference points appear to be different to the current diagnostic established by ICES. Considering 20% of connectivity among the three subpopulations, reference points $SSB_{MSY}$, $C_{MSY}$, were estimated at 20,086t, 4,870t. Estimates of $F_{MSY}$ depend upon subpopulations and where estimated at 0.29, 0.23, and 0.28 for the West-FR, the UK and the East-FR subpopulation, respectively.

### 4.1.2) Developing the foundations for the tag-integrated stock assessment model

Second, the tag-integrated model developed in this work provides the foundations of the modelling framework allowing to embed tag-recapture data into an integrated hierarchical life cycle model to infer connectivity of the Sole population in the Eastern Channel.

One of the main objectives of the study was to provide first guidance to the tag-recapture protocol that will be carried out during the SMAC project. SMAC planned a main tagging campaign with professionals during winter, including two working days per year and per subpopulations and which will be done over spawning grounds. A second type trip, more opportunistic, will be carried out during scientific surveys (UKBTS, NOURSOM, COMOR). Finally, this scenario therefore include 6 days per year for around 300 fish tagged per subpopulation and per year, which corresponds to a total of 3,600 fish tagged throughout 2016 and 2017.

### a) A sufficient number of tags must be released

Our Simulation-Estimation approach clearly emphasized that one of the main limit of tag-recapture data is the need to get sufficient number of tags recovered (and declared) to be able to derive accurate inferences on fish movements (Hulson et al., 2011).

Provided that the hypotheses on the spatial structure in three subpopulations are exact, and provided that the hypotheses on movement model are correct (parameters, e.g. box transfer model with parameters constant over time and space), our results show that the tagging experiments which will be undertaken during the SMAC project should provide enough information (through tagging data), in both quality and quantity, to infer connectivity parameters among the three subpopulations in the EC. Our baseline realistic scenario has been established on the basis of the tagging design which has been planned in the SMAC project (the same number of both fish tagged and tagging years (two years at minimum)).

Thanks to the integrated modelling approach, fishery mortality can be estimated, and tag-recapture rate of 17%, 22%, and 26% for the West-FR, the UK, and the East-FR subpopulations, respectively, can be expected the first year after tagging. The average recapture rate is drastically decreasing the second and third years (11%, 16%, and 18% for the the West-FR, the UK, and the East-FR subpopulations, respectively), and is expected to be only residual after three years.

Under the optimistic hypothesis of a high tag-declaration rate, expected to be high (90%) and homogeneous among subpopulations (90% in our baseline scenario), the average tag-return rate would be around 19.5% and 13.5% for the first and second year, respectively.

In this configuration, results show that connectivity parameters were estimated with rather low bias and uncertainty. An additional analysis pointed out the non-linear decrease of bias and uncertainty of parameters estimates when the number of tags released increases. Indeed, bias and uncertainty in posterior estimates drastically increase when the number of tag released falls below 150-200.

Therefore, given the additional uncertainty about the declaration rate, the first recommendation for the tagging protocol is to maintain a minimum number of 300 tags released in each subpopulation. Following Hulson et al. (2011), we also recommend to release an equal number of tags in all subpopulations to minimize bias and uncertainty in parameters estimates.

### b) Quality of inferences would be drastically penalized by low or misspecified tag-recapture declaration rate

Results also emphasized the importance of the tag-recapture declaration rate from the commercial fishery. Indeed, the baseline scenario was conducted under the very optimistic hypothesis that the tag-recapture declaration rate is known, spatially homogeneous and fixed when analyzing tag-recapture data, what probably not be possible in the true life.

Our analysis about the tag-recapture declaration rate emphasized the key importance of a good knowledge of the tag-recapture declaration to ensure precise and reliable inferences. Our results show that an overestimation of the tag-recapture declaration rate (but no misspecification in the spatial homogeneity of the declaration rate) drastically increases uncertainty of posterior estimates, but do not impact average relative bias. However a misspecification of the declaration rate (e.g. by considering the declaration rate as spatially homogeneous when it is heterogeneous in the “reality”) would drastically increases bias in posterior estimates of connectivity parameters. Because estimates of key population dynamics parameters are highly sensitive to the connectivity level, any bias in connectivity parameters would diffuse within the model and would drastically impact all inferences on key population parameters, stock productivity and stock assessment. Therefore, this spatial misspecification in the tag-recapture declaration rate leads to a bas interpretation of the population dynamics and the to a stock assessment leading to over/under exploitation of the stock.

For instance, when a spatial misspecification occurred in both the UK and the West-FR subpopulations, movements towards the UK subpopulation were highly negatively biased (($\sim -21\%$, which corresponds to a relative bias of $100\%$). The connectivity was consequently estimated to 40% instead of 20% (i.e. 60% of residency instead of 80%). As a consequence, the ratio $F/F_{MSY}$ was highly impacted (from 1.96 for a connectivity level of 20% to 1.12 for a connectivity level of 40%). Thus, such an estimation would lead to an over exploitation of this subpopulation due to maintaining the same fishery mortality rate instead of to decrease it.

Our results then emphasized the importance of a careful consideration of the hypotheses made on the tag-recapture declaration rate when analyzing tag-recapture data. Because the tag-recapture declaration rate is difficult to estimate and would remain essentially unknown, we formulate three recommendations.

First, the tag-recapture declaration should be maximized. Communication about the project towards fishermen should be enhanced. Some mark-recapture protocol use the high-reward tagging method to maximize tag-recapture declaration (Pollock et al., 2002, 2001). In the SMAC project, some kind of reward protocol could be organized through a lottery with some gift (T-shirt …) to be randomly distributed to fisherman that reported tags to the project.

Second, instead of fixing the tag-recapture reporting declaration rate (and hence of keeping the risk to introduce strong misspecification between the fixed and the true value), we recommend to use an informative prior on the recapture rate, and that all available information should be used to provide best guest informative prior for the declaration rate.
The Bayesian framework developed in this work provided the flexibility to incorporate knowledge about the tag-recapture declaration rate through the use of an informative prior with a higher/medium variability around the mean of this tag recapture declaration rate (i.e. without fixing the recapture rate in the Bayesian estimation procedure) while estimating population dynamics parameters and connectivity parameters. Results show that provided that the informative prior embeds the true value of the declaration rate, movements were estimated with rather low bias and uncertainty. This particularity of the Bayesian modelling framework is greatly encouraging for the SMAC project. Some data are available that would allow a better specification of the declaration rate. In particular, the current parameterization of this informative prior allows to incorporate a subpopulation-specific prior in the case where spatial knowledge about the tag-recapture declaration rate would be available. In particular, Burt and Milner (2008) emphasized a spatial heterogeneity of the declaration rate among the three subpopulations.

## 4.2. Towards a multimarker approach for an holistic understanding of the connectivity along the life cycle

Our tag-integrated model is to be considered as a first contribution towards an holistic understanding of the spatially structured life cycle of the common sole in the EC. But the model suffers from several limits and gaps in the knowledge, some of which could be addressed within the SMAC project, other being to be considered as food for through for further research projects.

### 4.2.1) A need to improve knowledge on dispersion and mortality of eggs and larvae

As already detailed in Rochette et al. (2013) or Archambault et al. (2016), our model already assimilates a large body of knowledge on the spatial distribution of the early life stages of the Sole population in the EC. Eggs and larvae stages are described by a larval-drift model with a high control from hydro-climate conditions implying a specific larval transport and larval support towards specific nursery grounds (Rochette et al., 2012). However, outputs from this model used in our work only cover the period between 1982 and 2007. Therefore an updating of those outputs for the entire time series would contribute to improve our understanding of both the way and the variability with which these stages undergo natural mortality and hydroclimate conditions. Also additional surveys of the spatio-temporal dynamics of the migration of larvae to the coast are planned in the SMAC project that should provide useful information to this critical part of the life cycle.

### 4.2.2) How do juvenile spread when they leave coastal nursery?

The transition from coastal nursery sectors to offshore habitats is key in the life cycle. Following Rochette et al. (2013) and Archambault et al. (2016), our model assumes that fish leave nursery grounds to reach offshore habitats at age -2 (Riou et al., 2001), and assumes that fish leaving nursery ground directly contribute to the adjacent subpopulation (Veys and Seine for the West-FR subpopulation, UK West and Rye for the UK subpopulation, and Somme for the East-FR subpopulation). Under this hypothesis, differences in productivity of nurseries (emphasized in Archambault et al., 2016; and also highlighted in our results) lead to a heterogeneous supply of the three subpopulations which then could induce heterogeneity in abundances at ages -3 and after.

Furthermore, the temporal seasonality of such movement has also to be investigated. Differences between nurseries could lead to specific temporal pattern in supply for each subpopulation. Therefore, considering that fishes leave nursery grounds at the same time over the EC and undergo fishing mortality over an entire year could lead to a mis-interpretation of the renewal dynamics of each subpopulation. Collecting data that would allow to infer movements from nurseries to offshore habitats is a priority to improve our understanding of this phase in the life cycle.

Within this perspective, one of the key research axis in the SMAC project will consists in using otolith microchemistry to identify origin, movements and finally to help discriminate some spatial units (Merigot et al., 2007: Cuveliers et al., 2010).

Tagging experiments carried out on juveniles (age 2) during beam trawl survey on nursery sectors will also be used as a complementary source of data to estimate connectivity parameters. Ultimately, those data could be assimilated within the integrated life cycle model to infer parameters of a connectivity matrix at the age -2, from nurseries to subpopulations. Information from otolith microchemistry could be first analyzed as ancillary data through “assignment models” and then plugged in the model as prior information.

### 4.2.3) Is the growth of juveniles different among nurseries?

Some data (not shown in this report) suggest that growth could be different among the three subpopulations (data Ifremer Boulogne). A question remains whether heterogeneity in growth of juveniles already exists during the juvenile phase on nursery sectors, or if growth differences appear latter in the life cycle. Then, investigating the heterogeneity of growth among nurseries would help to discriminate among subpopulations if any. Otolith gathered on juveniles within nurseries, supplemented by measure of the size of fish would help to the understanding of the spatial heterogeneity in growth.

### 4.2.4) A deeper investigation of the role of adult mediated connectivity

As established through our work and in Archambault et al. (2016), adult stages may have a significant role in structuring the sole population. A better understanding and modelling of the movements in both time and space is needed for more realistic model.

#### a) *Do the three subpopulations in the Eastern Channel represent an appropriate spatial scale?*

Our model currently considers movements among the three sole subpopulations in the EC as defined in Archambault et al. (2016). This choice of spatial scale to represent and to investigate connectivity and metapopulation dynamics must be questioned.

First, the model as currently proposed can only investigate movements from one subpopulation to another, without any possibility to integrate movements of smaller magnitude. Moving toward a more continuous representation of space could represent an interesting modelling perspective.

Second, the strong hypothesis is made that no movement occur between the EC and the adjacent areas like Western Channel or North Sea. However, some exchanges between the EC and adjacent ICES divisions (the Western Channel and the North Sea) have been identified (Burt and Milner, 2008). In their report, Burt and Milner highlighted that 71% of sole show a residency pattern within the EC but also that a significant number of sole tagged in the Eastern Channel were recaptured into the neighboring ICES divisions (IV and VIIe) and vice versa. Those movements can ecologically impact the sole population in EC by impacting abundance and genetic structure. In the case if those movements are really significant, the spawning stock biomass of each subpopulation can be altered, thus resulting in a strong impact on productivity and on stock assessment. During the SMAC project, some fish tagged in the EC are expected to be recapture outside the EC (and hopefully reported). Also, tag-recapture data available from the CEFAS (Burt and Milner, 2008) would provide a valuable source of information to infer movement at a broader spatial scale, including Western Channel and North Sea.

#### b) *A seasonal pattern of migrations?*

One of the strength of tagging experiments is the possibility to get information through the entire year (per month, or per day). Data available from the SMAC project are unlikely to provide enough information to precisely investigate the seasonality of migrations. Indeed, tagging will mainly be concentrated during a few days in the winter period, and recapture will depend upon the seasonality of the fishery. However, some recaptures are expected to be reported all along the year and may provide some exploitable information about the seasonality of migrations. Importantly, data already available from the CEFAS data base (Burt and Milner, 2008) could complement data from the SMAC project. Preliminary exploration of the CEFAS data base suggests a seasonality pattern with most of movements which occur during winter and autumn.

However, further model developments are needed to integrate such seasonality. Indeed, our model currently assumes an age-structured yearly time step such as most of tag-integrated models in order to match with stock assessment models used by ICES. As suggested by Burt and Millner (2008), most recapture of tags are expected to occur after a time at liberty < 1 year with around 20% of tagged fish recaptured in the next 90 days after release. A first model improvement could be to develop a model based on a quarter (4 months) time step in order to better account for all available data and to better inform this kind of seasonality.

# 5 Bibliography

Archambault, B., Le Pape, O., Baulier, L., Vermard, Y., Véron, M., Rivot, E., 2016. Adult-mediated connectivity affects inferences on population dynamics and stock assessment of nursery-dependent fish populations. Fish. Res. 198–213. doi:10.1016/j.fishres.2016.03.023

Ashford, J.R., Jones, C.M., Hofmann, E.E., Everson, I., Moreno, C.A., Duhamel, G., Williams, R., 2008. Otolith chemistry indicates population structuring by the Antarctic Circumpolar Current. Can. J. Fish. Aquat. Sci. 65, 135–146. doi:10.1139/f07-158

Bakun, A., 1996. Patterns in the ocean: ocean processes and marine population dynamics — University of Miami’s Research Profiles 382–384.

Begg, G.A., Friedland, K.D., Pearce, J.B., 1999. Stock identification and its role in stock assessment and fisheries management: an overview. Fish. Res. 43, 1–8. doi:10.1016/S0165-7836(99)00062-4

Buckland, S.T., Newman, K.B., Fernández, C., Thomas, L., Harwood, J., 2007. Embedding Population Dynamics Models in Inference. Stat. Sci. 22, 44–58. doi:10.1214/088342306000000673

Burt, G.J., Millner, R.S., 2008. Movement of sole in the southern North Sea and eastern Channel from tagging studies (1955-2004) (Sci.Ser.Tech.Rep. No. 44).

Campana, S.., Chouinard, G.., Hanson, J.., Fréchet, A., Brattey, J., 2000. Otolith elemental fingerprints as biological tracers of fish stocks. Fish. Res. 46, 343–357. doi:10.1016/S0165-7836(00)00158-2

Cooper, A.B., Mangel, M., 1999. The dangers of ignoring metapopulation. Fish. Bull. 97, 213–226.

Cunningham, C.L., Reid, D., McAllister, M., Kirkwood, G., Darby, C., 2007. A Bayesian state-space model for mixed-stock migrations, with application to Northeast Atlantic mackerel *Scomber scombrus*. Afr. J. Mar. Sci. 29, 347–367. doi:10.2989/AJMS.2007.29.3.4.334

Fässler, S.M.M., Payne, M.R., Brunel, T., Dickey-Collas, M., 2011. Does larval mortality influence population dynamics? An analysis of North Sea herring (Clupea harengus) time series: North Sea herring larval mortality. Fish. Oceanogr. 20, 530–543. doi:10.1111/j.1365-2419.2011.00600.x

Frank, K.T., Brickman, D., 2000. Allee effects and compensatory population dynamics within a stock complex. Can. J. Fish. Aquat. Sci. 57(3), 513–517.

Frisk, M.G., Jordaan, A., Miller, T.J., 2014. Moving beyond the current paradigm in marine population connectivity: are adults the missing link? Fish Fish. 15, 242–254. doi:10.1111/faf.12014

Gallego, A., North, E.W., Houde, E.D., 2012. Understanding and quantifying mortality in pelagic, early life stages of marine organisms — Old challenges and new perspectives. J. Mar. Syst. 93, 1–3. doi:10.1016/j.jmarsys.2011.10.012

Gelman, A., Carlin, J.B., Stern, H.S., Rubin, D.B., 2004. Bayesian Data Analysis. Chapman &

Hall/CRC, Boca Raton, London, New York (717 pp).

Goethel, D.R., Legault, C.M., Cadrin, S.X., 2014. Testing the performance of a spatially explicit tag-integrated stock assessment model of yellowtail flounder (Limanda ferruginea) through simulation analysis. Can. J. Fish. Aquat. Sci. 72, 582–601. doi:10.1139/cjfas-2014-0244

Goethel, D.R., Quinn, T.J., Cadrin, S.X., 2011. Incorporating spatial structure in stock assessment: Movement modeling in marine fish population dynamics. Rev. Fish. Sci. 19, 119–136. doi:10.1080/10641262.2011.557451

Grimm, V., Reise, K., Strasser, M., 2003. Marine metapopulations: a useful concept? Helgol. Mar. Res. 56, 222–228.

Grosberg, R.K., Levitan, D.R., 1992. For adults only? Supply-side ecology and the history of larval biology. Trends Ecol. Evol. 7, 130–133.

Halpern, B.S., Walbridge, S., Selkoe, K.A., Kappel, C.V., Micheli, F., D'Agrosa, C., Bruno, J.F., Casey, K.S., Ebert, C., Fox, H.E., Fujita, R., Heinemann, D., Lenihan, H.S., Madin, E.M.P., Perry, M.T., Selig, E.R., Spalding, M., Steneck, R., Watson, R., 2008. A Global Map of Human Impact on Marine Ecosystems. Science 319, 948–952. doi:10.1126/science.1149345

Hart, D.., Cadrin, S.X., 2004. Yellowtail flounder (Limanda ferruginea) off the Northeastern United States: Implications of movement among stocks, in: Applications in RAMAS (Resit Akc¸akaya, H. et Al., Eds.). New York: Oxford University Press, pp. 230–243.

Hastings, A., Harrison, S., 1994. Metapopulation Dynamics and Genetics. Annu. Rev. Ecol. Syst. 25, 167–188. doi:10.1146/annurev.es.25.110194.001123

Hilborn, R., 1990. Determination of fish movement patterns from tag recoveries using maximum likelihood estimators. Can. J. Fish. Aquat. Sci. 47, 635–643.

Hilborn, R., Liermann, M., 1998. Standing on the shoulders of giants: learning from experience in fisheries. Rev Fish Biol Fish 273–283.

Hilborn, R., Mangel, M., 1997. The ecological detective confronting models with data. Princeton University Press, Princeton, N.J.

Hinrichsen, H.-H., Dickey-Collas, M., Huret, M., Peck, M.A., Vikebo, F.B., 2011. Evaluating the suitability of coupled biophysical models for fishery management. ICES J. Mar. Sci. 68, 1478–1487. doi:10.1093/icesjms/fsr056

Hoenig, J.M., Barrowman, N.J., Pollock, K.H., Brooks, E.N., Hearn, W.S., Polacheck, T., 1998. Models for tagging data that allow for incomplete mixing of newly tagged animals. Can. J. Fish. Aquat. Sci. 55, 1477–1483.

Hulson, P.-J.F., Miller, S.E., Ianelli, J.N., Quinn, T.J., 2011. Including mark–recapture data into a spatial age-structured model: walleye pollock (Theragra chalcogramma) in the eastern Bering Sea. Can. J. Fish. Aquat. Sci. 68, 1625–1634. doi:10.1139/f2011-060

Hutchings, J.A., 2000. Collapse and recovery of marine fishes. Nature 406, 882–885. doi:10.1038/35022565

ICES. 2015. Report of the Working Group on the Assessment of Demersal Stocks in the

North Sea and Skagerrak (WGNSSK), 28 April-7 May, ICES HQ, Copenhagen, Denmark. ICES CM 2015/ACOM:13. 1229 pp.

ICES. 2015. Report of the Working Group on Mixed Ficheries Advice (WGMIXFISH-ADVICE), 25-29 May, ICES HQ, Copenhagen, Denmark. ICES CM 2015/ACOM:21. 171 pp

Jackson, J.B.C., 2001. Historical Overfishing and the Recent Collapse of Coastal Ecosystems. Science 293, 629–637. doi:10.1126/science.1059199

King, R., Morgan, B., Gimenez, O., Brooks, S., 2010. Bayesian Analysis for population Ecology., Chapman & Hall/CRC. ed.

Kritzer, J.P., Sale, P.F., 2004. Metapopulation ecology in the sea: from Levins' model to marine ecology and fisheries science. Fish Fish. 5, 131–140.

Le Pape, O., Chauvet, F., Mahévas, S., Lazure, P., Guérault, D., Désaunay, Y., 2003. Quantitative description of habitat suitability for the juvenile common sole (Solea solea, L.) in the Bay of Biscay (France) and the contribution of different habitats to the adult population. J. Sea Res. 50, 139–149. doi:10.1016/S1385-1101(03)00059-5

Le Pape, O., Gilliers, C., Riou, P., Morin, J., Amara, R., Désaunay, Y., 2007. Convergent signs of degradation in both the capacity and the quality of an essential fish habitat: state of the Seine estuary (France) flatfish nurseries. Hydrobiologia 588, 225–229. doi:10.1007/s10750-007-0665-y

Lotze, H.K., Lenihan, H.S., Bourque, B.J., Bradury, R.H., Cooke, R.G., Kay, M.., Kidwell, S.M., Kirby, M.X., Peterson, C.H., Jackson, J.B.C., 2006. Depletion, Degradation, and Recovery Potential of Estuaries and Coastal Seas. Science 312, 1806–1809. doi:10.1126/science.1128035

Maunder, M.N., 2005. IATTC Workshop on Stock Assessment Methods. La Jolla, CA.

Maunder, M.N., 1998. Integration of tagging and population dynamics models in fisheries stock assessment. (Ph.D. dissertation). University Washington, Seattle.

Maunder, M.N., 2001b. Integrated Tagging and Catch-at-Age Analysis (ITCAAN)., in: Kruse, G.H., Bez, N., Booth, A., Dorn, M.W., Hills, S., Lipcius, R.N., Pelletier, D., Roy, C., Smith, S.J., Witherell, D. (Eds.), Alaska Sea Grant College Program Report. Spatial Processes and Management of Fish Populations., University of Alaska, Fairbanks, pp. 123–146.

Maunder, M.N., Deriso, R.B., 2011. A state–space multistage life cycle model to evaluate population impacts in the presence of density dependence: illustrated with application to delta smelt ( *Hyposmesus transpacificus* ). Can. J. Fish. Aquat. Sci. 68, 1285–1306. doi:10.1139/f2011-071

Maunder, M.N., Punt, A.E., 2013. A review of integrated analysis in fisheries stock assessment. Fish. Res. 142, 61–74. doi:10.1016/j.fishres.2012.07.025

McAllister, M., Kirkwood, G.P., 1998. Bayesian stock assessment: a review and example application using the logistic model. ICES J. Mar. Sci. 55, 1031–1060. doi:10.1006/jmsc.1998.0425

Myers, R.A., Worm, B., 2003. Rapid worldwide depletion of predatory fish communities. Nature

423, 280–283. doi:10.1038/nature01610

Newman, K.B., Buckland, S.T., Morgan, B.J.T. (Eds.), 2014. Modelling population dynamics: model formulation, fitting and assessment using state-space methods, Methods in statistical ecology. Springer, New York, NY.

Ono, K., Punt, A.E., Rivot, E., 2012. Model performance analysis for Bayesian biomass dynamics models using bias, precision and reliability metrics. Fish. Res. 125, 173–183.

Parent, E., Rivot, E., 2013. Introduction to hierarchical Bayesian modeling for ecological data, Chapman & Hall/CRC applied environmental statistics. CRC Press, Boca Raton.

Patterson, K., Cook, R., Darby, C., Gavaris, S., Kell, L., Lewy, P., Mesnil, B., Punt, A., Restrepo, V., Skagen, D.W., Stefansson, G., 2001. Estimating uncertainty in fish stock assessment and forecasting. Fish Fish. 2, 125–157. doi:10.1046/j.1467-2960.2001.00042.x

Pauly, D., Watson, R., Alder, J., 2005. Global trends in world fisheries: impacts on marine ecosystems and food security. Philos. Trans. R. Soc. B Biol. Sci. 360, 5–12. doi:10.1098/rstb.2004.1574

Peterson, C.H., Grabowski, J.H., Powers, S.P., 2003. Estimated enhancement of fish production resulting from restoring oyster reef habitat: quantitative valuation. Mar. Ecol. Prog. Ser. 264, 249–264.

Petitgas, P., Rijnsdorp, A.D., Dickey-Collas, M., Engelhard, G.H., Peck, M.A., Pinnegar, J.K., Drinkwater, K., Huret, M., Nash, R.D.M., 2013. Impacts of climate change on the complex life cycles of fish. Fish. Oceanogr. 22, 121–139. doi:10.1111/fog.12010

Pollock, K.H., Hoenig, J.M., Hearn, W.S., 2001. Tag reporting rate estimation: 1 An evaluation of the high-reward tagging mehod. North Am. J. Fish. Manag. 21, 521–532.

Pollock, K.H., Hoenig, J.M., Hearn, W.S., Calingaert, B., 2002. Tag reporting rate estimation: 2. Use of high-reward tagging and observers in multiple-component fisheries. North Am. J. Fish. Manag. 22, 727–736.

Porch, C.E., Turner, S.C., Powers, J.E., 2001. Virtual population analyses of Atlantic bluefin tuna with alternative models of transatlantic migration: 1970-1997. Col Vol Sci Pap ICCAT 52, 1022–1045.

Punt, A.E., Butterworth, D.S., 1995. Use of tagging data within a VPA formalism to estimate migration rates of bluefin tuna across the north Atlantic. Col Vol Sci Pap ICCAT 44:166-182.

Punt, A.E., Hilborn, R., 1997. Fisheries stock assessment and decision analysis: the Bayesian approach. Rev. Fish Biol. Fish. 7, 35–63. doi:10.1023/A:1018419207494

Quinn II, T.J., Deriso, R.B., Neal, P.R., 1990. Migratory Catch-Age Analysis. Can. J. Fish. Aquat. Sci. 47, 2315–2327. doi:10.1139/f90-258

Quinn, T.J., Deriso, R.B., 1999. Quantitative fish dynamics. Oxford University Press, New York.

Raftery, A.E., Satagopan, J.M., Newton, M.A., Krivitsky, P.N., 2007. BAYESIAN STATISTICS

8, pp. 371-416. JM Bernardo, MJ Bayarri, JO Berger, AP Dawid, D. Heckerman, AFM Smith and M. West (Eds.)\copyright Oxford University Press, 2007, in: Bayesian Statistics 8: Proceedings of the Eighth Valencia International Meeting, June 2-6, 2006. Oxford University Press, USA, p. 371.

Riou, P., Le Pape, O., Rogers, S.I., 2001. Relative contributions of different sole and plaice nurseries to the adult population in the Eastern Channel: application of a combined method using generalized linear models and a geographic information system. Aquat. Living Resour. 14, 125–135. doi:10.1016/S0990-7440(01)01110-X

Rivot, E., Prévost, E., Parent, E., Baglinière, J.L., 2004. A Bayesian state-space modeling framework for fitting a salmon stage-structured population dynamic model to multpile time series of field data. Ecol. Model. 463–485. doi:10.1016/j.ecolmodel.2004.05.011

Robert, M., Faraj, A., McAllister, M.K., Rivot, E., 2010. Bayesian state-space modelling of the De Lury depletion model: strengths and limitations of the method, and application to the Moroccan octopus fishery. ICES J. Mar. Sci. J. Cons. 67, 1272–1290.

Rochette, S., Huret, M., Rivot, E., Le Pape, O., 2012. Coupling hydrodynamic and individual-based models to simulate long-term larval supply to coastal nursery areas: Modelling larval supply to coastal nurseries. Fish. Oceanogr. 21, 229–242. doi:10.1111/j.1365-2419.2012.00621.x

Rochette, S., Le Pape, O., Vigneau, J., Rivot, E., 2013. A hierarchical Bayesian model for embedding larval drift and habitat models in integrated life cycles for exploited fish. Ecol. Appl. 23, 1659–1676.

Rochette, S., Rivot, E., Morin, J., Mackinson, S., Riou, P., Le Pape, O., 2010. Effect of nursery habitat degradation on flatfish population: Application to Solea solea in the Eastern Channel (Western Europe). J. Sea Res. 64, 34–44. doi:10.1016/j.seares.2009.08.003

Sarmiento, J.L., Slater, R., Barber, R., Bopp, L., Doney, S.C., Hirst, A.C., Kleypas, J., Matear, R., Mikolajewicz, U., Monfray, P., Soldatov, V., Spall, S.A., Stouffer, R., 2004. Response of ocean ecosystems to climate warming. Glob. Biogeochem. Cycles 18, n/a-n/a. doi:10.1029/2003GB002134

Sippel, T., Paige Eveson, J., Galuardi, B., Lam, C., Hoyle, S., Maunder, M., Kleiber, P., Carvalho, F., Tsontos, V., Teo, S.L.H., Aires-da-Silva, A., Nicol, S., 2015. Using movement data from electronic tags in fisheries stock assessment: A review of models, technology and experimental design. Fish. Res. 163, 152–160. doi:10.1016/j.fishres.2014.04.006

Smedbol, R.K., McPherson, A., Hansen, M.M., Kenchington, E., 2002. Myths and moderation in marine “metapopulations”? Fish Fish. 3, 20–35. doi:10.1046/j.1467-2979.2002.00062.x

Tanner, S.E., Reis-Santos, P., Cabral, H.N., 2016. Otolith chemistry in stock delineation: A brief overview, current challenges and future prospects. Fish. Res. 173, 206–213. doi:10.1016/j.fishres.2015.07.019

Tuck, G.N., Possingham, H.P., 1994. Optimal harvesting strategies for a metapopulation. Bull. Math. Biol. 56, 107–127. doi:10.1007/BF02458291

# 6 Appendix

## Appendix I. Two extreme hypotheses on the spatial structure of the Sole population in the Eastern Channel tested in Archambault et al. (2016)

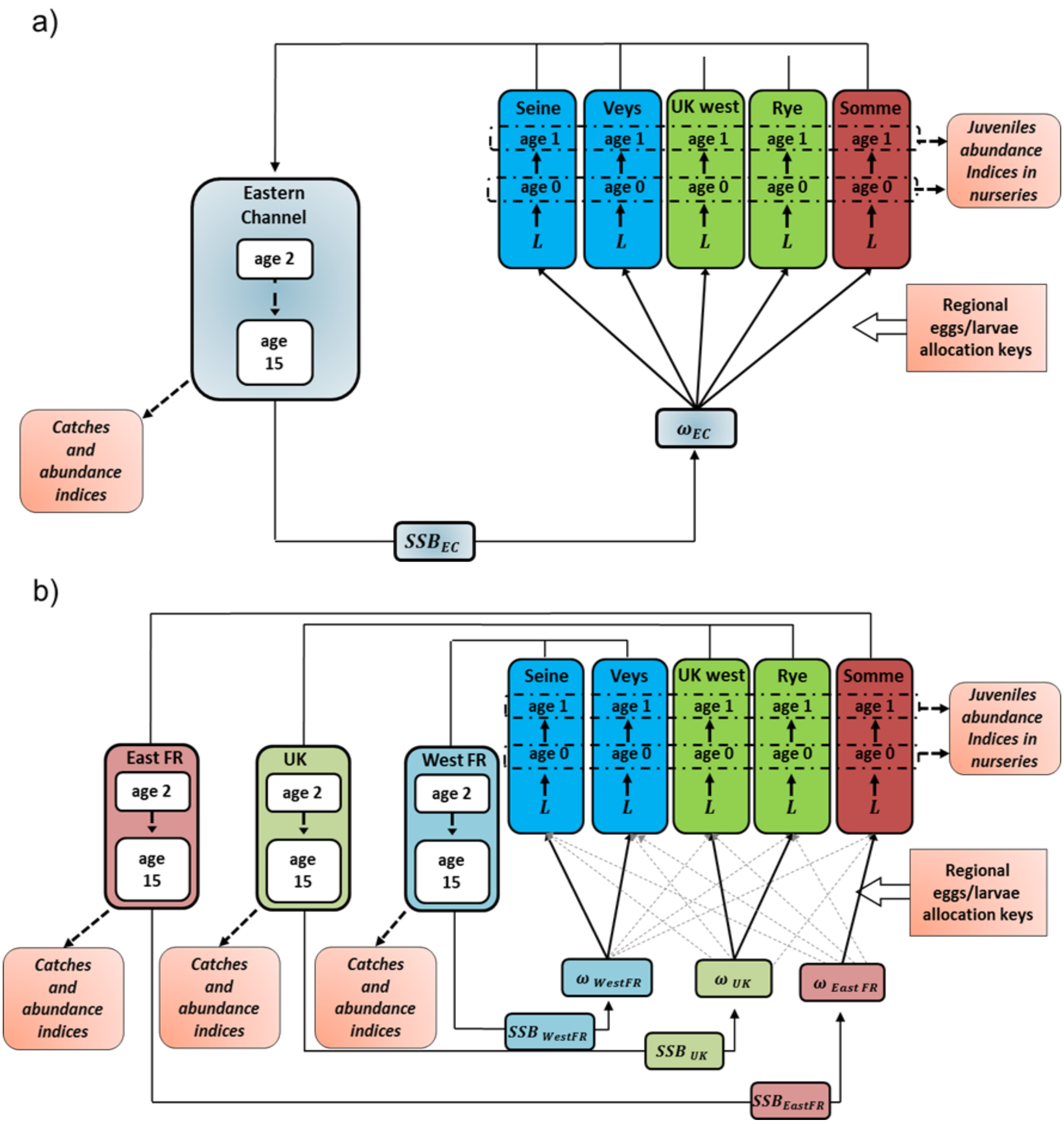

**Figure A-1.** Integrated life cycle models in a Bayesian framework. a) Model considering a homogeneous population within the Eastern Channel. b) Model considering three isolated subpopulations within the Eastern Channel with limited mixing occurring during the first pelagic stages. Data or external model outputs considered as data are represented by the orange boxes. (Adapted from Archambault et al. (2016))

The authors have compared inferences on population dynamics and stock assessment obtained under two extreme hypotheses: the first one assumes a single population, well-mixed and spatially homogeneous (***Fig. A-1a***). This hypothesis corresponds to the current hypothesis used in the stock assessment by ICES. The other one assumes existence of three subpopulations with a full spatial segregation (without connectivity between subpopulations) (***Fig. A-1b***).

## **Appendix II.** The main questions addressed in the SMAC project

### (1) Connectivity and spatial structure of the Sole population:

The first research axis seeks to improve understanding on the spatial structure of the Sole population in the Eastern Channel, and its consequences on population dynamics and stock assessment and management. This research axis addresses several questions:

(i) Identify in which nursery ground a given individual has spent his first two years, using otolith microchemistry;

(ii) Quantify adult movements within the Eastern Channel, using capture-mark-recapture;

(iii) Analyze the potential difference in growth of individuals between different zones in the Eastern Channel;

(iv) Integrate the new ecological knowledge on connectivity and spatial structure within population dynamics and stock assessment models and analyze how stocks assessment is impacted according to the connectivity level found.

### (2) Recruitment

This research axis is focused on the spatio-temporal variability in both larval and juvenile densities and the analysis of the asynchronicity of recruitment fluctuations over the five nursery sectors, taking in account their respective carrying capacity. The goals are two folds:

(i) Evaluate how the current unique scientific survey of recruitment in the Somme estuary can help to validate larval drift models

(ii) Evaluate how scientific survey of juvenile abundances can help to give full account of the recruitment variability. In particular, as predictions of recruitment in the current assessment are based on abundance indices from a single nursery sector (The Somme nursery ground, through the NOURSOM survey), this project seeks to evaluate how to optimize implementation of a new scientific survey in the Eastern Channel to supplement current available data and improve predictions of recruitment over the Easter Channel.

### (3) Selectivity

The last axis research aims at evaluating and improving catchability of fleets in the Eastern Channel by exploring technical and fishing strategies. This axis addresses several topics:

(i) Evaluate the current catchability of gears used in the Eastern Channel for the Sole population and ways to improve it;

(ii) Identify what are the current technical practices of professionals and how they can vary over time and space (between the three regions previously identified), using mapping. This item will investigate the way to improve the stock assessment and fisheries management through a better understanding of the spatio-temporal variability.

(iii) Analyze the effectiveness of the current management measures and those forthcoming concerning the current catchability, over spatio-temporal scales in order to improve them.

## **Appendix III.** Poster warning distributed durnig the SMAC project

# SOLE TAGGING

SMAC

**CONTACT IFREMER**
smac@ifremer.fr
+33 643040511
wwz.ifremer.fr/smac

If you catch a **tagged sole**, please send us the **tag** with the **date** and **location** of the catch (lat, long), as well as the fish **total length** if possible.

CRPMEM

COMITE REGIONAL DES PECHES MARITIMES BASSE NORMANDIE

Comité Régional des Pêches Maritimes et des Elevages Marins de Haute-Normandie

Organisation de Producteurs CME Manche-Mer du Nord

OPBN Marins Pêcheurs

FROM NORD

RÉGION NORD-PAS DE CALAIS

PICARDIE LA RÉGION

Liberté • Égalité • Fraternité
RÉPUBLIQUE FRANÇAISE

Ministère
de l'Environnement,
de l'Énergie
et de la Mer

FRANCE FILIÈRE PÊCHE

Ifremer

REGION NORMANDIE

AGRO CAMPUS OUEST

BOREA
Biologie des Organismes et Ecosystèmes Aquatiques

Eastern Channel Sole : Improving our knowledge for a better management of the stock

## **Appendix IV.** “Adult-mediated connectivity affects inferences on population dynamics and stock assessment of nursery-dependent fish populations”

**Authors:**

Benoit Archambault, Olivier Le Pape, Loic Baulier, Youen Vermard, Matthieu VERON, Etienne Rivot

**Publication:**

Fisheries Research 181 (2016) 198-213

Fisheries Research 181 (2016) 198–213

Contents lists available at ScienceDirect

Fisheries Research

journal homepage: www.elsevier.com/locate/fishres

# Adult-mediated connectivity affects inferences on population dynamics and stock assessment of nursery-dependent fish populations

Benoit Archambault[a,b], Olivier Le Pape[a], Loic Baulier[a,c], Youen Vermard[d,e], Matthieu Véron[a], Etienne Rivot[a,*]

[a] Agrocampus Ouest, UMR 985 ESE Ecologie et Santé des Écosystèmes, Rennes, France
[b] AgroParisTech, Paris, France
[c] Ifremer, Délégation de Guyane, Cayenne, France
[d] Channel and North Sea Fisheries Department, Ifremer, Boulogne Sur Mer, France
[e] Ifremer, Department of Fisheries Ecology and Modelling, Nantes, France

## ARTICLE INFO

*Article history:*
Received 22 May 2015
Received in revised form 24 March 2016
Accepted 29 March 2016
Handled by A.E. Punt

*Keywords:*
*Solea solea*
Spatial life-cycle model
Coastal nurseries
Connectivity
Stock assessment
Hierarchical bayesian model

## ABSTRACT

We explore how alternative hypotheses on the degree of mixing among local subpopulations affect statistical inferences on the dynamics and stock assessment of a harvested flatfish population, namely, the common sole population in the Eastern Channel (ICES area VIId). The current paradigm considers a single, well-mixed, spatially homogeneous population with juveniles from all coastal nursery grounds along the French and UK coasts that contribute to a single adult population and one pool of eggs. Based on the available data and ecological knowledge, we developed a spatial Bayesian integrated life-cycle model that consists of three subpopulations (one near the UK coast and two near the French coast, denoted UK, West FR and East FR, respectively) supported by their respective local nurseries, with the connectivity among the three components limited to low exchanges during larval drift. Considering the population dynamics among three subpopulations (instead of a single homogeneous one) drastically changes our inferences on the productivity of nursery sectors and their relative contribution to total recruitment. Estimates of the East FR subpopulation's contribution to total recruitment increase (29% in the single population model; 48% in the three subpopulation model), balanced by a decrease in the UK subpopulation's contribution (53%; 34%). Whereas an assessment based on the hypothesis of a single spatially homogeneous population in the EC indicates exploitation far above *MSY* (current $F/F_{MSY} = 1.8$), an assessment that considers a metapopulation with three loosely connected subpopulations revealed a different status, with the UK and East FR subpopulations being exploited above *MSY* (current $F/F_{MSY} = 1.9$ and 2, respectively) and the West FR subpopulation approaching full exploitation (current $F/F_{MSY} = 1.05$). This approach contributes to the quantitative assessment of spatial fishery and coastal habitat management plans.

## 1. Introduction

Integrated life-cycle modeling approaches that account for the spatial structure of populations are needed to improve our understanding of the impacts of multiple pressures on populations (Carson et al., 2011; Stelzenmuller et al., 2011; van de Wolfshaar et al., 2011; Petitgas et al., 2013). The concepts of metapopulation were introduced long ago in the optimal harvesting theory for fisheries (Tuck and Possingham, 1994 and references therein; Hilborn and Walters, 1992). Spatially explicit models can help decision making in spatial management plans either to adapt fisheries management to local productivities (Carruthers et al., 2011; Ying et al., 2011; Guan et al., 2013) or to design networks for marine protected areas (Botsford et al., 2009; Gaines et al., 2010; Grüss et al., 2011).

However, the current paradigm in population dynamics for the assessment of the most exploited marine stocks continues to ignore metapopulation structure. One often assumes a fish stock as a single, well-mixed and spatially homogeneous population that produces a single larval pool that undergoes extensive dispersal and

---

[*] Corresponding author at: Agrocampus Ouest, UMR 985 ESE Ecologie et Santé des Écosystèmes, Rennes, France.

*E-mail addresses:* benarcha@gmail.com (B. Archambault), Olivier.Le.Pape@agrocampus-ouest.fr (O. Le Pape), loic.baulier@ifremer.fr (L. Baulier), youen.vermard@ifremer.fr (Y. Vermard), matthieu.veron@agrocampus-ouest.fr (M. Véron), etienne.rivot@agrocampus-ouest.fr (E. Rivot).

http://dx.doi.org/10.1016/j.fishres.2016.03.023
0165-7836/© 2016 Elsevier B.V. All rights reserved.

massive export covering the population's entire distribution area. When it is addressed at all, the question of connectivity and population structure is mostly focused on early life stages (Petitgas et al., 2013; Frisk et al., 2014), with a large body of studies designed to evaluate the influence of physical and biological processes on the survival and dispersion of eggs and larvae (Miller, 2007; Savina et al., 2010; Hinrichsen et al., 2011; Peck and Hufnagl, 2012) that govern the variability of recruitment in space and time (Chambers and Trippel, 1997; Gallego et al., 2012). The importance of larval retention in marine populations has also been emphasized (Cowen et al., 2000; Warner and Cowen, 2002), because populations that display strong retention may be locally more vulnerable to local recruitment overfishing or depletion caused by catastrophic events (Strathmann et al., 2002). However, although adult-mediated connectivity is suspected to play a major role in population functioning, much less attention has been paid to its role (Frisk et al., 2014). The movements of adults may determine the structure and dynamics of metapopulations (Stelzenmuller et al., 2011; Cianelli et al., 2013), especially when larval and juvenile retention occurs (Grosberg and Levitan, 1992), thus indicating the need for population models that account for spatial structure and connectivity at all stages (Petitgas et al., 2013; Frisk et al., 2014).

New challenges arise when building and parameterizing population models that account for the spatial structure along the life cycle: (i) Long spatial data series of catches, abundance indices and fishing effort are rarely available; (ii) Coupling oceanographic circulation models and larval individual-based models provides a way to explore larval dispersal, but larval stages are rarely accessible to observation and the validation of those models remains an open question (Miller 2007); and (iii) Movements in the adult stage are difficult to quantify. Mark-recapture data (Drouineau et al., 2010; Carruthers et al., 2011), natural markers and genetic studies (Hellberg et al., 2002) are costly and sometimes fail to reveal the metapopulation structure (Ward et al., 1994; Smedbol et al., 2002; Rolland et al., 2007).

It thus remains a methodological challenge to embed spatial life-cycle models within a statistical approach to derive inferences on key parameters (Planque et al., 2011). The Hierarchical Bayesian modeling (HBM) framework has proven successful for embedding complex demographic processes with various sources of noisy and incomplete data on various spatial and temporal scales (Clark, 2005; Buckland et al., 2007; Parent and Rivot, 2013); thus it can help address some of these challenges. HBM has been successfully applied to build fish population dynamic models that assimilate various sources of field surveys (Rivot et al., 2004; Massiot-Granier et al., 2014), integrate mark-recapture data to capture the spatial structure of populations (Cunningham et al., 2007; Taylor et al., 2011), and incorporate complex interactions with environmental drivers of recruitment (Ruiz et al., 2009; Rochette et al., 2013).

In this paper, using the common sole (*Solea solea*) population in the Eastern Channel (EC; ICES area VIId; Fig. 1a) as a case study, we investigate how considering alternative hypotheses about adult-mediated connectivity can affect statistical inferences on population dynamics and stock assessment. The common sole is a coastal and estuarine nursery-dependent flatfish species (Le Pape et al., 2003a; Gibson, 2005). Its population in the EC is exploited, with annual landings of approximately 4,000t. The sole's life cycle in the EC is well described (Rochette et al., 2013 and references therein): adults reproduce in early spring; pelagic eggs and larvae drift and survivors will eventually settle and metamorphose into benthic juveniles in late spring in restricted nurseries in which they grow for 2 years (Riou et al., 2001; Rochette et al., 2010). Afterwards, the fish move to wider and deeper adult areas, where their migrations remain limited (Burt and Millner, 2008).

Rochette et al. (2013) have proposed an integrated life-cycle model for the EC's sole population that combines approaches that are usually considered independently: (i) Outputs of an individual-based model for larval drift that provided yearly estimates of the dispersion and mortality of eggs and larvae from spawning grounds to settlement in several coastal nurseries; (ii) A habitat suitability model based on juvenile trawl surveys combined with habitat maps to estimate the surface of each nursery sector and juvenile densities; and (iii) A statistical catch-at-age model for estimation of numbers-at-age and the fishing mortality of subadults and adults. A strong assumption in Rochette et al. (2013) considers that various nurseries contribute to the recruitment of a single homogeneous population in the EC. This hypothesis is consistent with the stock-assessment model (ICES, 2013). However, results from the larval drift model (Rochette et al., 2012) suggest consistent larval retention areas with strong relationships between spawning areas and nursery sectors. Additionally, ancillary data and expertise suggest only very low displacement of juveniles on nurseries (Coggan and Dando, 1988; Anon., 1989; Riou et al., 2001; Le Pape and Cognez, 2016) and only moderate movements of adults (Kotthaus, 1963; Anon., 1965; Burt and Millner, 2008) that would result in a low adult-mediated connectivity (Frisk et al., 2014). Thus, there is a strong presumption that very low connectivity exists among the three isolated subpopulations associated with different nurseries sectors, thus fostering an exploration of the impact of considering various spatial structures on (meta)population dynamics.

In this paper, we elaborate on the HBM framework proposed by Rochette et al. (2013) to explore how considering three (quasi)isolated subpopulations instead of a single homogeneous one (as considered by ICES (2013) and Rochette et al. (2013)) can affect statistical inferences on population dynamics. In particular, we assess how considering three subpopulations of adults (instead of a single homogeneous one) can change our evaluation of the productivity of each nursery area and its contributions to recruitment. We point out how consideration of three adult subpopulations ultimately affects not only the estimation of management reference points but also the assessment of the stock status with respect to the fishery's spatial dynamics.

## 2. Materials and methods

We first describe the model considering three (quasi)isolated subpopulations of sole in the EC (Fig. 2a), together with the available data and other model inputs based on results from previous models (Table 1). The second model that assumes a single, homogeneous adult population is derived as a simplification of the first model (Fig. 2b). Third, we provide details of the simulation method used to derive management reference points.

The life-cycle model is written in a state-space form (hierarchical) that integrates stochasticity in both the process equations for the population dynamics (process errors) and the observation equations (observation errors). All of the model equations, priors and values on fixed parameters are fully detailed in Appendix A. Posterior distributions were approximated via Monte Carlo Markov Chain methods using JAGS software (see Sup. Mat. S1 for details about the MCMC simulations and the convergence diagnostics).

### 2.1. Model considering three quasi-isolated populations

### 2.1.1. Spatial structure

The EC population is supported by five nursery areas (Rochette et al., 2010) along the French (Veys, Seine and Somme nurseries) and UK coasts (UK West and Rye nurseries) (Fig. 1a). Rochette et al. (2012) demonstrate the low dispersion of eggs and larvae during the pelagic stages of the common sole (Fig. 1b). Indications of the reduced movements of juveniles and adults suggest that connectivity is almost null for juveniles (Riou et al., 2001) and

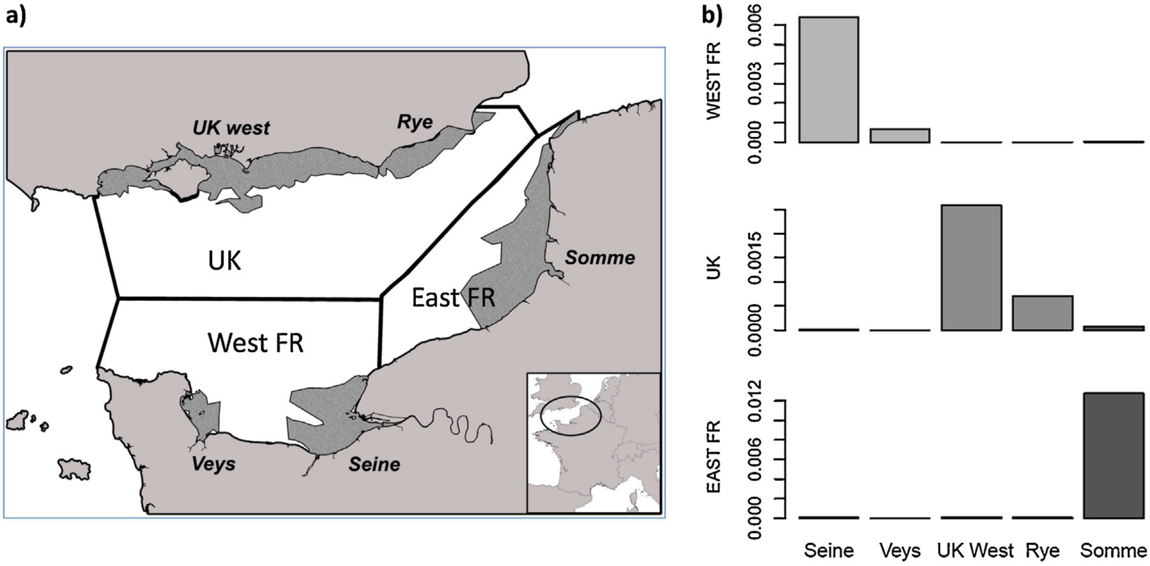

**Fig. 1.** (a) Eastern Channel area with the spatial limits of the three subpopulations (West Fr, UK, East Fr) based on larval retention as suggested by results of the larval drift model. Dark grey: coastal nursery sectors. (b) Probability of successful settlement in one of the three nurserygrounds (in column) given the origin of the eggs (three subpopulations as raws).

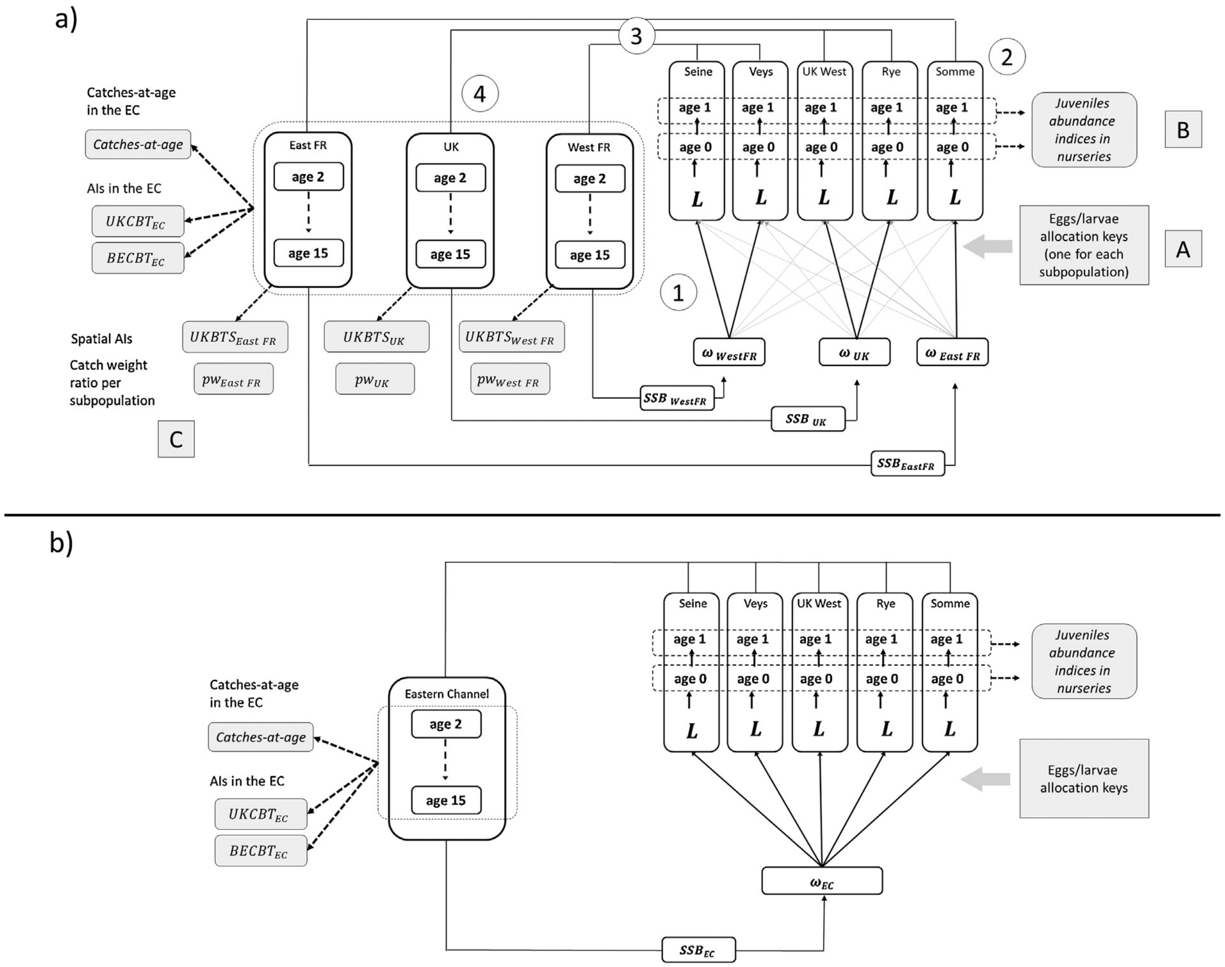

**Fig. 2.** Hierarchical Bayesian Models for the life cycle. (a) Model with three isolated subpopulations in which only very limited mixing occurs through egg and larval drift; (b) Model considering a single population. Lettering and numbering refer to corresponding points in Section 2. White boxes: non-observed state variables; Shaded boxes: data or external model outputs considered as data. Dashed arrows indicate observation equations to link latent state variables to observations.

**Table 1**
Synthesis of data and results of previous models used as inputs for the integrated life-cycle model.

| | | Nature of the information used | Source | Time series |
|---|---|---|---|---|
| Eggs & Larvae | Survival and allocation from spawning areas to the five nursery sectors | Outputs of biophysical IBM model | Upgraded run of Rochette et al. (2012); Savina et al. (2016). | 1982–2007 |
| Juveniles | Abundance indices available for each nursery sector | | | |
| | West UK | Outputs of a habitat suitability model | Rochette et al. (2010) | 1982–1999 |
| | Rye | // | Rochette et al. (2010) | 1982–2006 |
| | Somme | // | Rochette et al. (2010) | 1982–1983; 1987–2011 |
| | Seine | // | Rochette et al. (2010) + GIP Seine Aval | 1995–2002; 2006; 2008–2011 |
| | Veys | // | Rochette et al. (2010) | 2006;2010–2011 |
| Adults | Available on the scale of the Eastern Channel | | | |
| | Catches at age | Data | ICES | 1982–2011 |
| | UK commercial CPUE (UKCBT) | Data | ICES | 1986–2011 |
| | Belgium commercial CPUE (BECBT) | Data | ICES | 1982–2011 |
| | Available for the three subpopulations | | | |
| | Spatial repartition of catches (total weights, no age structure) among the three areas (East FR, UK, West FR) | Data | ICES (2003–2011)<br>Y. Vermard, Pers. comm. (1982–2002) | 1982–2011 |
| | Spatial Scientific Abundance Index (UKBTS) | Data | Y. Vermard, Pers. comm. | 1990–2004; 2006–2011 |

only very limited for adults. Considering this limited connectivity along the life cycle and the presence of natural barriers (e.g., rocky shores in the central southern coast and deep gravel grounds in the central part of the EC; Rochette et al., 2010), three subpopulations associated with three spawning areas (denoted $r = 1$–$3$) and attached nursery sectors were identified (Fig. 1a): the Western French subpopulation (West FR; Seine and Veys nursery sectors), the UK subpopulation (UK West and Rye nursery sectors) and the Eastern French subpopulation (East FR; Somme nursery sector).

### 2.1.2. Population dynamics

The population dynamics were modeled for 30 years from 1982 to 2011. The model is stage-structured from eggs to settled larvae and then age-structured from juveniles to adults (Fig. 2a).

*2.1.2.1. Eggs and larvae (see 1 in Fig. 2a).* Egg hatching is parameterized following the characteristics of the spawning season and the spatial distribution of eggs (Rochette et al., 2012), and the annual quantity of eggs spawned in each of the three subpopulations directly depends on the spawning biomass. Eggs and larvae are transported from spawning areas and settle in the five identified nursery sectors according to a drift/survival matrix estimated from a biophysical model (Rochette et al., 2012). Outputs from the larval-drift model (Rochette et al., 2012; Fig. 1b) indicate very low connectivity between the three spawning areas and distant nursery sectors over the time series, each spawning area almost exclusively feeding the closest coastal and estuarine nursery grounds. Only very limited mixing of individuals between the three subpopulations then occurs through larval drift (Fig. 2a). The UK – and in lesser proportions the East FR – subpopulations were also subject to larval inputs from the North Sea's (NS) sole population (Savina et al., in press), which were integrated into the model as a constant term (not shown in Fig. 2).

*2.1.2.2. Juvenile from age 0 to age 2 (see 2 in Fig. 2a).* Because of competition for space and food resources (Iles and Beverton, 2000; Le Pape and Bonhommeau, 2015), settled larvae experience density-dependent post-settlement mortality over nursery sectors between settlement (late spring) and the end of summer (growth period). Following previous modeling work in Rochette et al. (2013) and Archambault et al. (2014), the resulting expected number of age-0 juveniles is modeled through a compensatory density-dependent Beverton-Holt (BH) relationship parameterized with local parameters $\alpha_i$, the maximum survival rate (i.e., the survival rate without density dependence) and $K_i$, the carrying capacity per unit of surface (i.e., the maximum number of age-0 juveniles that can survive per unit of surface), which is then scaled to the total surface of each nursery, $S_i$ (fixed). Unexplained random variations are captured by independent lognormal random noise.

Because only limited information is available to estimate site-specific parameters, exchangeable hierarchical structures (Gelman et al., 2004) were used to model the between-nursery variability of parameters $\alpha_i$ and $K_i$, enabling "borrowing strength" between nursery sectors (Rivot and Prévost, 2002; McAllister et al., 2004). Available juvenile abundance indices on nursery sectors may contain enough information to estimate the carrying capacity parameters $K_i$. However, because very few observations are available at low levels of settling larvae, the maximum survival rates $\alpha_i$ could be difficult to estimate. Informative priors were set on the $\alpha_i$ (see Appendix A) based on a *meta*-analysis of flatfish stock-recruitment relationships (Archambault et al., 2014).

Late age-0 juveniles (in September, after the summer growth period) experience a fixed natural mortality during 4 months until they reach age 1 in January. Age-1 juveniles spend one year in nursery grounds with both natural (fixed) and fishing (estimated) mortalities.

*2.1.2.3. From nurseries to sub-adults (see 3 in Fig. 2a).* Young fish are assumed to leave their nurseries at age 2, in January. No quantitative data were directly available on the connectivity from nursery sectors to deeper areas where older fish (ages 2–15) live. Therefore, age-2 fish leaving nurseries are supposed to contribute directly to the subpopulation adjacent to the nursery (Fig. 1a).

*2.1.2.4. Sub-adults and adults (see 4 in Fig. 2a).* Fish from ages 2–15 are structured in three different subpopulations, with cohort dynamics accounting for both natural (age-specific, fixed) and fishing (age-/year-/subpopulation-specific, estimated) mortalities. All of the remaining fish are then assumed to die at age 15. Because the cumulative natural mortality up to age 12 is near 1, including an age+ group in the model would not change the results. Fishing mortality is a function of fishing effort (estimated) and age-specific gear selectivity (estimated).

Fish between the age of 3 and 15 participate in reproduction. The number of eggs for each year and each subpopulation is calculated from the spawning stock biomass.

### *2.1.3. Integration of results of previous models, data sources and observation models*

*2.1.3.1. Eggs and larvae survival and allocation key (see A in Fig. 2a).* Egg and larval survival and allocation from spawning areas to the five nursery sectors over 26 years between 1982 and 2007 were available as outputs from an upgraded run of Rochette et al.'s (2012) biophysical model (Savina et al., in press). That model ultimately provided the 3 × 5 × 26 probability key that eggs from each of the 3 subpopulations would reach one of the 5 different nursery sectors, accounting for inter-annual variability over the 26 years of simulation. No outputs of larval drift model were available for the last 4 years (2008–2011; Table 1). Because no particular time trend appears in the time series, the 3 × 5 probability key for years 2008–2011 was set equal to the average over the entire series.

*2.1.3.2. Abundance indices of juveniles in each nursery sector (see B in Fig. 2a).* The abundance indices (AI) of juveniles and the total surface of each nursery sector are outputs from the habitat suitability model developed by Rochette et al. (2010) and used in Rochette et al. (2013). Juvenile (ages 0 and 1) AIs over the five nursery sectors were obtained from an upgrade of Rochette et al.'s (2010) habitat-suitability model, using updated scientific trawl survey data. They were considered as lognormal random observations of juvenile abundance accounting for gear/age-specific catchability.

*2.1.3.3. Catches-at-age (see C in Fig. 2a).* Annual catches-at-age were available from stock assessment reports only at the scale of the EC; however, they were not available separately for the three subpopulations. Catches-at-age predicted by the model for each subpopulation were aggregated at the scale of the EC and considered observed with lognormal errors.

Ancillary data for the catch weight ratio per subpopulation (total weight; no age structure) also exist, showing that higher proportions of catches are regularly realized in the East FR area. An additional likelihood term for the catch weight ratio per subpopulation was added to assimilate this information in the model.

*2.1.3.4. Abundance indices of adults (see C in Fig. 2a).* Different AIs for adults were available at various spatial scales (EC and subpopulations). Two time series of AIs were available at the scale of the EC: the UK (UKCBT) and the Belgium (BEBCT) commercial fleet catch-per-unit effort. The scientific UK Bottom Trawl Survey (UKBTS) provided AIs at the adult stage for each of the three subpopulations. One observation equation is written for each time series of AIs, each contributing to the whole likelihood function. All of the AIs were considered as lognormal random observations of abundance at age, but with catchability parameters specific to the fleet (UKBCT, BEBCT, UKBTS), age and year.

### *2.1.4. Choice of priors and values of fixed parameters*

Some parameters were fixed from the literature (Appendix A, Table A.1). All of the estimated parameters except for the selectivity curve parameters and the slopes of the BH relationships over nursery areas ($\alpha_i$) were given weakly informative *a priori* distributions in the sense of Gelman et al. (2004), i.e., they let the data speak while excluding unrealistic values (Appendix A).

**Table 2**

Configuration of the three model runs to explore the respective contributions of data sources to the fit of the model with three subpopulations.

| Run | Spatial Abundance Index (UKBTS) | Proportion of total catches among subpopulations (total catches in weight, no age structure) |
|---|---|---|
| a | Yes | No |
| b | No | Yes |
| c | Yes | Yes |

### *2.2. Simplifying the model to a single, homogeneous adult population*

The model considering three isolated subpopulations can easily be simplified into a single population model that corresponds to the structure of Rochette et al. (2013) and to the stock-assessment working group (ICES, 2013). This single population model assumes that the five nursery sectors contribute to one single population covering the whole EC (Fig. 2b). The distribution of eggs over the spawning area is assumed to follow the distribution observed in 1991 (Rochette et al., 2012). All other processes (e.g., juvenile dynamics) are unchanged except for the fishing mortality of adults that is now considered homogeneous at the EC scale. The same sources of data are used, but no catch weight ratios per subpopulation are considered and only the adult AIs available at the EC scale (i.e., UKCBT and BECBT) are used (Fig. 2b).

### *2.3. Evaluating the fit to each data sources*

We conducted posterior predictive checking to evaluate the fit of the model to each data source assimilated in the model. For each data source, observed data (denoted $y^{\rm obs}$) were compared to the distribution of replicated data sets ($y^{\rm pred}$) simulated from their posterior predictive distribution (Gelman et al., 2004). To check that the model was able to replicate data similar to the observations, we compare synthetic statistics calculated from the observed data ($T\left(y^{obs}\right)$) with statistics calculated from replicated data ($T(y^{rep})$). We calculated Bayesian *p-values* (Gelman et al., 2004), defined as the probability that the statistics calculated from the replicated data $T(y^{rep})$ are more extreme than the statistics calculated from the observed data $T\left(y^{obs}\right)$:

$$\text{p-values} = \Pr\left(T\left(y^{rep}\right) \geq T\left(y^{obs}\right)\right) \tag{1}$$

We chose the standard discrepancy statistic calculated for the observed and simulated data as follows:

$$T\left(y^{obs}\right) = \sum\left(y^{obs} - E\left(y\right)\right)^2 \text{ and } \mathrm{T}\left(y^{pred}\right) = \sum\left(y^{pred} - E\left(y\right)\right)^2 \tag{2}$$

where $y^{obs}$ is an observation, $y^{pred}$ is a simulated value in the posterior predictive distribution of the state variable $y$ and $E\left(y\right)$ is the expected mean of $y$ in the model (the fit of the model). $y^{obs}$, $y^{pred}$ and $E\left(y\right)$ were log-transformed for all variables observed with lognormal random noise. Depending upon the data source, the sums in Eq. (2) are calculated either across the entire time series of available data (for age-0 and age-1 AIs in nursery sectors and for the catch weight ratio per subpopulation) or across both time and age classes (for adults AIs and aggregated catches-at-ages). *p-values* close to 0 or 1 reveal the potential failure of the model (Gelman et al., 2004).

In addition, we assessed the contribution of the various data sources in the model, considering three loosely connected populations by examining how the final inferences change when cumulating the data sources. Three runs of the model were conducted, successively adding the various spatial data series (i.e., spatial UKBTS AIs and catch weight ratio per subpopulation; Table 2). In run (a), only spatial UKBTS AIs are introduced in the likelihood. Run (b) considers a likelihood function for the catch weight ratio per subpopulation, but does not integrate spatial UKBTS AIs. Finally, run (c) corresponds to the final model that assimilates both the spatial UKBTS AIs and the catch weight ratio per subpopulation.

### 2.4. Stock-assessment and management reference points

The spawning stock biomass (*SSB*), recruitment (*R*), fishing mortality (*F*), and Maximum Sustainable Yield (*MSY*), the associated fishing mortality ($F_{MSY}$) and spawning stock biomass ($SSB_{MSY}$) were estimated on different scales (for each subpopulation and on the scale of the EC).

The evaluation of *MSY*, $F_{MSY}$, and $SSB_{MSY}$ is not analytically straightforward, because the production of each subpopulation results from a combination of stochastic BH relationships fitted on each nursery sector (two in West Fr: Veys and Seine; two in the UK: UK West and Rye; and one in East FR: Somme; Fig. 1a). The empirical equilibrium curves were obtained using Monte Carlo simulations to integrate both process and parameter uncertainty (see the methods in Appendix B). In the model considering three subpopulations, reference equilibrium points for each subpopulation *r*, denoted $B_{MSY,r}$, $F_{MSY,r}$ and $C_{MSY,r}$, were estimated conditionally by fixing the fishing pressure for the two other subpopulations equal to the estimates averaged over the last five years of the data series (2007–2011).

## 3. Results

### 3.1. Model evaluation

For both of the model configurations, the convergence diagnostics indicate convergence of the MCMC chains after $10^6$ iterations for all variables (see Sup. Mat. S1 for more details about the MCMC simulations and the convergence diagnostics). To reduce the autocorrelation in the sample used for final inferences, one out of 100 iterations was kept (thinning = 100). Final inferences were derived from a sample of 3 × 10,000 iterations that resulted from merging the three chains.

Because the two models integrate different sources of data (e.g., the spatial AIs of adults and catch weight ratios that are not included in the model considering a single, homogeneous adult population), the usual goodness of fit criteria cannot be used directly to compare the two model structures. The component of deviance associated with the data shared by the two model structures (i.e., the juvenile AIs in the five nursery sectors and the non-spatial AIs for ages 2–15) was revealed as slightly lower for the model with one single population than for the model with three isolated subpopulations (not shown). However, the difference is very low, indicating that the likelihood of the two models is quite comparable when considering the data shared by the two model structures.

Although this is not formally considered in the likelihood function, we also compared egg distribution among the three spawning areas (i.e., the function of the *SSB* associated with each subpopulation) to the spatial distribution of eggs given by the single available observation originating from the 1991 eggs survey (Rochette et al., 2012). Results indicate that the spatial distribution of eggs derived from the fit of the model with three isolated subpopulations (West FR, 29%; UK, 33%; East FR, 38%) was highly consistent with the egg distribution observed in 1991 (25%, 34% and 41%), thus providing evidence that the spatial repartition of the SSB inferred from the model considering three subpopulation is consistent with some external data sources.

Overall, a posterior predictive check conducted for the two model configurations (one homogeneous population and three isolated subpopulations) did not reveal any strong and general inconsistencies between the fitted model and the data. Almost all of the *p-values* are between 0.05 and 0.95 for all model compartments (Table 3). The additional figures included in Sup. Mat. S2 (Fig. S2.1–S2.9) show a good consistency between the posterior predictive distributions and the data, providing additional evidence of a lack of conflict between the different sources of observations assimilated in the model. Interestingly, the *p-values* associated with the data sources that are common to the two model configurations (juveniles AIs, aggregated catches-at-ages and commercial CPUEs) were quite similar between the two model configurations (Table 3).

There was however evidence of poor fit between the posterior predictive distribution from the model and the observed data for the abundance indices of age-0 juveniles in the Solent nursery sector in the case of a model considering three subpopulations (*p-value* = 0.92) (Fig. S2.1). Additionally, *p-values* for commercial AIs (UKCBT and BECBT) and for the spatial AIs of adults (UKBTS) for the UK subpopulation are relatively high, indicating that the dispersion of the predictive distribution around the model fit is higher than the dispersion of observations (see also Fig. S2.1 and S2.8).

### 3.2. Posterior estimates of parameters

Marginal posterior distributions of all of the parameters obtained under both model configurations reveal that the parameters are generally estimated with low uncertainty (Sup. Mat. S3, Figs. S3.2 and S3.5 and Tabs. S3.1 and S3.2). Overall, the differences between the prior and the posterior reveal that the distributions are mostly driven by the data (Sup. Mat. S3, Figs. S3.2 and S3.5).

Interestingly, considering the more complex spatial structure of the population (three subpopulations of adults versus a single, homogeneous population) does not increase the posterior uncertainty about parameters. In contrast, uncertainty about posterior estimates of biomass, recruitment, and fishing mortality is higher in the model that considers three subpopulations (Fig. 3).

Nevertheless, one exception to this rule relates to the parameters for the density-dependent recruitment process in each nursery sector; those parameters are estimated with much more uncertainty than are the other parameters for both model configurations (Sup. Mat. S3, Fig. S3.1 and S3.4). Uncertainty is particularly high for the maximum survival rate $\alpha$ for the Somme and Rye nursery sectors. The posterior distribution of $\alpha$ for the Bay of Veys is not different from the posterior predictive distribution because juvenile abundance indices are only available for three years for this nursery sector.

For both model configurations, the selectivity parameters are estimated with very low uncertainty that leads to a knife-edge selectivity curve, with selectivity near 0 for age-1 fish, near 0.5 for age-2 fish and 1 for older fish.

As expected, the process error variance of the larvae to age-0 transition is greater than for the age-0 to age-1 transition (Sup. Mat. S3, Tabs. S3.1 and S3.2). This residual variability does not reveal any particular departure from the hypotheses of constant variance across the five nursery grounds and of the time independence of residuals (not shown).

In both model configurations, the variance of observation error in catches is very low. In the model considering a single, homogeneous population, the observation error on juveniles and adults' abundance indices are of the same order of magnitude. In contrast, the variance of observation error on juveniles is much higher in the model that considers three subpopulations.

Additional results (Sup. Mat. S3, Tabs. S3.3 and S3.4) reveal that some parameters are correlated and thus partially confounded. Results are similar for the two model configurations. In particular, parameters ($\alpha$,*K*) for each nursery sector are negatively correlated. Catchabilities associated with age-0 and age-1 abundance indices ($q_0$ and $q_1$) are positively correlated; moreover, they are positively correlated with the variance of observation errors on juveniles

**Table 3**
*p-values* of posterior predictive checking calculated for each source of observation and for the two model configurations: the model considering a single, homogeneous adult population and the model considering three subpopulations. *p-values* are the probability that the discrepancy static calculated for predicted values is greater than the one calculated with observed values (see text for details).

| | | One single population | | Three subpopulations | |
|---|---|---|---|---|---|
| JUVENILES | AI in each nursery sector | Age-0 | Age-1 | Age-0 | Age-1 |
| | Solent (West UK) | 0.72 | 0.74 | 0.92 | 0.51 |
| | Rye | 0.29 | 0.84 | 0.33 | 0.80 |
| | Somme | 0.12 | 0.26 | 0.23 | 0.11 |
| | Seine | 0.65 | 0.70 | 0.71 | 0.83 |
| | Veys | 0.61 | 0.55 | 0.72 | 0.64 |
| ADULTS | Aggregated data (Eastern Channel) | | | | |
| | Catches-at-age | 0.54 | | 0.56 | |
| | UK commercial CPUE (UKCBT) | 0.82 | | 0.88 | |
| | Belgium commercial CPUE (BECBT) | 0.72 | | 0.78 | |
| | Spatial data | | | | |
| | Proportion of total catches (weight) among the three areas (East FR, UK, West FR) | | | | |
| | West FR | – | | 0.54 | |
| | UK | – | | 0.57 | |
| | East FR | – | | 0.47 | |
| | Spatial Scientific AI Index (UKBTS) | | | | |
| | West FR | – | | 0.85 | |
| | UK | – | | 0.91 | |
| | East FR | – | | 0.27 | |

($\sigma^2_{Ijuv}$). Similarly, catchabilities associated with adults' abundance indices ($q_{UKCBT}$, $q_{BECBT}$ and $q_{UKBTS}$) are positively correlated, and they are positively correlated with the variance of observation error ($\sigma^2_{IAd}$).

### 3.3. Contribution of the different data sources to posterior estimates

We assessed the contribution of each dataset to the final estimations of the model with three subpopulations. Three runs of the model were conducted, successively assimilating the different sources of spatial data series (i.e., spatial UKBTS AIs and proportion of catches among areas; Table 2). The spatial AIs and the spatial distribution of aggregated catches make different contributions to the final estimates. In the run with spatial AIs only, although the uncertainty about local *SSB* is relatively high, the total SSB at the scale of the EC is precisely estimated (not shown) and the repartition is relatively balanced among the three subpopulations (Fig. 4a), which is consistent with the information provided by the spatial UKBTS AIs. When including spatial catches only (no spatial AIs), differences in *SSB* among subpopulations are higher (Fig. 4b), with higher estimates of *SSB* in the UK and East FR areas than in the West FR area, which is consistent with the higher proportion of catches observed in the East FR area (see Fig. S2.6 in Sup. Mat. S2). Finally, when assimilating all available data, uncertainty in SSB estimates is drastically reduced and the variability across subpopulations is shrunken (Fig. 4c) according to the information provided by the spatial AIs, and unbalanced catch ratios translate into unbalanced fishing mortality among subpopulations.

### 3.4. The effect of considering three isolated subpopulations on stock productivity

The effect of considering three isolated populations (instead of one homogeneous population) depends upon the spatial scale considered. The single-population model and the model considering three subpopulations provide similar estimates of *SSB*, recruitment and fishing mortality considered on the EC scale (Fig. 3a–c). These estimates were also consistent with ICES estimates, although overall they displayed a slightly higher *SSB* balanced by a lower *F*. However, the consideration of three subpopulations provides a spatial perspective on population dynamics. It also impacts inferences on stock productivity and therefore the assessment of stock status with respect to reference points.

#### 3.4.1. Reevaluation of the productivity of nurseries

The hypothesis on the spatial structure of the population strongly affects estimates of the carrying capacity per unit of surface (Fig. 5a), with *K* for the Somme nursery sector being largely reevaluated when considering a model structure with three isolated subpopulations, balanced by a decrease in estimates of *K* for all other nursery sectors. Estimates of parameters $\alpha$ for the UK West and Veys decrease when considering a model with three subpopulations, whereas the estimate increases for the Somme (Fig. 5b). Additional Figs. S3.3 and S3.6 in Sup. Mat. S3 provide a plot of the resulting Beverton-Holt curve in each nursery sector that illustrates the change in the local recruitment dynamics between the two model configurations.

As a result, the contributions of each nursery sector to recruitment in the EC are also strongly affected. In the single-population model, the Seine, Veys, UK West, Rye and Somme sectors contributed an average of 16, 3, 28, 24 and 29%, respectively, but with high variability among years (Fig. 6a). When considering three isolated subpopulations (Fig. 6b), these contributions were estimated at 14, 4, 17, 17 and 48% and were much less variable in time. At the subpopulation level, this translates into a strong increase in the contribution from East FR subpopulation (Somme: from 29% to 48%) balanced by decreases in contributions from West FR (Seine + Veys: from 19% to 18%) and UK subpopulations (UK West + Rye: from 52% to 34%).

Overall, those results are consistent with the high proportion of catches recorded in the East FR area (the area associated with the Somme nursery sector), logically leading to a high *SSB* in this area in the model that considers three subpopulations (Fig. 3d); in turn, this leads to higher recruitment in the Somme nursery sector.

#### 3.4.2. Management reference points and stock assessment

Whereas the results obtained on the scale of the entire EC indicate that the sole population is overexploited, the results obtained when considering a three-subpopulation structure revealed highly contrasting levels of exploitation among subpopulations.

When considering a single population, the average *SSB* and $F_{3-8}$ over the past four years were approximately 12,950 t and 0.38, respectively (Fig. 3a–c). $SSB_{MSY}$, $C_{MSY}$ and $F_{MSY}$ are estimated at

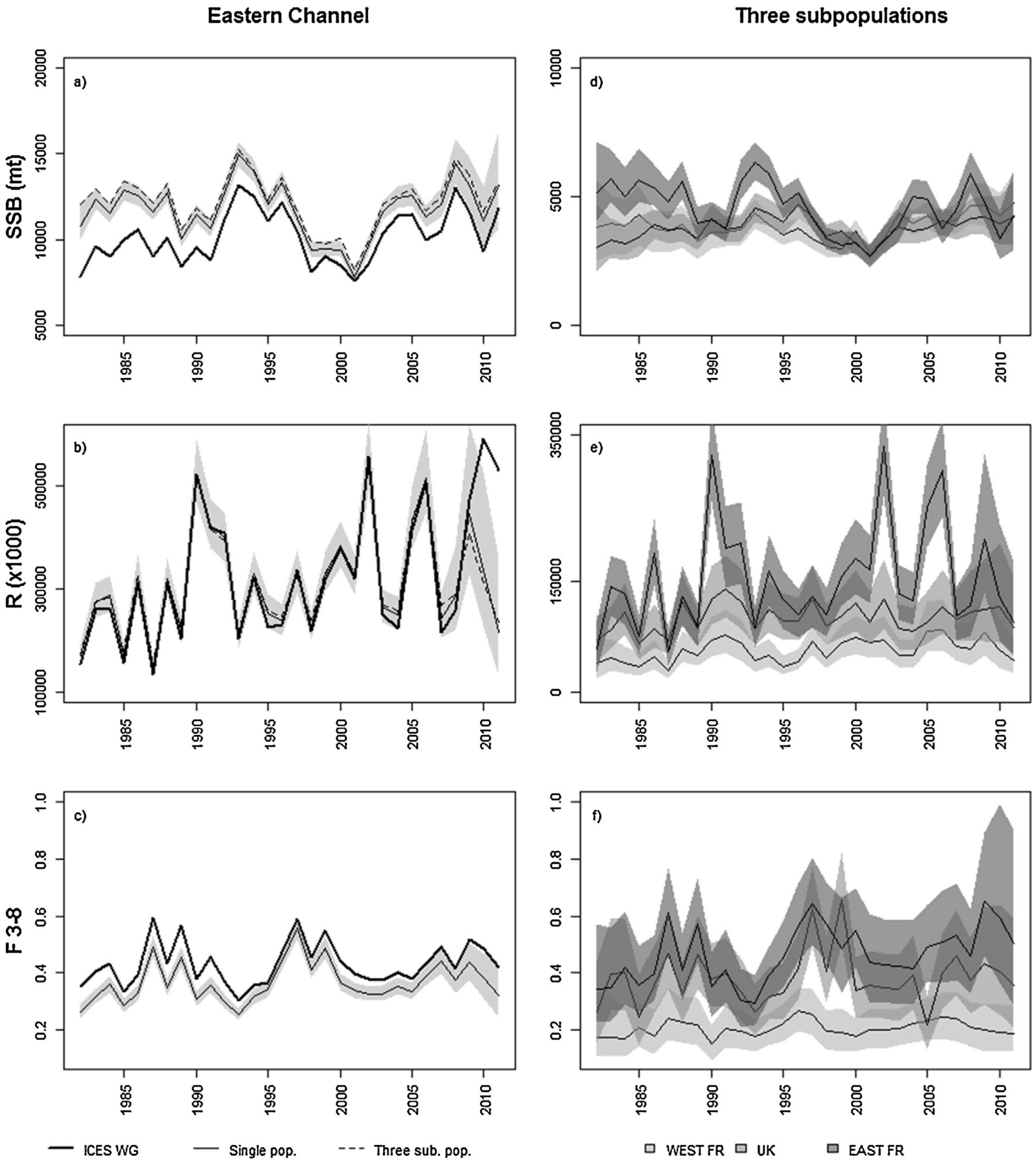

**Fig. 3.** Left column (a–c). Comparison of estimates of *SSB*, *R* and $F_{3-8}$ at the Eastern Channel scale obtained by the ICES WG (bold line), by the model considering one homogeneous adult population (solid line) and by the model considering three components of the adult population (dotted line). Right column (d–f). Estimates of *SSB*, *R* and $F_{3-8}$ for the three subpopulations. Solid lines: posterior medians. Shaded areas: 95% Bayesian credible intervals.

**Table 4**
Summary of point estimates of the management reference points $SSB_{MSY}$, $C_{MSY}$ and $F_{MSY}$ obtained in the models considering (i) a single population and (ii) three isolated subpopulations.

| Reference points | One single population | Three subpopulations | |
|---|---|---|---|
| $SSB_{MSY}$ | 28,090 | West FR | 4,880 |
| | | UK | 8,540 |
| | | East FR | 8,300 |
| $C_{MSY}$ | 5,470 | West FR | 870 |
| | | UK | 1,670 |
| | | East FR | 2,150 |
| $F_{MSY}$ | 0.21 | West FR | 0.19 |
| | | UK | 0.21 |
| | | East FR | 0.28 |

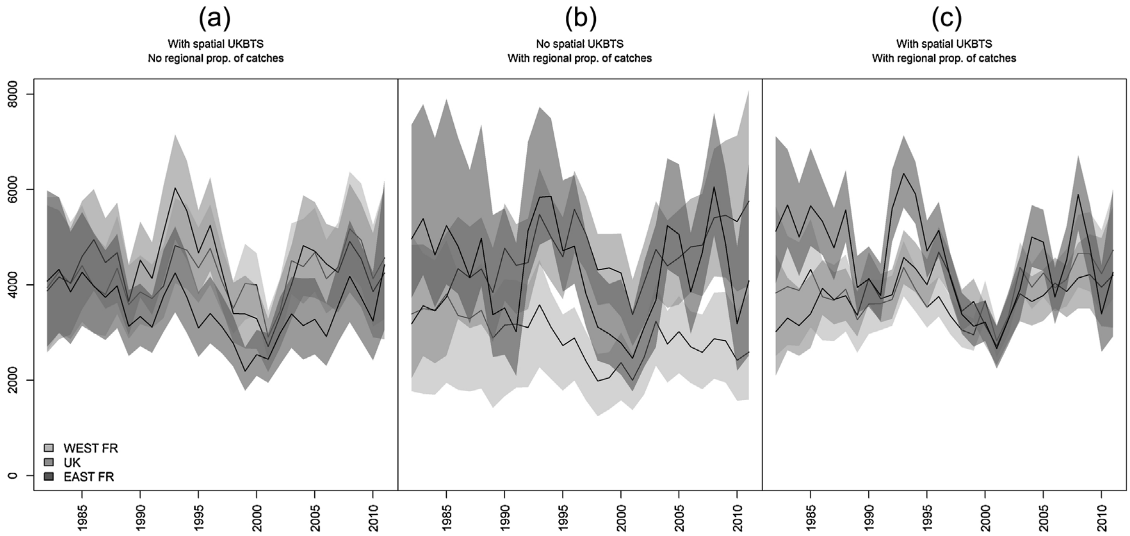

**Fig. 4.** Time series of posterior estimates of *SSB* for the three subpopulations obtained with the three data configurations of Table 2. Solid lines: posterior medians. Shaded areas: 95% Bayesian credibility intervals.

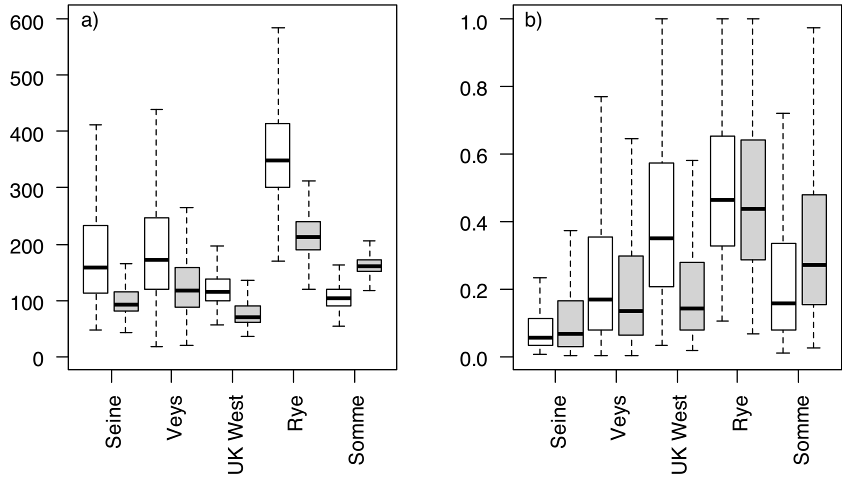

**Fig. 5.** Marginal posterior distributions of the nursery-specific Beverton-Holt parameters $K$ (a) and $\alpha$ (b) obtained with the model considering one homogeneous adult population (white) and with the model considering three isolated subpopulations (gray). $K$ is in thousands of fish per km$^2$. $\alpha$ is a maximum survival rate.

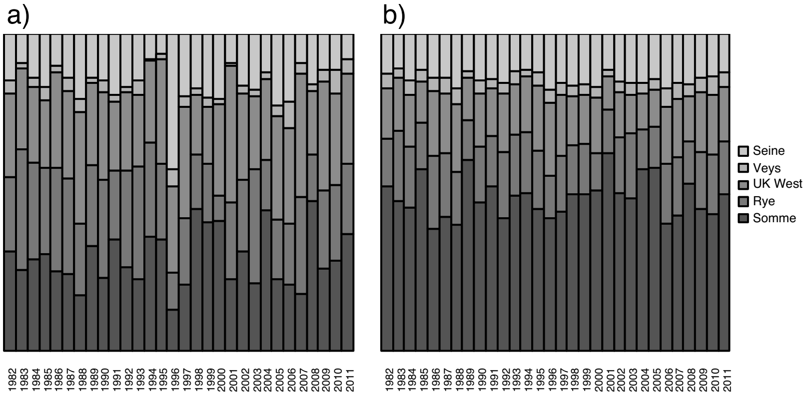

**Fig. 6.** Contributions of the five nursery sectors to the total 0+ recruitment obtained from the model considering (a) one single adult population and (b) three isolated subpopulations. The contribution is calculated from the posterior median estimates of the recruitment (age-0 abundance).

28,090 t, 5,470 t and 0.21, respectively (Table 4; Fig. 7a), thus indicating that the sole population is currently overexploited, with an average ratio of $F/F_{MSY}$ near 1.8 and that of $SSB/SSB_{MSY}$ near 0.5 during the last four years.

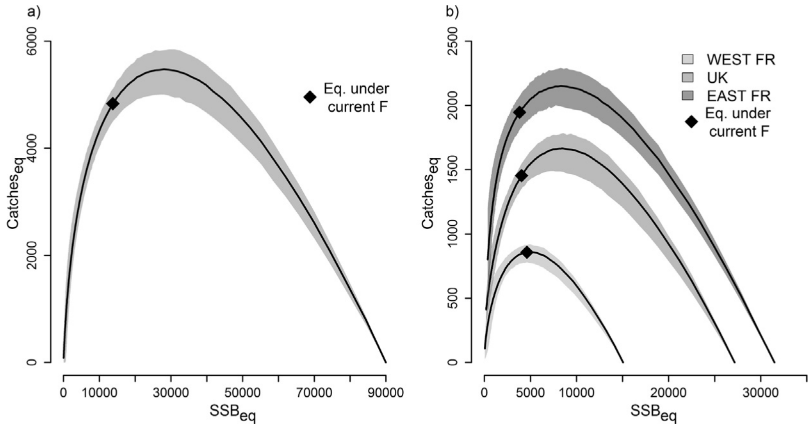

**Fig. 7.** Relation between the *SSB* and catches at equilibrium obtained through the simulation approach in the model considering (a) a single population and (b) three isolated subpopulations. Shaded area: 50% credibility interval obtained from the Monte Carlo simulation integrating both process and parameters uncertainty. Solid lines: posterior medians Black diamond: Eq. under current F represents the position on the equilibrium curve obtained with the current fishing mortalities (average over the 4 most recent years).

The model with three isolated populations provides a spatial perspective on the population dynamics and the impact of fishing pressure. Estimates of *SSB* among the various subpopulations (Fig. 3d) are essentially equivalent, with an average *SSB* of 4,570 t for the West FR subpopulation, 4,130 t for the UK subpopulation, and 4,590 t for the East FR subpopulation. By contrast, average *F* are highly contrasted among populations, with average *F* over the past 4 years estimated at 0.20, 0.39 and 0.55 for the West FR, UK and East FR subpopulations, respectively.

The reference points $SSB_{MSY}$, $C_{MSY}$, $F_{MSY}$ (Table 4; Fig. 7b) associated with each subpopulation were estimated at 4,880t, 870 t and 0.19 for West FR, 8,540 t, 1,670 t and 0.21 for UK and 8,300 t, 2,150 t and 0.28 for East FR, respectively. When considering the current state of exploitation (average over four years), it appears that the West FR subpopulation is at full exploitation level, with $F/F_{MSY}$ at 1.05 and $SSB/SSB_{MSY}$ at 0.94, whereas the UK and East FR subpopulations are overexploited (Fig. 7b), with $F/F_{MSY}$ dramatically greater than 1 (1.9 and 2.0, respectively) and $SSB/SSB_{MSY}$ dramatically lower than 1 (0.48 and 0.54, respectively).

## 4. Discussion

### 4.1. An integrated modeling framework for a better understanding of metapopulation dynamics

Our results make a significant contribution to the understanding of the sole population dynamics in the EC. The model used to assess the stock of the sole population in the EC considers a simple, homogeneous population with no spatial structure (ICES, 2013). Using the HBM framework, Rochette et al. (2013) make an important contribution by establishing the fundamental basis for a population model that embeds egg and larval drift and survival derived from an oceanic circulation model within a stage-structured life cycle, accounting for the spatial nature of the recruitment process in distinct coastal nursery sectors. The model presented here elaborates on Rochette et al. (2013) and provides additional insights into population dynamics by exploring a metapopulation structure with very low connectivity among three subpopulations. The capacity of Bayesian models to incorporate prior information also presented the possibility of an efficient use of the available information through the informative prior distribution for the maximum survival rate between settled larvae and 0+ juveniles derived from a meta-analysis on flatfish (Archambault et al., 2014).

The consideration of three loosely connected subpopulations increased the model's state-space dimension of the model. But because the two models integrate different sources of data (e.g., spatial AIs of adults and catches that are not included in the model considering one single homogeneous adult population), the usual goodness-of-fit criteria such as the deviance information criterion (Spiegelhalter et al., 2014) are not adapted to compare the trade-off between the two model structures' complexity and quality of fit. A posterior predictive check conducted for both model configurations did not reveal any strong, general inconsistencies between the fitted model and the different sources of data for both model configurations. Interestingly, when considering the data sources that are common to the two model configurations (*i.e.*, juveniles AIs, catch-at-ages and commercial CPUEs aggregated at the scale of the EC), both model configurations showed similar quality of fit. Additional results (not shown) indicate that the likelihood components restricted to the data shared by the two model structures are comparable between the two models.

However, although we were unable to demonstrate that the model considering three isolated subpopulations provides a better fit to the data, a body of ecological knowledge and clues continues to strongly argue for *a priori* consideration of such a metapopulation structure, and posterior inferences provide a portfolio of ecologically meaningful results.

First, strong prior knowledge exists in favor of the limited movements of juveniles (Coggan and Dando, 1988; Anon., 1989; Le Pape and Cognez, 2016) and adults (Kotthaus, 1963; Anon., 1965; Burt and Millner, 2008), and barriers linked to sediment structure limit exchanges between regions (Rochette et al., 2010, 2012). This knowledge was used *a priori* to define the spatial contours of three subpopulations of the common sole in the EC.

Second, taking into account the moderate connectivity between the successive life stages, we were able to produce a diagnosis of the population that, while consistent with ICES estimates at the scale of the EC, provided contrasting, meaningful results on a local scale. This approach allowed us to reconstruct local biomasses' evolution during the past three decades that were revealed as consistent with the time series of spatial abundance indices and catches. The consideration of three subpopulations also led to a substantial reevaluation of the productivity of the various nursery sectors that are quantitatively consistent with the juveniles AIs, catches and local biomasses estimated for their associated subcomponents. It also drastically reduced the between-years variability of the relative contribution of each nursery sector to total 0+ recruitment, which is consistent with both the concentration hypothesis (Rijnsdorp et al., 1992; Iles and Beverton, 2000; Rooper et al., 2004) and the low recruitment variability described for common sole (Le Pape et al., 2003b; Archambault et al., 2014).

Finally, results indicate that the spatial distribution of eggs derived from the fit of the model with three subpopulations with low connectivity matches the observed egg repartition derived from the 1991 eggs survey (Rochette et al., 2012). Because the comparison between the spatial distribution of eggs observed (1991) and simulated *a posteriori* by the model is not included in the likelihood function, this result can be considered as an element that validates the spatial structure of the adult population.

### 4.2. Weaknesses and directions for future research

Our modeling approach has some weaknesses. Below, we discuss some of those weaknesses along with some critical needs for knowledge and data about the spatial ecological process that the modeling approach has helped identify. Finally, we highlight a few research avenues that would improve both the knowledge and the models.

#### 4.2.1. Simulations to explore the tradeoff between model complexity and data availability

Several studies have shown that in the case of complex spatial population dynamics, the explicit consideration of spatial structures in stock-assessment models that are better aligned with ecological reality (instead of simpler models) provide better estimates, when sufficiently informative data are available (Hulson et al., 2013; Hintzen et al., 2015). However, our case study is a data-poor situation because only a few data provide information about the spatial structure of the population. In particular, no time series of spatial catch-at-age data are available. Thus, it is difficult to formally conclude that fitting a spatial structure to the available data results in reliable estimates of abundance and population dynamics. To reinforce the analysis, one interesting perspective for future work would consist of conducting simulations that would cross a few hypotheses about how the dynamics of the true population work with various model and data configurations for the statistical stock-assessment model. This would enable us not only to show which type of assessment might provide reliable estimates given our data limitations but also to illustrate how gathering more informative data about the spatial processes (for instance spatial catch-at-age or mark-recapture data) would improve the quality of our inferences.

#### 4.2.2. Sensitivity to priors

Uncertainty about estimates and sensitivity to the prior choice varied according to model compartment. As analyzed (with respect to a previous version of the model) by Rochette et al. (2013), numbers-at-age and all other variables associated with the demographic of ages 1–15, such as *SSB*, recruitment and fishing mortality, are estimated with low uncertainty. Indeed, the demographics of ages 1–15 consist of a catch-at-age model for 14 age classes tracked over 30 years; both catch and abundance indices are available for almost all years and ages.

By contrast, parameters for the density-dependent recruitment process in nursery sectors are estimated with much more uncertainty and are partly confounded. Those parameters are generally difficult to estimate from the data alone (Conn et al., 2010) and we therefore developed a method based on a previous *meta*-analysis on flatfish (Archambault et al., 2014) to build an informative prior distribution about the maximum survival rates of settled larvae on nursery ground ($\alpha$). Relying on a previous analysis by Rochette et al. (2013), our results are likely to be sensitive to the choice of priors on those parameters, and using weakly informative priors on the $\alpha_i$'s would certainly lead to poor inferences about stock productivity. Because the models developed in this manuscript have many similarities and the data are the same, and to keep the main message centered on the impact of changing the spatial structure of the model, we did not report any additional sensitivity analysis.

#### 4.2.3. Improving the model for the recruitment process

Based on previous modeling work by Rochette et al. (2013), strong hypotheses were made on the recruitment process: (i) Within each nursery sector, variability of the recruitment process was modeled as independent lognormal random noise, with no time series autocorrelation; (ii) The variance of lognormal process noise was considered homogeneous among nurseries; and (iii) Between-years random variations were considered as independent among nursery sectors. Consistent with results found by Rochette et al. (2013), a careful examination of the residual variability did not reveal any particular departure from the hypotheses of constant variance across the five nursery grounds and the time independence of residuals. This is consistent with previous analysis on the low synchronicity in inter-annual variability of juvenile abundance between the nursery sectors (Riou et al., 2001). Because there are many gaps in the time series of juvenile-abundance indices on nursery sectors (47% missing data; see Table 1), data are lacking to estimate parameters for the covariance in the recruitment process among nursery sectors. Including covariance in the recruitment process among nursery sectors would likely impact the population dynamics and stock assessment (Ranta et al., 1997; Liebhold et al., 2004). Therefore, an investigation of how the inclusion of covariance in the time series of recruitment process noise among nursery sectors would change estimates and population dynamics for the sole population in the EC would be an interesting focus for future research.

#### 4.2.4. The need for better knowledge of adult-mediated connectivity

Data on sub-adult and adult migration were lacking, and we were unable to estimate the degree of mixing among the three subpopulations. Our approach thus considered two extreme scenarios of adult-mediated connectivity: full connectivity and full spatial segregation between subpopulations associated with nursery sectors. Whereas a body of ecological knowledge advocates for a loose connectivity among the three subpopulations, improved data collection on movements and connectivity is a top priority. Natural markers, which include genetic markers, xenobiotics, stable isotopes, otolith microchemistry and parasites and their possible combination (Selkoe et al., 2008; Fodrie and Herzka, 2013), are a first source of data. The analysis of genetic-neutral markers could help infer population structure (Smedbol et al., 2002), although the open nature of the marine environment may prevent a significant signal from emerging (Waples, 1998; Exadactylos et al., 2003; Rolland et al., 2007). Recent approaches using genetic-adaptive markers (Diopere et al., 2013) and combined multi-marker approaches (Cuveliers et al., 2012) provide fruitful perspectives to quantify connectivity among marine subpopulations with a finer spatial resolution. Analyses of the differences in otolith elemental composition have been used to identify the estuarine origin of individuals (Cuveliers et al., 2010). Mark-recapture is also widely used to quantify migration (Hilborn, 1990; Rijnsdorp and Pastoors, 1995; Polacheck et al., 2010). Recent work focusing on older juvenile, sub-adult and adult flatfish emphasizes the interest of these approaches (Sackett et al., 2008; Fairchild et al., 2009; Furey et al., 2013). Future methodological work should include the development of integrated models that enables the consideration of multiple sources of data into space-structured population models (Darnaude and Hunter, 2008; Korman et al., 2012; Goethel et al., 2014).

### 4.3. *Implications for spatial management*

The sole population in the EC, like most exploited marine fish stocks, is currently assessed as a single population. However, our results suggest that the consideration of metapopulation dynamics strongly impacts inferences on stock productivity and conclusions about both stock assessment and (ultimately) fisheries advice.

The consideration of three subpopulations induced a substantial reevaluation of the productivity of the various nursery sectors; estimates of the contribution of the East FR subpopulation to the total recruitment doubled, balanced by a decrease in contributions from the West FR and UK subpopulations. Whereas results obtained on the scale of the entire EC indicate that the sole population is exploited far above MSY, assessments obtained when considering a three-subpopulation structure revealed highly contrasting levels of exploitation among subpopulations, with over-exploitation of some of the metapopulation components. Indeed, estimates of local management reference points associated with each subpopulation revealed that the West FR subpopulation is approaching full exploitation, whereas the UK and East FR subpopulations are over-exploited. The practical consequences of our conclusions may even increase when considering the local fisheries, which are characterized by fleets with limited movement, without large-scale tracking of fish (Tidd et al., 2015).

Beyond our case study, this work emphasizes the role of space in population functioning for species whose different life-history stages are segregated among specific habitats. Larval retention in marine populations is suspected to occur more than originally thought (Cowen et al., 2000; Warner and Cowen, 2002). Juvenile segregation in restricted nursery areas is also a common feature of fish populations (Vasconcelos et al., 2014). As noted by Frisk et al. (2014), our case study stresses the need to more thoroughly assess the importance of adult-mediated connectivity. Spatial integrated life-cycle models such as the one developed in this work provides a contribution to the quantitative assessment of spatial fishery and coastal habitat management plans. First, as previously shown by several authors, ignoring metapopulation structure in stock assessment models could result in local over/under exploitation (Tuck and Possingham, 1994; Ying et al., 2011; Yau et al., 2014) and improving data collection and statistical methods to estimate the parameters of spatial life-cycle models is a top priority for the optimal allocation of fishing pressure. Second, accounting for metapopulation dynamics is critical for an optimal assessment of essential habitat preservation and/or restoration that could be at least as efficient as assessing fishing pressure for restoring populations of nursery-dependent species (Levin and Stunz, 2005; van de Wolfshaar et al., 2011).

## Acknowledgements

This work was funded partly by the European Community's Seventh Framework Programme (FP7 2007–2013) under Grant Agreement No. 266445 for the project Vectors of Change in Oceans and Seas Marine Life, Impact on Economic Sectors (VECTORS). The authors thank the various people and institutes that provided data: the GIP Seine-Aval and Marie Laure Cochard, Paul Marchal and Marie Savina-Rolland (Ifremer). We are grateful to Sophie Pasquier for compiling the References.

## Appendix A.

### *Equations for the hierarchical Bayesian life-cycle model*

The equation below stand for the model considering three loosely connected subpopulations. The model is written in a state-space form that integrates stochasticity in both the process equations of the population dynamics (process errors) and the observation equations (observation errors). Following this logic, the Appendix below first provides the equation for the population dynamics and then provides the equation for the observation process.

Subscript $y$ denotes the years in the time series, $i$ denotes the nursery sector ($i = 1,\ldots,5$, with 1 = Seine, 2 = Veys, 3 = UK West, 4 = Rye, 5 = Somme), and $r$ denotes the component of the metapopulation ($r = 1$–$3$ with 1 = West FR, associated with nursery grounds Seine and Veys; 2 = UK, associated with nursery grounds UK West and Rye; 3 = East FR, associated with nursery ground Somme).

Prior distribution or fixed values for parameters are defined in Table A.1. The surface of each nursery sector (in $km^2$) is given in Table A.2.

#### *Process equations*

#### *Eggs and larval drift*

The number of settling larvae (i.e., post-larvae) in nursery sector $i$ at year $y$, $L_{y,i}$, is defined as follows:

$$L_{y,i} = \sum\nolimits_{r=1}^{r=3} \omega_{y,r} \cdot D_{y,r,i} \tag{A.1}$$

where $\omega_{y,r}$ is the egg pool for the subpopulation $r$ at year $y$ and $D_{y,r,i}$ is the probability of success for an egg from the egg pool $r$ to reach the nursery sector $i$ at year $y$ (fixed). The egg pool for each year and each subpopulation is calculated from the spawning stock biomass (all fish between age 3 and 15 take part in reproduction; ICES (2010)):

$$\omega_{y,r} = \sum\nolimits_{a\geq 3} N_{a,y,r} \cdot pf_a \cdot fec_{a,y} \tag{A.2}$$

where $pf_a$ is the proportion of females for age class $a$ (known, considered constant over the time series and homogeneous across areas), and $fec_{a,y}$ is the number of eggs per female of age $a$, calculated from the weight at age $w_{a,y}$ as (ICES, 2010; Rochette et al., 2012):

$$fec_{a,y} = e^{5.6+1.17*\log\left(w_{a,y}\right)} \tag{A.3}$$

#### *Post-larvae to juvenile on nursery grounds, from settlement to summer's end.*

The expected number of age-0 fish at year $y$ in nursery $i$, $E\left(N_{0_{y,i}}\right)$, is defined from a density dependent lognormally distributed around an expected mean defined from a Beverton-Holt equation parameterized with $\alpha_i$, the nursery-specific maximum survival rate (estimated); $K_i$, the nursery-specific carrying capacity per unit of surface (1000 fish$\cdot km^{-2}$, estimated); and $S_i$, the surface of nursery sector $i$ ($km^2$, fixed; Table A.2):

$$E\left(N_{0_{y,i}}\right) = \frac{\alpha_i \cdot L_{y,i}}{1 + \frac{\alpha_i}{K_i \cdot S_i} \cdot L_{y,i}} \tag{A.4}$$

Unexplained random variations are captured by independent lognormal random noise with the same variance $\sigma^2_{BH}$ for all nurseries (estimated):

$$N_{0,y,i} = E\left(N_{0_{y,i}}\right) \cdot e^{\varepsilon_{L,y,i} - 0.5\cdot\sigma^2_{BH}} \tag{A.5}$$

#### *Natural mortality of age 0 from summer's end to December*

The number of age-1 fish in nursery $i$, $N_{1,y+1,i}$, is defined as

$$N_{1,y+1,i} = N_{0,y,i} \cdot e^{-1/3\cdot M_0} \,.\, e^{\varepsilon_{0,y,i} - 0.5\cdot\sigma_0^2} \tag{A.6}$$

where $N_{0,y,i}$ is the number of age-0 fish in the nursery $i$, $M_0$ is the annual natural mortality rate at age 0 (fixed) and $\varepsilon_{0,y,i}$ is normal environmental noise with variance $\sigma_0^2$ (estimated).

**Table A.1**
Prior distribution (or fixed values) for the parameters of the Hierarchical Bayesian Life-cycle Model.

| Parameters | Value/prior/structure | Description |
|---|---|---|
| $M_a$ | Age 0: 1.5; Age 1: 2.6; Age 3–11: 0.1; Age 12: 0.2; Age 13: 0.3; Age 14: 0.4; Age 15: 0.5 | Natural mortality at age $a$ ($y^{-1}$) |
| $S_a$ | $a_{50} \sim Gamma\left(E=3, CV=0.1\right)$<br>$\delta \sim Gamma\left(E=1, CV=0.2\right)$ | Age-specific gear selectivity<br>Logistic curve parameterized with ($a_{50}$, $\delta$).<br>$a_{50}$: the age at which $S_a=0.5$; $\delta$: the difference (in years) between $S_a=0.25$ and $S_a=0.75$<br>$S_a$ is scaled to 1 for a=15. |
| $\sigma_p^2$ | $\sigma_p^2=0.001$ | Variance of process errors on the dynamics of adult stages (fixed to a very low value) |
| $E_{y,r}$ | $log\left(E_{y=1,r}\right) \sim Norm\left(E=0, \sigma=\sqrt{10}\right)$ | Fishing effort |
| | $\log\left(E_{y,r}\right) \sim Norm\left(E=log\left(E_{y-1,r}\right), \sigma_E\right)$<br>$\sigma_E \sim Unif\left(0.01, 0.5\right)$ | Prior defined as a random walk in the log-scale |
| $\mathrm{F_{a,y,r}}$ | $\mathrm{F_{a,y,r} \sim Gamma\left(E=E_{y,r}\cdot S_a, CV_F\right)}$ | Fishing mortality |
| | $\mathrm{CV_F \sim Unif\left(0, 1\right)}$ | Exchangeable hierarchical structure |
| $\alpha_i$ | $log\left(\alpha_i\right) \sim Norm\left(E=\mu_{log\alpha}, \sigma=\sigma_{log\alpha}\right)[,0]$ | Nursery-specific maximum survival rates |
| | $\mu_{log\alpha} \sim Norm\left(E=-3, \sigma=\sqrt{0.1}\right)$<br>$\sigma_{log\alpha} \sim \mathrm{Unif}\left(0, 2.5\right)$ | Hierarchical structure with informative priors derived from Archambault et al. (2014) |
| $K_i$ | $K_i \sim Norm\left(E=\mu_K, \sigma=\sigma_K\right)1_{>0}$<br>$\mu_K \sim Norm\left(E=100, \sigma=100\right)$ | Nursery-specific carrying capacity per unit of surface (1000 fish · km$^{-2}$) |
| | $\sigma_K \sim \mathrm{Unif}\left(10, 300\right)$ | Hierarchical structure with weakly informative priors |
| $\sigma_{BH}^2$ | $log({\sigma^2}_{BH}) \sim \mathrm{Unif}(-10{,}10)$ | Variance of process errors on the post-larvae to juvenile BH relationship |
| $\sigma_0^2$ | $\log({\sigma^2}_0) \sim \mathrm{Unif}(-10{,}10)$ | Variance of process errors from age-0 to age-1 fish |
| $\sigma_{I_{juv}}^2$ | $\sigma_{I_{juv}}^2 \sim Unif\left(-10, 10\right)$ | Variance of observation errors on surveys of juveniles on nurseries |
| $\sigma_{I_{Ad}}^2$ | $\sigma_{I_{Ad}}^2 \sim Unif\left(-10, 10\right)$ | Variance of observation errors on all abundance indices of adults (UKCBT, BECBT, UKBTS) |
| $\sigma_C^2$ | $\sigma_C^2 \sim Unif\left(-10, 10\right)$ | Variance of observation errors on catches |
| $q_0$ | $log\left(q_0\right) \sim Unif\left(-10, 10\right)$ | Catchability of age-0 |
| $q_1$ | $log\left(q_1\right) \sim Unif\left(-10, 10\right)$ | Catchability of age-1 |
| $q_{fleet}$ | $log\left(q_{fleet}\right) \sim Unif\left(-10, 10\right)$ | Catchability related to abundance indices of adults (fleet: UKCBT, BECBT, UKBTS) |

**Table A.2**
Surface of nursery sector $i$ ($km^2$). All surfaces are derived from the habitat suitability model in Rochette et al. (2010).

| Subpopulation | Nursery sector | Surface (km$^2$) |
|---|---|---|
| West | Seine ($i=1$) | 967 |
| Fr | Veys ($i=2$) | 320 |
| UK ($r=1$) | UK West ($i=3$) | 1650 |
| ($r=2$) | Rye ($i=4$) | 504 |
| East FR ($r=3$) | Somme ($i=5$) | 1680 |

*Natural and fishing mortality at age 1 and emigration from nursery to adult population*

The number of age-2 fish in nursery $i$ at the very beginning of year $y+1$, $N_{2,y+1,i}$, is defined as

$$N_{2,y+1,i} = N_{1,y,i}.e^{-Z_{1,y,i}} \cdot e^{\varepsilon_{1,y,i}-0.5\cdot\sigma_p^2} \tag{A.7}$$

where $Z_{1,y,i} = M_1 + F_{1,y,r}$ is the total mortality, $M_1$ is the annual natural mortality rate at age 1 (fixed), $F_{1,y,r}$ is the fishing mortality in subpopulation $r$ associated with nursery $i$ (estimated), and $\varepsilon_{1,y,i}$ is normal environmental noise with variance $\sigma_p^2$.

Age-2 fish leave nurseries at the very beginning of the year and are supposed to contribute directly to the subpopulation $r$ adjacent to the nursery. Fish from the Seine and Veys nurseries contribute to subpopulation $r=1=$ West FR; UK West and Rye nurseries contribute to subpopulation $r=2=$ UK; and the Somme nursery contributes to subpopulation $r=3=$ East FR. Starting from $N_{2,y+1,i}$ as defined in Eq. (A.7), the number of age-2 fish in each subpopulation $r$, $N_{2,y+1,r}$ (note the subscript $r$ and not $i$), is defined as follows:

$$\begin{cases} \mathrm{N}_{2,y+1,r=1} = \sum_{i=1}^{i=2} \mathrm{N}_{2,y+1,i} \\ \mathrm{N}_{2,y+1,r=2} = \sum_{i=3}^{i=4} \mathrm{N}_{2,y+1,i} \\ \mathrm{N}_{2,y+1,r=3} = \mathrm{N}_{2,y+1,i=5} \end{cases} \tag{A.8}$$

*Natural and fishing mortality at the adult stage*

The number of fish from age 2–15 then follows the classical dynamics:

$$N_{a+1,y+1,r} = N_{a,y,r}.e^{-Z_{a,y,r}} \cdot e^{\varepsilon_{a,y,r}-0.5\cdot\sigma_p^2} \tag{A.9}$$

where $N_{a,y,r}$ is the number of fish of age $a$ in component $r$ at year $y$, $Z_{a,y,r}$ is the total mortality rate and $\varepsilon_{a,y,r}$ is a normal environmental noise with variance $\sigma_p^2$. All remaining fish are assumed to die at age 15.

*Model for total mortality Z*

$Z_{a,y,r}$ is defined as the sum of natural mortality $M_a$, considered constant across years and subpopulations (Table A.1), and fishing mortality $F_{a,y,r}$. For any given age, year and subpopulation r, the expected mean of the fishing mortality is defined as $E\left(F_{a,y,r}\right) = S_a \cdot E_{y,r}$ with $S_a$ as an age-specific selectivity (logistic function considered homogeneous in time and space, estimated, Table A.1) and $E_{y,r}$ as the fishing effort specific to each year and subpopulation. The time variability of fishing effort $E_{y,r}$ was a priori modeled as a random walk in the log-scale (Table A.1). Additional random variability of $F_{a,y,r}$ around the expected mean $E\left(F_{a,y,r}\right)$ was captured through a random gamma hierarchical structure with the coefficient of variation $CV_F$ (Table A.1).

*Observation equations*

*Juvenile abundance indices*

The abundance indices of age-0 and age-1 juveniles in nursery $i$ are considered as lognormal random observations of abundance $N_{0,y,i}$ and $N_{1,y,i}$, respectively:

$$I_{0,y,i} = q_0 \cdot N_{0,y,i} \cdot e^{\varepsilon_{I_{0,y,i}}-0.5\cdot\sigma_{I_{juv}}^2} \tag{A.10}$$

$$I_{1,y,i} = q_1 \cdot N_{1,y,i} \cdot e^{\varepsilon_{I_{1,y,i}}-0.5\cdot\sigma_{I_{juv}}^2} \tag{A.11}$$

with $q_0$ and $q_1$ the age-specific catchability, $\varepsilon_{I_0,y,i}$ and $\varepsilon_{I_1,y,i}$ independent normal random noise with the same observation error variance $\sigma^2_{I_{juv}}$ (estimated).

*Adult abundance indices*

In the model considering three subpopulations, three time series of abundance indices (AI) of age-2 to age-15 fish are used: CPUEs from the UK and Belgium commercial fleet (UKBCT and BEBCT, respectively), both of which are available on the scale of the entire Eastern Channel, and UK bottom-trawl surveys available for each subpopulations ($r = 1, 2, 3$). One observation equation is written for each AI, with each observation equation contributing to the whole likelihood function. The same general form of observation equation is used for all AIs, which are all considered as lognormal random observations of the abundance at age but with parameters specific for the fleet (UKBCT, BEBCT, UKBTS) age, year (and eventually subpopulation for UKBTS):

$$AI_{fleet_{a,y,(r)}} = q_{fleet} \cdot S_a \cdot N_{a_{y,i,(r)}} \cdot e^{\varepsilon_{\mathrm{fleet,a},y,(r)} - 0.5 \cdot \sigma^2_{I_{Ad}}} \tag{A.12}$$

where $AI_{fleet_{a,y,(r)}}$ is the observed AI of age $a$ at year $y$ on a different spatial scale (in subpopulations $r$ for the UKBTS survey; in the whole EC for other indices),$q_{fleet}$ is the fleet-specific catchability, $S_a$ is the age-specific selectivity (considered homogeneous among fleets), and $\varepsilon_{\mathrm{fleet,a},y,(r)}$ is independent random noise with the same observation error variance $\sigma^2_{I_{Ad}}$ (estimated; homogeneous among fleets).

*Catches-at-age aggregated on the scale of the Eastern Channel*

Catches-at-age predicted by the model ($H_{a,y,r}$) were calculated for each subpopulation with the standard Baranov equation:

$$H_{a,y,r} = N_{a,y,r} \cdot \left( \frac{F_{a,y,r}}{F_{a,y,r} + M_a} \right) \cdot (1 - e^{-(F_{a,y,r} + M_a)}) \tag{A.13}$$

Annual catches-at-age ($C_{a,y}$; observed) were available from stock assessment reports only on the scale of the Eastern Channel; however, they were not available separately for the three subpopulations. Catches-at-age predicted by the model were then first aggregated at the scale of the Eastern Channel ($H_{a,y} = \sum_{r=1}^{r=3} H_{a,y,r}$) and considered observed with lognormal errors:

$$C_{a,y} = H_{a,y} \cdot e^{\varepsilon_{Ca,y} - 0.5 \cdot \sigma^2_C} \tag{A.14}$$

where $\varepsilon_{Ca,y}$ are independent normal random noise with observation error variance $\sigma^2_C$ (estimated).

*Spatial repartition of catches (weight) among subpopulations*

A likelihood function for the catch weight ratio per subpopulation ($pw_{t,r}$, $\sum_{r=1:3} pw_{t,r} = 1$) was also incorporated into the model. The catch weight ratio was originally available using the ICES statistical rectangle from 2003 to 2011; however, it was here aggregated at the scale of the three areas associated with each subpopulation. Before 2003, the catch weight ratio per subpopulation was derived from the catch ratio per country (weight; known for the entire time series) combined with the average repartition of catches (weight) among the three areas calculated for each country over the most recent time series 2003–2011. This procedure only assumes a constant spatial repartition of national fleets among the three areas and is a reasonable hypothesis because no major change in the national fleet strategies has been observed between 1982 and 2011 (Y. Vermard, com. Pers.). The catch ratio predicted by the model ($\pi_{y,r}$) was calculated from the catches-at-age predicted by the model ($C_{a,y,r}$) and the weight-at-age ($w_{a,y}$; observed). A Dirichlet likelihood function was used to capture observation errors between the observed and predicted catch ratio. The predicted catch weight ratio was scaled to mimic the precision that would be obtained with a sample of 500 tones:

$$(pw_{t,r=1}, pw_{t,r=2}, pw_{t,r=2}) \sim \mathrm{Dirichlet}(500 \times (\pi_{t,r=1}, \pi_{t,r=2}, \pi_{t,r=3})) \tag{A.15}$$

*Parameters and priors*

Prior distributions or fixed values of parameters are given in Table A.1. Following Rochette et al. (2013), informative priors were set for parameters of the selectivity $S_a$, based on ICES (2013). The priors on the carrying capacity of nursery sectors, $K_i$'s, were weakly informative in the sense of Gelman (2009), i.e., it allows the data to speak while being strong enough to exclude unrealistic values (the 90% percentile of the prior predictive distribution is more than 100 times greater than the highest estimated density in nurseries of the Bay of Biscay; Le Pape et al., 2003a).

Informative priors were set on the nursery-specific maximum survival rates $\alpha_i$. Taking away the EC sole dataset from the database used for the meta-analysis in Archambault et al. (2014), the posterior predictive distribution of $\alpha$ was derived and considered to build an informative prior for this study. The method developed in Archambault et al. (2014) provides a predictive distribution for the slope at origin calculated from a Beverton-Holt relationship calculated from egg-to-egg (denoted $\alpha_{meta}$). By contrast, parameter $\alpha$ in our model (denoted $\alpha_{HBM}$) stands for the survival rate from settled larvae to 0+ juveniles (in September). To transfer the information from $\alpha_{meta}$ to $\alpha_{HBM}$, average demographic parameters specific to the Eastern Channel were used to complete the life cycle from the age-0 juveniles in September to eggs:

$$S_{\omega-L} \cdot \alpha_{HBM} \cdot e^{-M_0 \cdot 4/12} \cdot \overline{Fec} \cdot SPR_{F=0} = \alpha_{meta} \tag{A.16}$$

with $S_{\omega-L}$ as the average eggs to post-larvae survival, $\overline{Fec}$ as the average fecundity, $SPR_{F=0}$ the spawning biomass produced in the absence of fishing and $e^{-M_0 \cdot 4/12}$ as the natural mortality from observation in September to recruitment at age 1 in January. Finally, because the meta-analysis of Archambault et al. (2014) was derived using recruitment estimated by ICES (recruitment at age 1 back-calculated from age 2), we also took into account the differences between the mortality used by ICES $\left(\mathrm{M}_{1_{\mathrm{ICES}}} = 0.1\right)$ and the one used in our model $\left(\mathrm{M}_{1_{\mathrm{ICES}}} = 2.6\right)$. The following final equation was then used to scale the posterior predictive of $\alpha_{meta}$ to obtain the informative prior of $\alpha_{HBM}$:

$$\alpha_{\mathrm{HBM}} = \frac{\alpha_{\mathrm{meta}}}{\mathrm{S}_\omega - \mathrm{L} \cdot \mathrm{e}^{-\mathrm{M}_0 \cdot 4/12 \cdot \mathrm{Fec} \cdot \mathrm{SPR}_{\mathrm{F}=0}}} . \mathrm{e}^{\mathrm{M}_{1_{\mathrm{HBM}}} - \mathrm{M}_{1_{\mathrm{ICES}}}} \tag{A.17}$$

## Appendix B.

*Catches at equilibrium as a function of fishing mortality*

Empirical equilibrium curves were obtained by Monte Carlo simulations. The population was simulated with constant $F$ in time and space during 200 years to reach an equilibrium state. Results obtained by varying $F$ in a wide range (from 0 to 2, with a step of 0.01) were used to empirically construct the equilibrium curve relating Catches and $SSB$ at equilibrium, thus enabling the estimation of management reference points such as $B_{MSY}$, $F_{MSY}$ and $C_{MSY}$. Drift and survival parameters for eggs and larvae were considered constant during the simulations and set to their average values (1982–2007). In the model considering three subpopulations, reference equilibrium points for each subpopulation $r$ (denoted $B_{MSY,r}$, $F_{MSY,r}$ and $C_{MSY,r}$) were estimated conditionally by fixing the fishing pressure for the two other subpopulations equal to the estimates averaged over the last five years of the data series (2007–2011).

Monte Carlo simulations were run to account for both process errors and parameters uncertainty. For a given value of $F$, the population dynamics was simulated over 200 years, including process error. The equilibrium (ergodic) state is considered after 100 years of simulation and the process error was integrated out by considering the distribution of the results between year 101 and 200. To integrate the parameter uncertainty, the procedure was repeated

1500 times with 1500 sets of parameters directly drawn in the joint posterior distribution of model parameters, ensuring that the statistical covariance structure between the parameters is fully accounted for (Punt and Hilborn, 1997; Parent and Rivot, 2013).

## Appendix C. Supplementary data

Supplementary data associated with this article can be found, in the online version, at http://dx.doi.org/10.1016/j.fishres.2016.03.023.

## References

Anon, 1965. Report of the working group on sole. ICES Coop. Res. Rep. 5, 1–126.

Anon., 1989. Report of ad hoc study group on juvenile sole tagging. ICES CM 1989/G: 21, 34pp.

Archambault, B., Le Pape, O., Bousquet, N., Rivot, E., 2014. Density-dependence can be revealed by modelling the variance in the stock–recruitment process: an application to flatfish. ICES J. Mar. Sci. 71 (8), 2127–2140.

Botsford, L.W., Brumbaugh, D.R., Grimes, C., Kellner, J.B., Largier, J., O'Farrell, M.R., Ralston, S., Soulanille, E., Wespestad, V., 2009. Connectivity, sustainability, and yield: bridging the gap between conventional fisheries management and marine protected areas. Rev. Fish Biol. Fish. 19, 69–95.

Buckland, S.T., Newman, K.B., Fernández, C., Thomas, L., Harwood, J., 2007. Embedding population dynamics models in inference. Stat. Sci. 22 (1), 44–58.

Burt, G.J., Millner, R.S., 2008. Movements of sole in the southern North Sea and eastern English Channel from tagging studies (1955–2004). Sci. Ser. Tech. Rep. 44.

Carruthers, T.R., McAllister, M.K., Taylor, N.G., 2011. Spatial surplus production modeling of Atlantic tunas and billfish. Ecol. Appl. 21, 2734–2755.

Carson, H.S., Cook, G.S., López-Duarte, P.C., Levin, L.A., 2011. Evaluating the importance of demographic connectivity in a marine metapopulation. Ecology 92, 1972–1984.

Chambers, R.C., Trippel, E.A., 1997. Early Life History and Recruitment in Fish Populations. Chapman and Hall, New York.

Cianelli, L., Fisher, J., Skern-Mauritzen, M., Hunsicker, M., Hidalgo, M., Frank, K., Bailey, K., 2013. Theory, consequences and evidence of eroding population spatial structure in harvested marine fishes: a review. Mar. Ecol. Prog. Ser. 480, 227–243.

Clark, J.S., 2005. Why environmental scientists are becoming Bayesians? Ecol. Lett. 8, 2–14.

Coggan, R.A., Dando, P.R., 1988. Movements of juvenile dover sole, *solea solea* (L.), in the tamar estuary, south-western england. J. Fish Biol. 33, 177–184.

Conn, P.B., Williams, E.H., Shertzer, K.W., 2010. When can we reliably estimate the productivity of fish stocks? Can. J. Fish. Aquat. Sci. 67, 511–523.

Cowen, R.K., Lwiza, K.M.M., Sponaugle, S., Paris, C.B., Olson, D.B., 2000. Connectivity of marine populations: open or closed? Science 287, 857–859.

Cunningham, C., Reid, D., McAllister, M., Kirkwood, G., Darby, C., 2007. A Bayesian state-space model for mixed-stock migrations, with application to Northeast Atlantic mackerel Scomber scombrus. Afr. J. Mar. Sci. 29 (3), 347–367.

Cuveliers, E.L., Geffen, A.J., Guelinckx, J., Raeymaekers, J.A.M., Skadal, J., Volckaert, F.A.M., Maes, G.E., 2010. Microchemical variation in juvenile *Solea solea* otoliths as a powerful tool for studying connectivity in the North Sea. Mar. Ecol. Prog. Ser. 401, 211–220.

Cuveliers, E., Larmuseau, M., Hellemans, B., Verherstraeten, S., Volckaert, F., Maes, G., 2012. Multi-marker estimate of genetic connectivity of sole (*Solea solea*) in the North-East Atlantic Ocean. Mar. Biol. 159, 1239–1253.

Darnaude, A., Hunter, E., 2008. Coupled use of data storage tags and otolith microchemistry to assess population dispersal and intra-specific diversity in migratory behaviour in North Sea plaice (*Pleuronectes platessa* L.). Comp. Biochem. Phys. A 150, S205.

Diopere, E., Hellemans, B., Volckaert, F.A.M., Maes, G.E., 2013. Identification and validation of single nucleotide polymorphisms in growth- and maturation-related candidate genes in sole (*Solea solea* L.). Mar. Genom. 9, 33–38.

Drouineau, H., Mahévas, S., Bertignac, M., Duplisea, D., 2010. A length-structured spatially explicit model for estimating hake growth and migration rates. ICES J. Mar. Sci. 67 (8), 1697–1709.

Exadactylos, A., Geffen, A.J., Panagiotaki, P., Thorpe, J.P., 2003. Population structure of Dover sole *Solea solea*: rAPD and allozyme data indicate divergence in European stocks. Mar. Ecol. Prog. Ser. 246, 253–264.

Fairchild, E.A., Rennels, N., Howell, H., 2009. Using telemetry to monitor movements and habitat use of cultured and wild juvenile winter flounder in a shallow estuary. In: Tagging and Tracking of Marine Animals with Electronic Devices. Springer, Netherlands, pp. 5–22.

Fodrie, F., Herzka, S., 2013. A comparison of otolith geochemistry and stable isotope markers to track fish movement: describing estuarine ingress by larval and post-larval halibut. Estuaries Coasts 39, 906–917.

Frisk, M.G., Jordaan, A., Miller, T.J., 2014. Moving beyond the current paradigm in marine population connectivity: are adults the missing link? Fish Fish. 15 (2), 242–254.

Furey, N., Dance, M., Rooker, J., 2013. Fine-scale movements and habitat use of juvenile southern flounder Paralichthys lethostigma in an estuarine seascape. J. Fish Biol. 82, 1469–1483.

Gaines, S.D., White, C., Carr, M.H., Palumbi, S.R., 2010. Designing marine reserve networks for both conservation and fisheries management. Proc. Natl. Acad. Sci. 107, 18286–18293.

Gallego, A., North, E.W., Houde, E.D., 2012. Understanding and quantifying mortality in pelagic, early life stages of marine organisms—old challenges and new perspectives. J. Mar. Syst. 93, 1–3.

Gelman, A., Carlin, J.B., Stern, H.S., Rubin, D.B., 2004. Bayesian Data Analysis. Chapman & Hall/CRC, Boca Raton, London, New York (717 pp.

Gelman, A., 2009. Bayes, Jeffreys, prior distributions and the philosophy of statistics. Stat. Sci. 24 (2), 176–178.

Gibson, R.N., 2005. Flatfishes: Biology and Exploitation. Wiley, Oxford, UK (419 pp).

Goethel, D.R., Legault, C.M., Cadrin, S.X., 2014. Demonstration of a spatially explicit, tag-integrated stock assessment model with application to three interconnected stocks of yellowtail flounder off of New England. ICES J. Mar. Sci. 72 (1), 164–177.

Grüss, A., Kaplan, D., Guenette, S., Roberts, C., Botsford, L., 2011. Consequences of adults and juvenile movement for marine protected areas. Biol. Conserv. 144, 692–702.

Grosberg, R.K., Levitan, D.R., 1992. For adults only?: supply-side ecology and the history of larval biology. Trends Ecol. Evol. 7, 130–133.

Guan, W., Cao, J., Chen, Y., Cieri, M., 2013. Impacts of population and fishery spatial structures on fishery stock assessment. Can. J. Fish. Aquat. Sci. 70, 1178–1189.

Hellberg, M.E., Burton, R.S., Neigel, J.E., Palumbi, S.R., 2002. Genetic assessment of connectivity among marine populations. Bull. Mar. Sci. 70, 273–290.

Hilborn, R., Walters, C.J., 1992. Quantitative fisheries stock assessment: choice, dynamics and uncertainty. Rev. Fish Biol. Fish. 2, 177–178.

Hilborn, R., 1990. Determination of fish movement patterns from tag recoveries using maximum likelihood estimators. Can. J. Fish. Aquat. Sci. 47, 635–643.

Hinrichsen, H.-H., Dickey-Collas, M., Huret, M., Peck, M.A., Vikebø, F.B., 2011. Evaluating the suitability of coupled biophysical models for fishery management. ICES J. Mar. Sci. 68, 1478–1487.

Hintzen, N.T., Roel, B., Benden, D., Clarke, M., Egan, A., Nash, R.D.M., Rohlf, N., Hatfield, E.M.C., 2015. Managing a complex population structure: exploring the importance of information from fisheries-independent sources. ICES J. Mar. Sci. 72 (2), 528–542.

Hulson, P.J.F., Quinn, T.J., Hanselman, D.H., Ianelli, J.N., 2013. Spatial modeling of Bering Sea walleye pollock with integrated age-structured assessment models in a changing environment. Can. J. Fish. Aquat Sci. 70 (9), 1402–1416.

ICES, 2010. Report of the Working Group on the Assessment of Demersal Stocks in the North Sea and Skagerrak (WGNSSK), 5–11 May 2010. ICES CM 2010/ACOM:13. Copenhagen, ICES Headquarters, 1058 pp.

ICES, 2013. Report of the Working Group on the Assessment of Demersal Stocks in the North Sea and Skagerrak (WGNSSK), 24–30 April 2013, ICES Headquarters, Copenhagen. ICES Document CM 2013/ACOM:13. 1435 pp.

Iles, T.C., Beverton, R.J.H., 2000. The concentration hypothesis: the statistical evidence. ICES J. Mar. Sci. 57, 216–227.

Korman, J., Martell, S.J.D., Walters, C.J., Makinster, A.S., Coggins, L.G., Yard, M.D., Persons, W.R., 2012. Estimating recruitment dynamics and movement of rainbow trout (*Oncorhynchus mykiss*) in the Colorado River in Grand Canyon using an integrated assessment model. Can. J. Fish. Aquat. Sci. 69 (11), 1827–1849.

Kotthaus, A., 1963. Tagging experiments with the North Sea sole (*Solea solea*) in 1959 and 1960. In: Special Publication Number 4 of the International Commission for the Northwest Atlantic Fisheries. Headquarters of the Commission, Darthmouth, Nova Scotia, Canada, pp. pp. 123–129.

Le Pape, O., Bonhommeau, S., 2015. The food limitation hypothesis for juvenile marine fish. Fish Fish. 16 (3), 373–398.

Le Pape, O., Cognez, N., 2016. The range of juvenile movements of estuarine and coastal nursery dependent flatfishes: estimation from a meta-analytical approach. J. Sea Res. 107 (1), 43–55.

Le Pape, O., Chauvet, F., Mahévas, S., Lazure, P., Guérault, D., Désaunay, Y., 2003a. Quantitative description of habitat suitability for the juvenile common sole (*Solea solea*, L.) in the Bay of Biscay (France) and the contribution of different habitats to the adult population. J. Sea Res. 50, 139–149.

Le Pape, O., Chauvet, F., Désaunay, Y., Guérault, G., 2003b. Relationship between interannual variations of the river plume and the extent of nursery grounds for the common sole (*Solea solea*, L.) in Vilaine Bay. Effects on recruitment variability. J. Sea Res. 50, 177–185.

Levin, P.S., Stunz, G.W., 2005. Habitat triage for exploited fishes: can we identify essential 'Essential Fish Habitat? Estuarine Coastal Shelf Sci. 64, 70–78.

Liebhold, A., Koenig, W.D., Bjørnstad, O.N., 2004. Spatial synchrony in population dynamics. Annu. Rev. Ecol. Evol. Syst. 35 (1), 467–490.

Massiot-Granier, F., Prévost, E., Chaput, G., Potter, T., Smith, G., White, J., Mantyniemi, S., Rivot, E., 2014. Embedding stock assessment within an integrated hierarchical Bayesian life cycle modelling framework: an application to Atlantic salmon in the Northeast Atlantic. ICES J. Mar. Sci. 71 (7), 1653–1670.

McAllister, M., Hill, S., Agnew, D., Kirkwood, G., Beddington, J., 2004. A Bayesian hierarchical formulation of the De Lury stock assessment model for abundance estimation of Falkland Islands' squid (*Loligo gahi*). Can. J. Fish. Aquat. Sci. 61, 1048–1059.

Miller, T.J., 2007. Contribution of individual-based coupled physical-biological models to understanding recruitment in marine fish populations. Mar. Ecol. Prog. Ser. 347, 127–138.

Parent, E., Rivot, E., 2013. Introduction to hierarchical bayesian modeling for ecological data. In: Applied Environmental Statistics. Chapman & Hall/CRC, Boca Raton, London, New York (427 pp).

Peck, M., Hufnagl, M., 2012. Can IBMs tell us why most larvae die in the sea?: Model sensitivities and scenarios reveal research needs. J. Mar. Syst. 93, 77–93.

Petitgas, P., Rijnsdorp, A., Dickey-Collas, M., Engelhard, G., Peck, M., Pinnegar, J., Drinkwater, K., Huret, M., Nash, R.D.M., 2013. Impacts of climate change on the complex life cycles of fish. Fish. Oceanogr. 22, 121–139.

Planque, B., Loots, C., Petitgas, P., Lindstrom, U., Vaz, S., 2011. Understanding what controls the spatial distribution of fish populations using a multi-model approach. Fish. Oceanogr. 20, 1–17.

Polacheck, T., Paige Eveson, J., Laslett, G.M., 2010. Classifying tagging experiments for commercial fisheries into three fundamental types based on design, data requirements and estimable population parameters. Fish and Fish. 11 (2), 133–148.

Punt, A.E., Hilborn, R., 1997. Fisheries stock assessment and decision analysis: the Bayesian approach. Rev. Fish Biol. Fish. 7, 35–63.

Ranta, E., Kaitala, V., Lindström, J., Helle, E., 1997. The Moran effect and synchrony in population dynamics. Oikos 78 (1), 136–142.

Rijnsdorp, A.D., Pastoors, M.A., 1995. Modelling the spatial dynamics and fisheries of North Sea plaice (*Pleuronectes platessa* L.) based on tagging data. ICES J. Mar. Sci. 52, 963–980.

Rijnsdorp, A.D., Van Beek, F.A., Flatman, S., Millner, R.M., Riley, J.D., Giret, M., De Clerck, R., 1992. Recruitment of sole stocks, *Solea solea* (L.), in the Northeast Atlantic. Neth. J. Sea Res. 29, 173–192.

Riou, P., Le Pape, O., Rogers, S.I., 2001. Relative contributions of different sole and plaice nurseries to the adult population in the Eastern Channel: application of a combined method using generalized linear models and a geographic information system. Aquat. Living Resour. 14, 125–135.

Rivot, E., Prévost, E., 2002. Hierarchical bayesian analysis of capture-mark-recapture data. Can. J. Fish. Aquat. Sci. 59, 1768–1784.

Rivot, E., Prévost, E., Parent, E., Baglinière, J.L., 2004. A Bayesian state-space modelling framework for fitting a salmon stage-structured population dynamic model to multiple time series of field data. Ecol. Modell. 179, 463–485.

Rochette, S., Rivot, E., Morin, J., Mackinson, S., Riou, P., Le Pape, O., 2010. Effect of nursery habitat degradation on flatfish population: application to *Solea solea* in the Eastern Channel (Western Europe). J. Sea Res. 64, 34–44.

Rochette, S., Huret, M., Rivot, E., Le Pape, O., 2012. Coupling hydrodynamic and individual-based models to simulate long-term larval supply to coastal nursery areas. Fish. Oceanogr. 21, 229–242.

Rochette, S., Le Pape, O., Vigneau, J., Rivot, E., 2013. A hierarchical Bayesian model for embedding larval drift and habitat models in integrated life cycles for exploited fish. Ecol. Appl. 23, 1659–1676.

Rolland, J.-L., Bonhomme, F., Lagardere, F., Hassan, M., Guinand, B., 2007. Population structure of the common sole (*Solea solea*) in the Northeastern Atlantic and the Mediterranean Sea: revisiting the divide with EPIC markers. Mar. Biol. 151, 327–341.

Rooper, C.N., Gunderson, D.R., Armstrong, D.A., 2004. Application of the concentration hypothesis to English sole in nursery estuaries and potential contribution to coastal fisheries. Estuaries 27, 102–111.

Ruiz, J., González-Quirós, R., Prieto, L., Navarro, G., 2009. A Bayesian model for anchovy (*Engraulis encrasicolus*): the combined forcing of man and environment. Fish. Oceanogr. 18, 62–76.

Sackett, D.K., Able, K.W., Grothues, T.M., 2008. Habitat dynamics of summer flounder Paralichthys dentatus within a shallow USA estuary, based on multiple approaches using acoustic telemetry. Mar. Ecol. Prog. Ser. 364, 199–212.

Savina, M., Lacroix, G., Ruddick, K., 2010. Modelling the transport of common sole larvae in the southern North Sea: influence of hydrodynamics and larval vertical movements. J. Mar. Syst. 81, 86–98.

Savina, M., Lunghi, M., Archambault, B., Baulier, L., Huret, M., Le Pape, O., 2016. Sole larval supply to coastal nurseries: interannual variability and connectivity at interregional and interpopulation scales. J. Sea. Res., http://dx.doi.org/10.1016/j.seares.2015.11.010 (in press).

Selkoe, K., Henzler, C., Gaines, S., 2008. Seascape genetics and the spatial ecology of marine populations. Fish and Fish. 9, 363–377.

Smedbol, R.K., McPherson, A., Hansen, M.M., Kenchington, E., 2002. Myths and moderation in marine 'metapopulations'? Fish Fish. 3, 20–35.

Spiegelhalter, D.J., Best, N.G., Carlin, B.P., van der Linde, A., 2014. The deviance information criterion: 12 years on. J. R. Stat. Soc. Ser. B 76 (3), 485–493.

Stelzenmuller, V., Schulze, T.F.H.O., Berkenhagen, J., 2011. Integrating modelling tools to support risk-based decision-making in marine spatial management. Mar. Ecol. Prog. Ser. 441, 197–212.

Strathmann, R.R., Hughes, T.P., Kuris, A.M., Lindeman, K.C., Morgan, S.G., Pandolfi, J.M., Warner, R.R., 2002. Evolution of local recruitment and its consequences for marine populations. Bull. Mar. Sci. 70, 377–396.

Taylor, N.G., McAllister, M.K., Lawson, G.L., Carruthers, T., Block, B.A., 2011. Atlantic bluefin tuna: a novel multistock spatial model for assessing population biomass. PLoS One 6 (12), e27693.

Tidd, A.N., Vermard, Y., Marchal, P., Pinnegar, J., Blanchard, J.L., Milner-Gulland, E.J., 2015. Fishing for space: fine-scale multi-sector maritime activities influence fisher location choice. PLoS One 10 (1), e0116335.

Tuck, G., Possingham, H., 1994. Optimal harvesting strategies for a metapopulation. Bull. Math. Biol. 56 (1), 107–127.

Vasconcelos, R., Eggleston, D.B., Le Pape, O., Tulp, I., 2014. Patterns and processes of habitat-specific demographic variability in exploited marine species. ICES J. Mar. Sci. 71, 638–647.

van de Wolfshaar, K.E., HilleRisLambers, R., Grdmark, A., 2011. Effect of habitat productivity and exploitation on populations with complex life cycles. Mar. Ecol. Prog. Ser. 438, 175–184.

Waples, R.S., 1998. Separating the wheat from the chaff: patterns of genetic differentiation in high gene flow species. J. Hered. 89, 438–450.

Ward, R.D., Woodwark, M., Skibinski, D.O.F., 1994. A comparison of genetic diversity levels in marine, freshwater, and anadromous fishes. J. Fish Biol. 44, 213–232.

Warner, R.R., Cowen, R.K., 2002. Local retention of production in marine populations: evidence, mechanisms, and consequences. Bull. Mar. Sci. 70, 245–249.

Yau, A.J., Lenihan, H.S., Kendall, B.E., 2014. Fishery management priorities vary with self-recruitment in sedentary marine populations. Ecol. Appl. 24 (6), 1490–1504.

Ying, Y., Chen, Y., Lin, L., Gao, T., Quinn, T., 2011. Risks of ignoring fish population spatial structure in fisheries management. Can. J. Fish. Aquat. Sci. 68, 2101–2120.

## **Appendix V.** MCMC methods used to obtained Bayesian estimates of all unknown quantities of the model

All computations were performed using the R platform ("The R Project for Statistical Computing" - www.R-project.org). All the Bayesian posterior distributions were approximated via Monte Carlo Markov Chain (MCMC) methods and were run within R using the ***rjags*** package (JAGS software; http://mcmc-jags.sourceforge.net, version 4.2.0 ). Two MCMC-independent chains with dispersed initialization points were used for all computations. The Gelman-Rubin test was applied to all posterior sampling to check convergence of the MCM chains. The Gelman-Rubin test is based on the computation of the R-ratio which allows comparison within and between-chain variances. Its values have to be much closed to 1 as implemented in the Coda package of R (Brooks and Gelman, 1998). Values substantially above 1 indicate lack of convergence.
For all computation, in order to reduce the autocorrelation in the sample used for inferences, one out of 100 iterations was kept (thinning = 100).

### ✓ Using Bayesian estimates for the stock assessment

For each of the two MCMC independent chains, an adapting phase of 10,000 iterations was realized. The two chains were run during 500,000 iterations. Due to the thin applied, final inferences were derived from a sample of 2 x 5,000 iterations resulting from merging of the two chains. The Gelman Rubin test revealed that all variables of each run had an R ratio R < 1.11 except for the run with 10% of connectivity (R < 1.17 for all variables) (see an example in Appendix V-a). The calculation was time-consuming; each model configuration took ~24h.

### ✓ Bayesian fit for the simulation estimation approach

For this case, convergence has been obtained with using a burnin phase of 250,000 iterations. This burnin was necessary to help to obtain the convergence at the sense of Gelman). However, inferences were derived from a same-length sample as for the first analysis, i.e. a sample of 2 x 5,000 iterations. The Gelman Rubin test revealed that all variables of each run had an R ratio R < 1.1 except for the run with 10% of connectivity (R < 1.17 for all variables). The calculation for the simulation-estimation approach was much more time-consuming; each scenario took ~50-60h.

Appendix V- a)

Example of posterior Checking (Gelman Rubin Test) of Bayesian posterior estimates ($F_{3-8}$) used to analyze the sensitivity of the stock assessment to the connectivity level

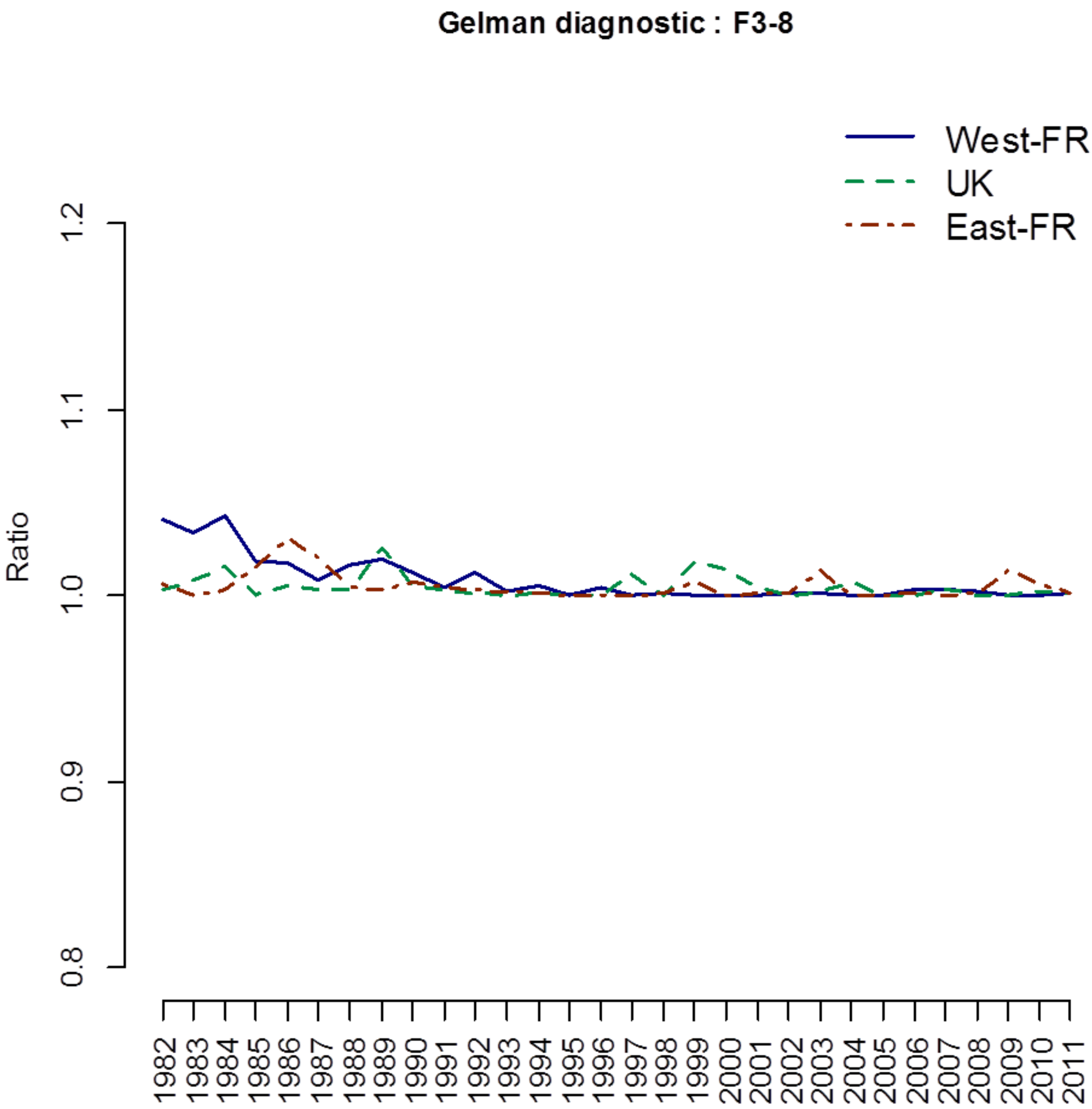

**Figure A 1.** Bayesian posterior checking (Gelman-Rubin Test). The test is realized on the$F_{3-8}$. If both the data and the model are consistent, observed data should be similar to replicated data simulated a posteriori by the model, with a value of the ratio near to 1.

## **Appendix VI.** Simulation methods used to estimate quantities at the MSY

Following the method described in Archambault et al. (2016), we used Monte Carlo simulations to integrate both process and parameter uncertainty in order to obtain the equilibrium curves. For a given value of F in each subpopulation, population dynamics was simulated including process error and using a constant F in time and space during 200 years to ensure achievement of equilibrium state.

Reference equilibrium points for each subpopulation r, denoted $\mathbf{B_{MSY,r}}$, $\mathbf{F_{MSY,r}}$ and $\mathbf{C_{MSY,r}}$, were estimated by varying simultaneously each F. Due to this complexity, access to the reference equilibrium points was performed in two steps. A first step allowing to identify a range of fishing pressure values, by varying each F in a range from 0 to 1, with a step of 0.05. Then a second step was to use a smaller range of fishing pressure values with a step of 0.01.

The equilibrium state was assumed to occur after 100 years of simulation and the process error was integrated out by considering the distribution of the results between year 101 and 200. Regarding the second step, procedure was repeated 500 times with 500 sets of parameters directly drawn in the joint posterior distribution of the model parameters in order to integrate the parameter uncertainty. Each run took approximately 4 days to obtain MSY values.

## **Appendix VII.** Statistical quantities of the parameters alpha and K obtained for each level of connectivity applied

| Connectivity level (%) | Parameters | Mean | Median | Sd | q10 | q90 |
|---|---|---|---|---|---|---|
| Isolated population | $\alpha_1$ | 0,22 | 0,14 | 0,2 | 0,051 | 0,53 |
| | $\alpha_2$ | 0,48 | 0,44 | 0,23 | 0,2 | 0,82 |
| | $\alpha_3$ | 0,34 | 0,27 | 0,24 | 0,096 | 0,72 |
| | $\alpha_4$ | 0,14 | 0,068 | 0,18 | 0,017 | 0,37 |
| | $\alpha_5$ | 0,22 | 0,14 | 0,22 | 0,034 | 0,56 |
| | $K_1$ | 82 | 71 | 39 | 53 | 125 |
| | $K_2$ | 220 | 212 | 43 | 172 | 270 |
| | $K_3$ | 160 | 160 | 19 | 140 | 190 |
| | $K_4$ | 110 | 93 | 47 | 72 | 150 |
| | $K_5$ | 130 | 120 | 65 | 66 | 210 |
| 5% | $\alpha_1$ | 0,2 | 0,13 | 0,19 | 0,051 | 0,47 |
| | $\alpha_2$ | 0,5 | 0,459 | 0,23 | 0,214 | 0,85 |
| | $\alpha_3$ | 0,35 | 0,38 | 0,23 | 0,1 | 0,72 |
| | $\alpha_4$ | 0,15 | 0,072 | 0,18 | 0,017 | 0,39 |
| | $\alpha_5$ | 0,25 | 0,169 | 0,23 | 0,043 | 0,63 |
| | $K_1$ | 84 | 73 | 38 | 53 | 131 |
| | $K_2$ | 202 | 197 | 37 | 162 | 250 |
| | $K_3$ | 164 | 161 | 17 | 134 | 175 |
| | $K_4$ | 107 | 97 | 40 | 75 | 152 |
| | $K_5$ | 135 | 126 | 57 | 74 | 204 |
| 10% | $\alpha_1$ | 0,21 | 0,139 | 0,2 | 0,051 | 0,5 |
| | $\alpha_2$ | 0,5 | 0,469 | 0,23 | 0,217 | 0,86 |
| | $\alpha_3$ | 0,35 | 0,281 | 0,23 | 0,106 | 0,72 |
| | $\alpha_4$ | 0,15 | 0,072 | 0,18 | 0,019 | 0,39 |
| | $\alpha_5$ | 0,29 | 0,208 | 0,24 | 0,056 | 0,68 |
| | $K_1$ | 82 | 70 | 37 | 52 | 130 |
| | $K_2$ | 196 | 191 | 35 | 157 | 240 |
| | $K_3$ | 145 | 143 | 17 | 126 | 165 |
| | $K_4$ | 114 | 104 | 41 | 80 | 160 |
| | $K_5$ | 140 | 134 | 52 | 82 | 206 |
| 20% | $\alpha_1$ | 0,22 | 0,144 | 0,21 | 0,052 | 0,53 |
| | $\alpha_2$ | 0,51 | 0,479 | 0,23 | 0,221 | 0,85 |
| | $\alpha_3$ | 0,34 | 0,261 | 0,24 | 0,095 | 0,7 |
| | $\alpha_4$ | 0,15 | 0,075 | 0,19 | 0,021 | 0,4 |
| | $\alpha_5$ | 0,38 | 0,318 | 0,26 | 0,094 | 0,79 |
| | $K_1$ | 81 | 69 | 35 | 52 | 128 |
| | $K_2$ | 196 | 192 | 35 | 157 | 238 |
| | $K_3$ | 130 | 129 | 16 | 113 | 150 |
| | $K_4$ | 129 | 119 | 44 | 91 | 176 |
| | $K_5$ | 172 | 162 | 61 | 107 | 249 |
| 30% | $\alpha_1$ | 0,24 | 0,154 | 0,21 | 0,053 | 0,57 |
| | $\alpha_2$ | 0,51 | 0,473 | 0,23 | 0,218 | 0,86 |
| | $\alpha_3$ | 0,31 | 0,237 | 0,23 | 0,082 | 0,68 |

| | Parameters | Mean | Median | Sd | q10 | q90 |
|---|---|---|---|---|---|---|
| 40% | $\alpha_1$ | 0,25 | 0,17 | 0,22 | 0,055 | 0,58 |
| | $\alpha_2$ | 0,5 | 0,468 | 0,23 | 0,212 | 0,85 |
| | $\alpha_3$ | 0,29 | 0,215 | 0,23 | 0,071 | 0,66 |
| | $\alpha_4$ | 0,15 | 0,066 | 0,19 | 0,017 | 0,4 |
| | $\alpha_5$ | 0,51 | 0,486 | 0,25 | 0,176 | 0,87 |
| | $K_1$ | 84 | 73 | 39 | 56 | 128 |
| | $K_2$ | 224 | 217 | 43 | 177 | 278 |
| | $K_3$ | 114 | 110 | 18 | 96 | 133 |
| | $K_4$ | 162 | 145 | 67 | 103 | 236 |
| | $K_5$ | 272 | 256 | 100 | 158 | 404 |
| 60% | $\alpha_1$ | 0,27 | 0,189 | 0,22 | 0,062 | 0,62 |
| | $\alpha_2$ | 0,5 | 0,476 | 0,24 | 0,211 | 0,85 |
| | $\alpha_3$ | 0,28 | 0,205 | 0,23 | 0,064 | 0,66 |
| | $\alpha_4$ | 0,12 | 0,046 | 0,17 | 0,013 | 0,33 |
| | $\alpha_5$ | 0,58 | 0,852 | 0,24 | 0,24 | 0,91 |
| | $K_1$ | 88 | 79 | 37 | 61 | 122 |
| | $K_2$ | 255 | 247 | 52 | 200 | 320 |
| | $K_3$ | 104 | 101 | 18 | 88 | 122 |
| | $K_4$ | 193 | 167 | 95 | 107 | 315 |
| | $K_5$ | 382 | 370 | 156 | 217 | 564 |
| 70% | $\alpha_1$ | 0,29 | 0,214 | 0,23 | 0,07 | 0,66 |
| | $\alpha_2$ | 0,5 | 0,468 | 0,24 | 0,206 | 20,85 |
| | $\alpha_3$ | 0,29 | 0,209 | 0,23 | 0,064 | 0,66 |
| | $\alpha_4$ | 0,11 | 0,037 | 0,16 | 0,013 | 0,3 |
| | $\alpha_5$ | 0,6 | 0,611 | 0,23 | 0,282 | 0,92 |
| | $K_1$ | 89 | 79 | 38 | 62 | 118 |
| | $K_2$ | 266 | 257 | 56 | 208 | 334 |
| | $K_3$ | 101 | 98 | 16 | 86 | 118 |
| | $K_4$ | 201 | 168 | 106 | 105 | 346 |
| | $K_5$ | 449 | 442 | 136 | 278 | 626 |

**Table A 1.** Mean, Median, Standard deviation (Sd) and quantiles (q10 and q90) obtained for each connectivity level applied to evaluate the sensitivity of parameter estimates when increasing connectivity among the three subpopulations.

## **Appendix VIII.** Effects of each connectivity level tested on the contributions of each nursery sector to recruitment in the Eastern Channel

### Appendix VIII – a)

| | | Connectivity level | | | | | | | | | |
|---|---|---|---|---|---|---|---|---|---|---|---|
| | | Isolated | 5% | 10% | 20% | 30% | 40% | 50% | 60% | 70% | Panmictic |
| Average contribution of nursery sector to the recruitment (Percent) | Seine | 14 | 15 | 17 | 19 | 20 | 21 | 20 | 20 | 19 | 16 |
| | Veys | 4 | 5 | 5 | 7 | 9 | 11 | 14 | 15 | 17 | 3 |
| | UK West | 17 | 17 | 17 | 17 | 17 | 18 | 18 | 19 | 19 | 28 |
| | Rye | 17 | 17 | 17 | 17 | 17 | 18 | 18 | 18 | 19 | 24 |
| | Somme | 48 | 47 | 45 | 40 | 36 | 32 | 30 | 28 | 27 | 29 |

**Table A 2.** Contributions of each nursery sector by increasing connectivity level

### Appendix VIII – b)

a) Three isolated populations

b) 20% of connectivity

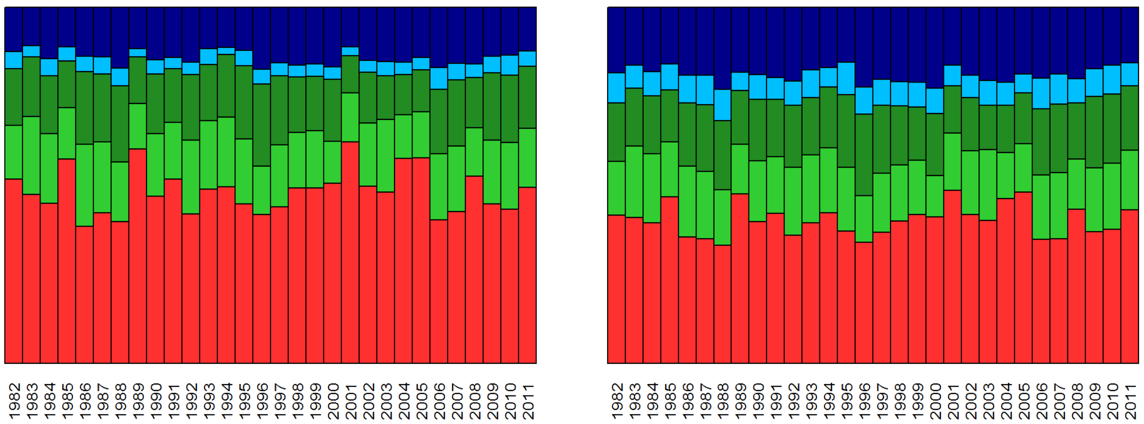

c) 40% of connectivity

d) 60% of connectivity

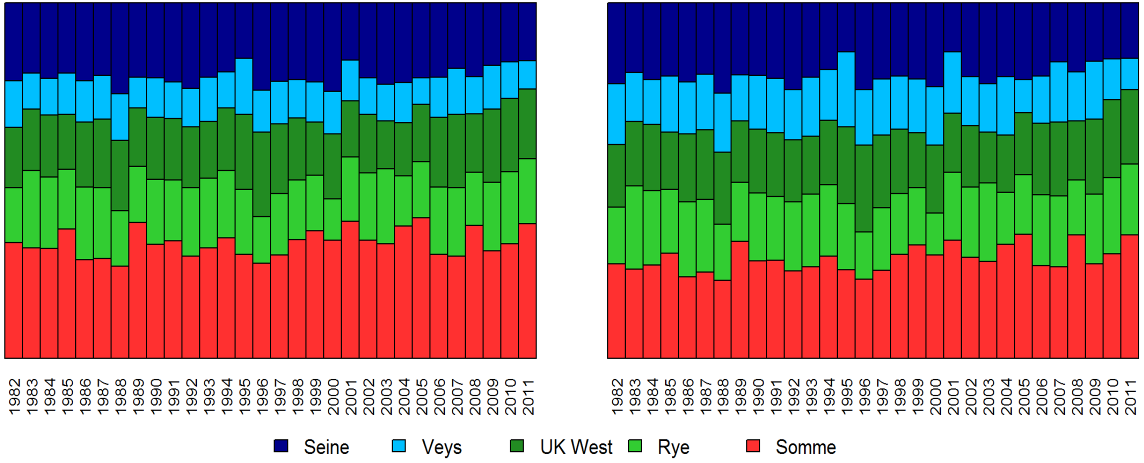

**Figure A 2.** Variability among years of each nursery sector by increasing connectivity level among subpopulations

**Appendix IX.** Sensitivity of the Spawning Stock biomass, Recruitment and Fishing mortality to the connectivity level for both (IX – a) the West-FR subpopulation and (IX – b) the UK subpopulation.

## Appendix IX – a): The West FR subpopulation

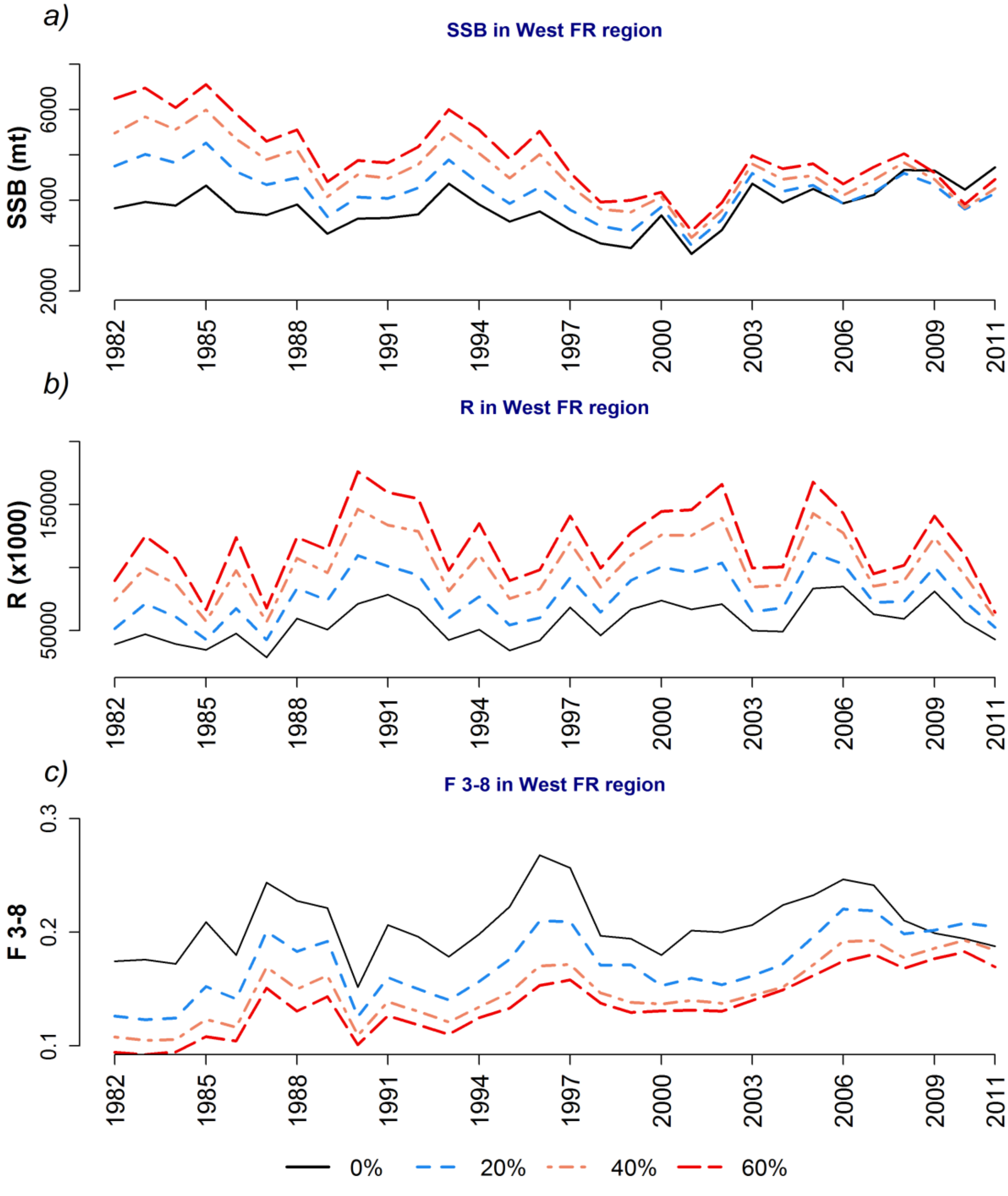

**Figure A 3.** Comparison of posterior median estimates of SSB (a), R (b) and F_(3-8) (c) obtained for models considering three isolated sub-populations, and connectivity levels of 20, 40, and 60% for the West-FR subpopulation.

## Appendix IX – b): The UK subpopulation

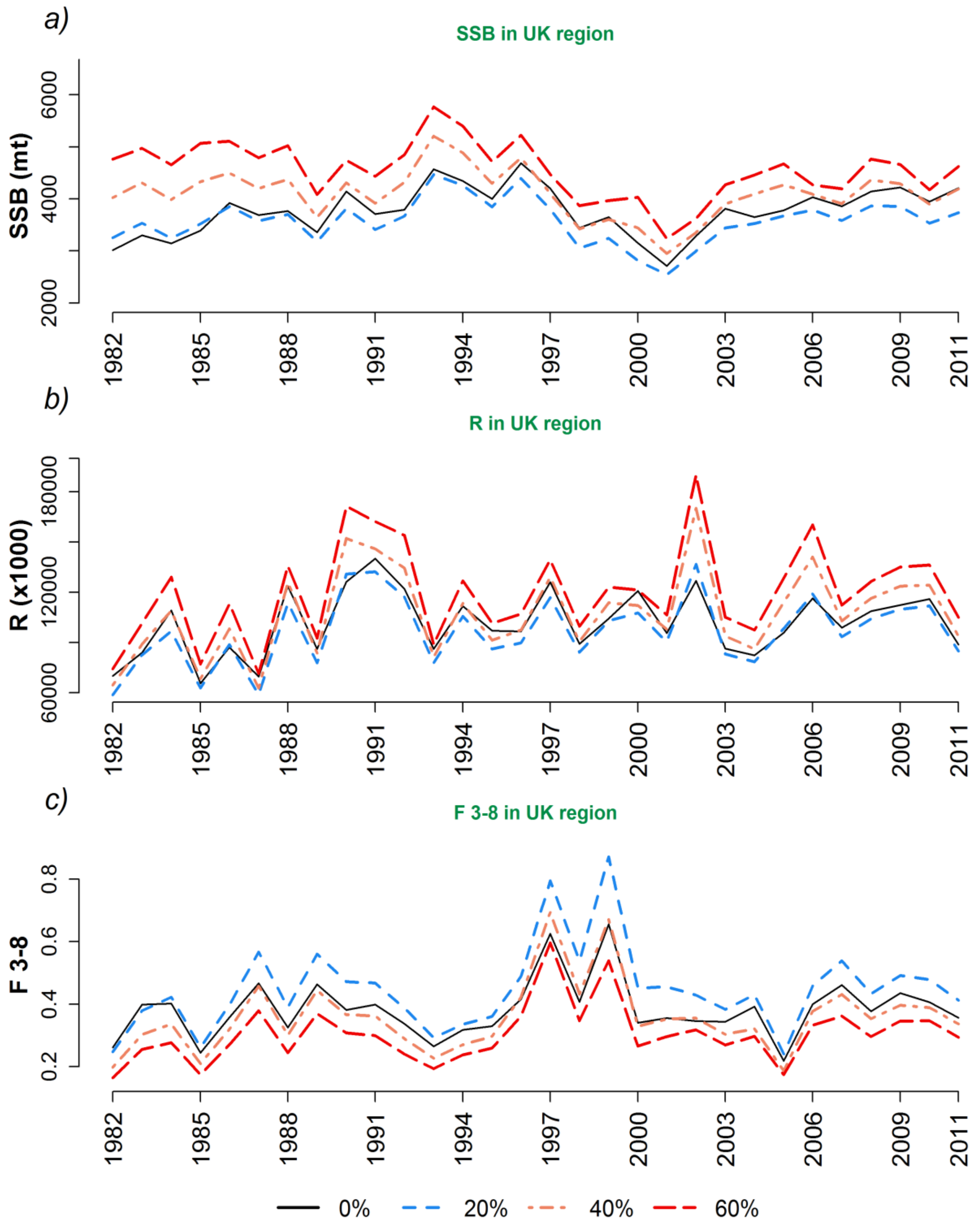

**Figure A 4.** Comparison of posterior median estimates of SSB (a), R (b) and F_(3-8) (c) obtained for models considering three isolated sub-populations, and connectivity levels of 20, 40, and 60% for the UK subpopulation.

## **Appendix X.** Additional boxplot and statistical quantities for each scenario of the Simulation-Estimation approach

### ✓ Inferences are sensitive to the number of tags released

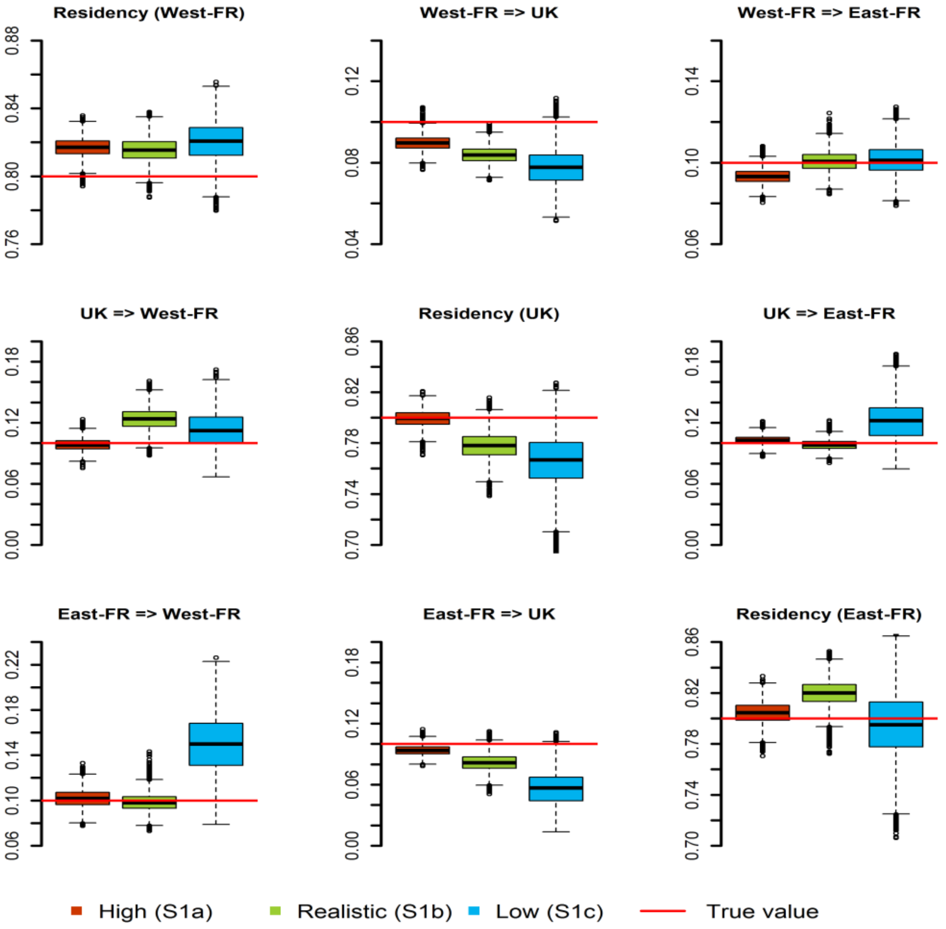

**Figure A 5.** Marginal posterior distributions of connectivity parameters obtained for each tag number scenario (high, realistic, and low number of tags). The solid line represents the true value of the connectivity parameter (10% and 80% for diagonal parameters) used for simulating the tag-recapture data.

**Table A 3.** Standard deviation and relative bias obtained from the three scenarios of the number of tags released: high number (1,800 tags released per year) (S1a), realistic number (900 tags released per year) (S1b), and low number (100 tags released per year) (S1c).

| | High number (S1a) | | Realistic number (S1b) | | Low number (S1c) | |
|---|---|---|---|---|---|---|
| | Sd | Relative bias | Sd | Relative bias | Sd | Relative bias |
| Residency (West FR) | 0.0057 | 2.1% | 0.0071 | 1.9% | 0.012 | 2.6% |
| West FR -> UK | 0.0037 | -10.32% | 0.0041 | -16.1% | 0.0086 | -22.2% |
| West FR -> East FR | 0.0037 | -6.6% | 0.005 | 0.7% | 0.0074 | 1.6% |
| UK -> West FR | 0.0061 | -1.5% | 0.011 | 23.7% | 0.018 | 12.8% |
| Residency (UK) | 0.0067 | -0.1% | 0.011 | -2.7% | 0.021 | -4.3% |
| UK -> East FR | 0.0048 | 2.5% | 0.005 | -1.7% | 0.019 | 21.6% |
| East FR -> West FR | 0.0079 | 1.9% | 0.0078 | -1.6% | 0.026 | 49.8% |
| East FR -> UK | 0.005 | -6.3% | 0.0081 | -18.4% | 0.017 | -44.7% |
| Residency (East FR) | 0.0084 | 0.6% | 0.010 | 2.5% | 0.026 | -0.6% |

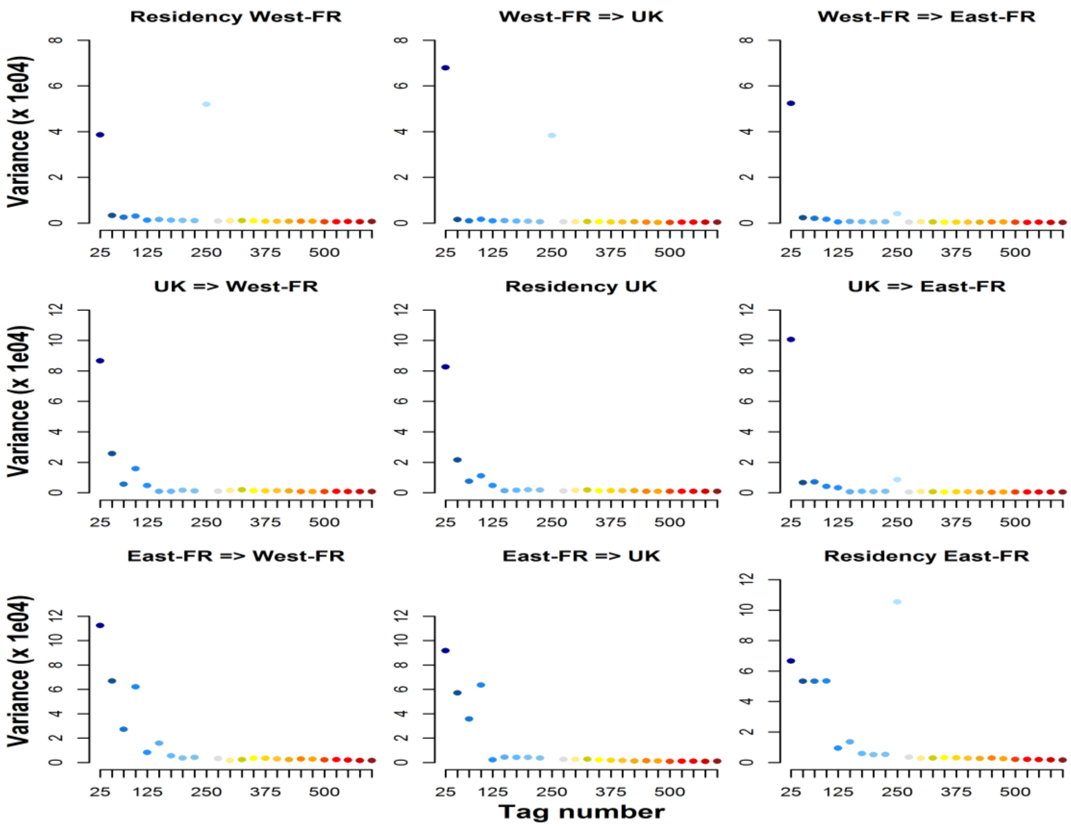

Figure A 6. Sensitivity of the estimation procedure to the tag number: analysis of the variance obtained by increasing the tag number for all movement directions (residency included).

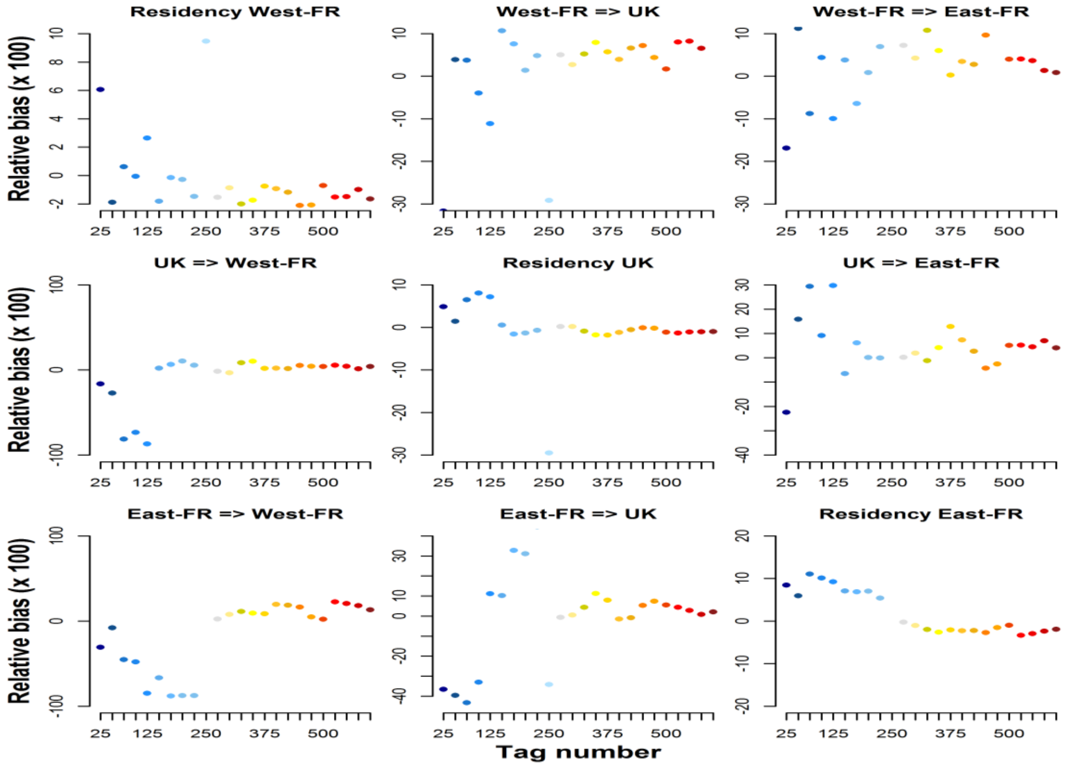

Figure A 7. Sensitivity of the estimation procedure to the tag number: analysis of the relative bias obtained by increasing the tag number for all movement directions (residency included).

### ✓ Inferences are sensitive to the value of the declaration rate

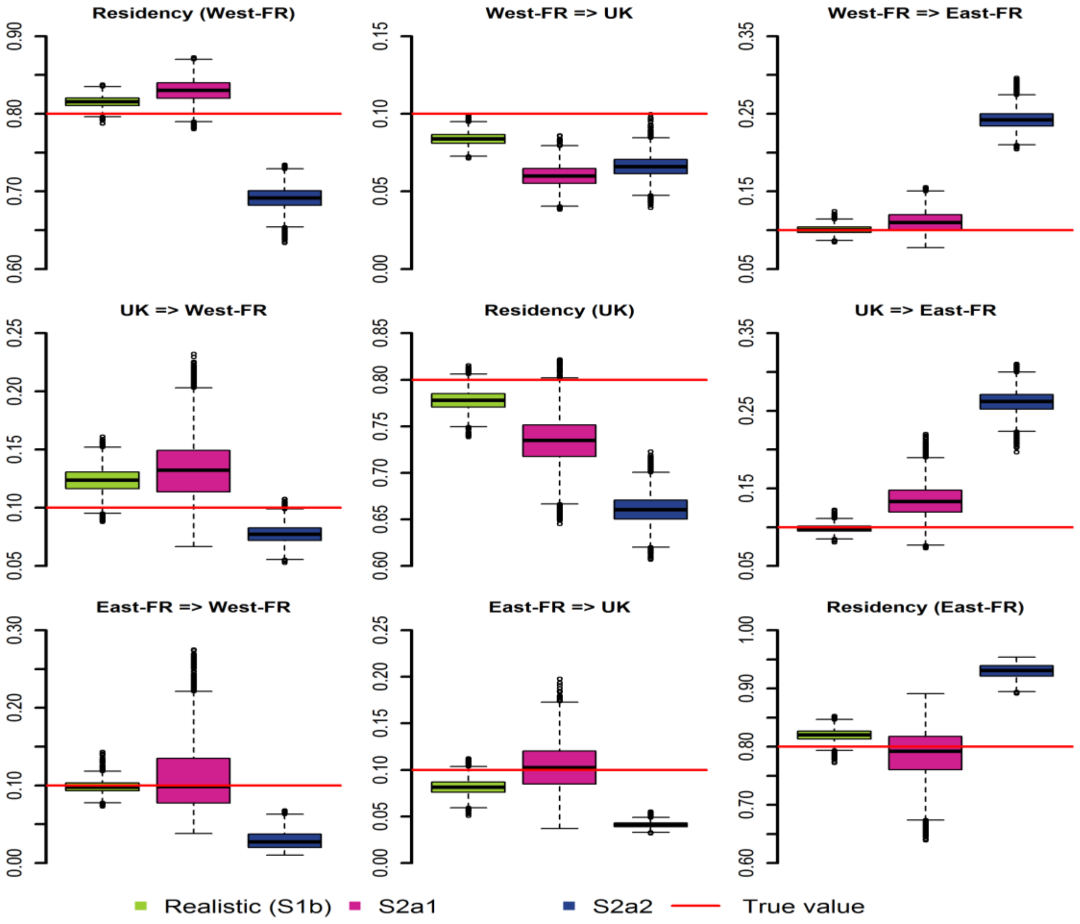

**Figure A 8.** Marginal posterior distributions of connectivity parameters obtained with the baseline realistic scenario (S1b), the scenario considering a declaration rate fixed to β=0.45 for both the simulation and estimation procedures (S2a1), and the scenario considering a declaration rate fixed to β=0.45 for simulation and fixed to β=0.90 in the estimation procedure (S2a2). The solid line represents the true value of connectivity parameters (10% and 80% of residency).

**Table A 4.** Standard deviation and relative bias obtained with the baseline realistic scenario (S1b), the scenario considering a declaration rate fixed to β=0.45 for both the simulation and estimation procedures (S2a1), and the scenario considering a declaration rate fixed to β=0.45 for simulation and fixed to β=0.90 in the estimation procedure (S2a2).

| | Realistic | | Scenario S2a1 | | Scenario S2a2 | |
|---|---|---|---|---|---|---|
| Connectivity direction | Sd | Relative bias | Sd | Relative bias | Sd | Relative bias |
| Residency (West FR) | 0.0071 | 1.92% | 0,0147 | 3,7% | 0,014 | -14% |
| West FR -> UK | 0.0041 | -16.12% | 0,0072 | -40,1% | 0,0072 | -34% |
| West FR -> East FR | 0.005 | 0.73% | 0,014 | 10,3% | 0,0127 | 143% |
| UK -> West FR | 0.0109 | 23.66% | 0,0278 | 32,4% | 0,0084 | -22% |
| Residency (UK) | 0.0108 | -2.74% | 0,0262 | -8,3% | 0,0151 | -17% |
| UK -> East FR | 0.005 | -1.71% | 0,0211 | 33,8% | 0,0149 | 162% |
| East FR -> West FR | 0.0078 | -1.64% | 0,0434 | 10,7% | 0,0113 | -71% |
| East FR -> UK | 0.0081 | -18.36% | 0,0252 | 2,3% | 0,0031 | -59% |
| Residency (East FR) | 0.0101 | 2.5% | 0,0433 | -1,6% | 0,0119 | 16% |

### ✓ Inferences are sensitive to a spatial mis-specification of the declaration rate

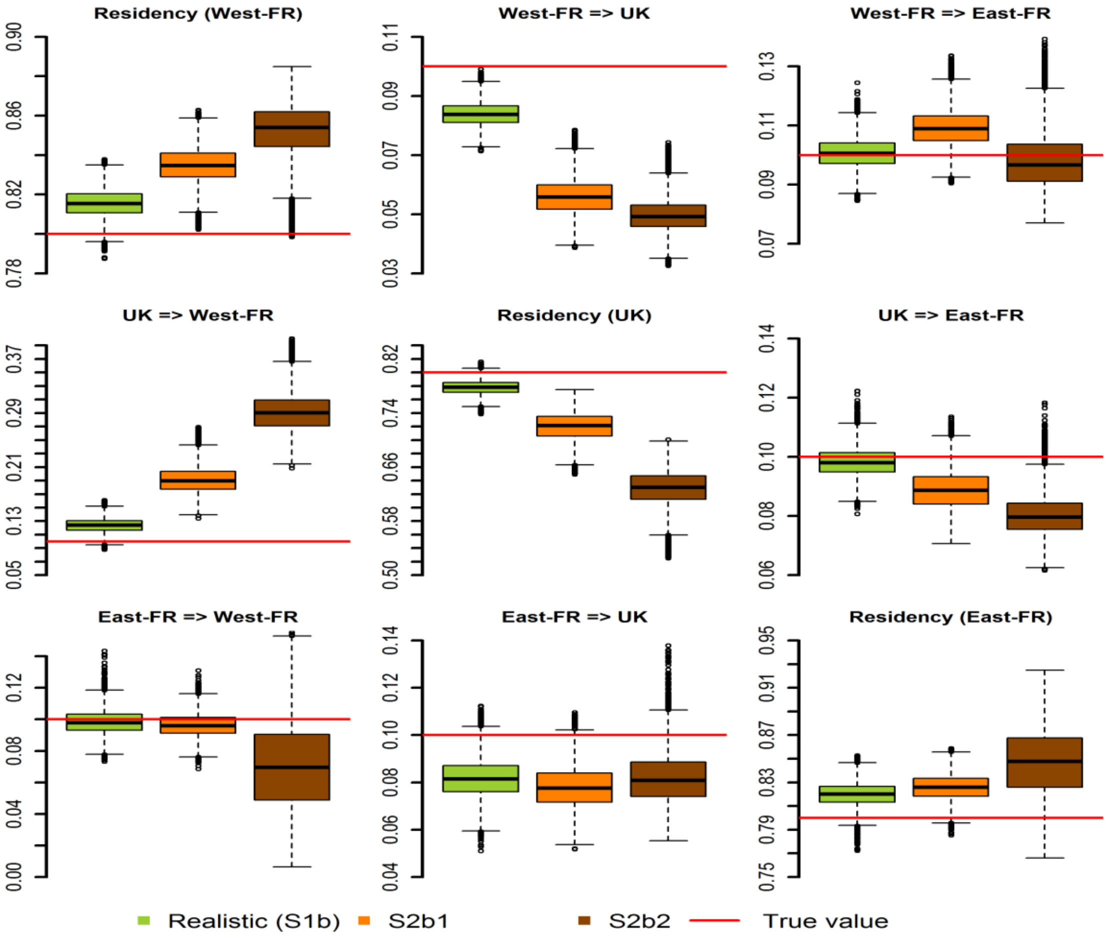

**Figure A 9.** Marginal posterior distributions of movement parameters obtained with the baseline scenario (denoted Realistic), the scenario considering a declaration rate fixed to β=0.45 for the UK sub-population in simulation (denoted S2b1), and the scenario considering a declaration rate fixed to $\boldsymbol{\beta} = \mathbf{0.45}$ in simulation for the both West-FR and UK sub-populations denoted S2b2). For all these scenarios estimation procedure was performed with a declaration rate fixed to $\boldsymbol{\beta} = \mathbf{0.90}$ for all sub-populations. The solid line represents the true value of connectivity (i.e. the value at which tagging datasets have been simulated).

**Table 10.** Standard deviation and relative bias obtained from scenarios considering a declaration rate fixed to β=0.45 in simulation for the UK region (S2b1), and the scenario considering a declaration rate fixed to β=0.45 in simulation for the both West-FR and East-FR regions (S2b2). For all these scenarios estimation procedure was performed with a declaration rate fixed to β=0.90.

| | Realistic | | Scenario S2b1 | | Scenario S2b2 | |
|---|---|---|---|---|---|---|
| Connectivity | Sd | Relative bias | Sd | Relative bias | Sd | Relative bias |
| Residency (West FR) | 0.0071 | 1.92% | 0.009 | 4.4% | 0.0135 | 6.5% |
| West FR -> UK | 0.0041 | -16.12% | 0.0063 | -44% | 0.0059 | -50.2% |
| West FR -> East FR | 0.005 | 0.73% | 0.0062 | 9.1% | 0.0099 | -2.1% |
| UK -> West FR | 0.0109 | 23.66% | 0.0207 | 91.7% | 0.0283 | 191.2% |
| Residency (UK) | 0.0108 | -2.74% | 0.0214 | -10.1% | 0.0258 | -21.5% |
| UK -> East FR | 0.005 | -1.71% | 0.0068 | -11% | 0.0071 | -19.6% |
| East FR -> West FR | 0.0078 | -1.64% | 0.0077 | -3.7% | 0.0286 | -29.5% |
| East FR -> UK | 0.0081 | -18.36% | 0.0089 | -22% | 0.011 | -17.9% |
| Residency (East FR) | 0.0101 | 2.5% | 0.0107 | 3.2% | 0.0296 | 5.9% |

### ✓ Using an informative prior on the declaration rate is workable

**Table A 5.** Summary of marginal posterior distribution of the declaration rate obtained with models considering an informative prior with medium variability (S2c1) and an informative prior with higher variability (S2c2) for the declaration rate.

| Scenario | Region | Mean | Sd | CV | q10 | q90 | Relative bias |
|---|---|---|---|---|---|---|---|
| **Scenario S2c1 Informative prior with medium variability** | West-FR | 0.93 | 0.021 | 2.3 | 0.9 | 0.96 | 3.4% |
| | UK | 0.93 | 0.017 | 1.8 | 0.91 | 0.95 | 3.2% |
| | East-FR | 0.91 | 0.015 | 1.6 | 0.9 | 0.93 | 1.6% |
| **Scenario S2c2 Informative prior with higher variability** | West-FR | 0.95 | 0.033 | 3.5 | 0.91 | 0.99 | 6.1% |
| | UK | 0.94 | 0.025 | 2.6 | 0.91 | 0.97 | 4.4% |
| | East-FR | 0.91 | 0.017 | 1.9 | 0.89 | 0.93 | 1.1% |

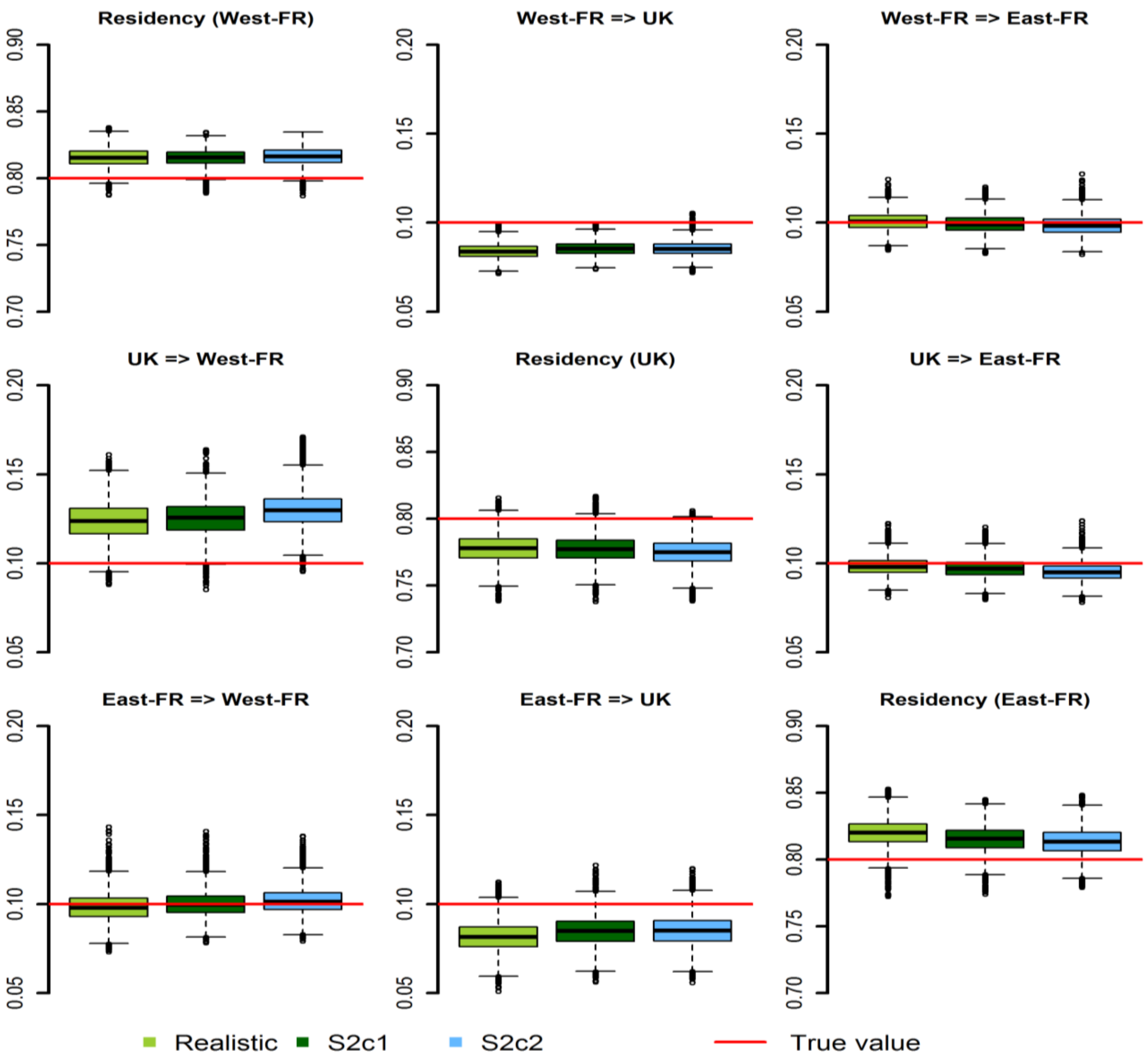

**Figure A 10.** Marginal posterior distribution of connectivity parameters obtained from the two scenarios introducing an informative prior on the declaration rate with a medium variability (S2c1) and a higher variability (S2c2). The solid line represents the true value used for simulating the tag-recapture data.

**Table A 6.** Standard deviation and relative bias obtained from the two scenarios of the set of an informative prior on the declaration rate (medium variability (S2c1) and higher variability (S2c2)).

| | Realistic | | Scenario S2c1 Informative prior with medium variability | | Scenario S2c2 Informative prior with higher variability | |
|---|---|---|---|---|---|---|
| Connectivity direction | Sd | Relative bias | Sd | Relative bias | Sd | Relative bias |
| Residency (West FR) | 0.0071 | 1.92% | 0.0063 | 1.89% | 0.0067 | 2,00% |
| West FR -> UK | 0.0041 | -16.12% | 0.0039 | 25.3% | 0.0098 | 29.9% |
| West FR -> East FR | 0.005 | 0.73% | 0.0052 | 0.04% | 0.0072 | 1.8% |
| UK -> West FR | 0.0109 | 23.66% | 0.0093 | -14.58% | 0.004 | -14.6% |
| Residency (UK) | 0.0108 | -2.74% | 0.0098 | -2.82% | 0.0102 | -3.1% |
| UK -> East FR | 0.005 | -1.71% | 0.0054 | -15.24% | 0.0085 | -15.2% |
| East FR -> West FR | 0.0078 | -1.64% | 0.0072 | -0.55% | 0.0055 | -1.5% |
| East FR -> UK | 0.0081 | -18.36% | 0.0084 | -2.71% | 0.0053 | -4.8% |
| Residency (East FR) | 0.0101 | 2.5% | 0.0099 | 1.9% | 0.0104 | 1.7% |

## ✓ Ability to estimate natural mortality

**Table A 7.** Statistical values of the posterior estimate for the Maximal natural mortality obtained with the model considering the realistic baseline scenario with a weighting function.

| Mean | Sd | CV | q10 | q90 | Relative bias |
|---|---|---|---|---|---|
| 2.95 | 0.046 | 1.56 | 2.88 | 2.99 | 13.4% |

**Table A 8.** Standard deviation and relative bias obtained from the model allowing estimation of the maximal natural mortality using the realistic baseline scenario.

| | Realistic | | S3 | |
|---|---|---|---|---|
| Connectivity direction | Sd | Relative bias | Sd | Relative bias |
| Residency (West FR) | 0.0071 | 1.92% | 0.0096 | 1.3% |
| West FR -> UK | 0.0041 | -16.12% | 0.0043 | -12.6% |
| West FR -> East FR | 0.005 | 0.73% | 0.0049 | 2.1% |
| UK -> West FR | 0.0109 | 23.66% | 0.0095 | 20.9% |
| Residency (UK) | 0.0108 | -2.74% | 0.0099 | -2.4% |
| UK -> East FR | 0.005 | -1.71% | 0.0052 | -1.5% |
| East FR -> West FR | 0.0078 | -1.64% | 0.0073 | -1.8% |
| East FR -> UK | 0.0081 | -18.36% | 0.0087 | -15.7% |
| Residency (East FR) | 0.0101 | 2.5% | 0.0097 | 2.2% |

Diplôme : Ingénieur Agronome

Spécialité : Agronomie

Spécialisation / option : Sciences halieutiques et aquacoles (REA)

Enseignant référent : GASCUEL Didier

Auteur(s) : VERON Matthieu

Date de naissance : 04/11/1992

Nb pages : 79 Annexe(s) : 35 pages

Année de soutenance : 2016

Organisme d'accueil : Agrocampus Ouest

Adresse :65, rue de St-Brieuc
35 000 RENNES

Maître de stage : RIVOT Etienne

Titre français : Développement d'un modèle Bayésien de cycle de vie intégré pour estimer les mouvements de la Sole en Manche Est à partir de données de marquage-recapture

Titre anglais : Developing an integrated Bayesian life cycle model to infer connectivity of the Sole population in the Eastern Channel from mark-recapture data

Résumé : Le projet SMAC vise à améliorer la compréhension du fonctionnement de la population de Sole en Manche Est afin d'optimiser la gestion. Ce travail s'inscrit dans un des axes principaux du projet SMAC qui vise à améliorer la connaissance sur le niveau de connectivité entre différentes sous-populations de Sole en Manche Est et de quantifier les conséquences pour l'évaluation des stocks et la gestion. L'objectif de ce travail est de développer un cadre méthodologique pour prendre en compte la structure spatiale de la population dans le modèle d'évaluation des stocks et pour pouvoir à terme intégrer des données de marquage-recapture afin d'estimer les mouvements. Les développements s'appuient sur une approche de modélisation hiérarchique Bayésienne développée par Rochette et al (2013) et étendue par Archambault et al (2016). Nous proposons ici une extension du modèle intégré de cycle de vie permettant la prise en compte de mouvements entre les trois populations identifiées et l'assimilation de données de marquage recapture pour estimer les mouvements de la Sole en Manche Est. Les résultats montrent une forte sensibilité de l'évaluation de stock aux niveaux de connectivité entre les trois sous-populations et renforcent la nécessité de mieux comprendre la connectivité au cours du cycle de vie. Le modèle est ensuite interrogé pour explorer dans quelle mesure le protocole de marquage envisagé peut-être optimisé pour optimiser la qualité des inférences sur le mouvement des poissons. L'analyse confirme que sous l'hypothèse d'un fort taux de déclaration des marques par les pêcheurs, le protocole de marquage prévu dans SMAC (300 poissons marqués par an et par zone sur 2 ans) peut permettre des inférences fiables des paramètres de mouvements. Cependant la qualité des inférences est conditionnée par certaines hypothèses qui n'ont pas pu être vérifiées dans le cadre de ce stage ; Notamment, une mauvaise connaissance de la distribution spatiale et de la valeur du taux de déclaration des marques induit des biais systématiques dans l'estimation des paramètres de mouvement. Les résultats nous amènent à recommander de maximiser le nombre de poissons marqués mais aussi la promotion auprès des pêcheurs afin de favoriser le taux de retour des marques.

Abstract : SMAC project aims at improving understanding of the Sole population functioning in the Eastern Channel for a better management. This work stands within one of the main Research axes of the SMAC project which aims at improving understanding on the connectivity level between different subpopulation of the Sole in the Eastern Channel and then quantifies consequences on both the stock assessment and the management. The objective of this work is to develop a modelling framework allowing to take into account the spatial structure of this population in the stock assessment model and then finally to be able to embed tag-recapture data in order to estimate movements. Developments are built on the basis of a Bayesian hierarchical modelling approach of the Sole population dynamics in the Eastern Channel developed by Rochette et al. (2013) and extended by Archambault et al. (2016). We provided here an extension to the integrated life cycle model allowing firstly to introduce the possibility to parameterize the connectivity between the three subpopulations previously identified and secondly to assimilate capture-mark-recapture data to infer connectivity parameters in the Sole life cycle in Eastern Channel. Results show that stock assessment is highly sensitive to the assumptions made on the connectivity strengthen the need of a better understanding of the connectivity among the life cycle. The model is then used to test how the planned protocol could be improved in order to optimize inferences quality on movement. Analyses emphasized that under the optimistic hypothesis of a high tag-reporting rate from commercial fishery, the protocol planned in SMAC (300 tagged fish per year and per region throughout 2 years) would allow to estimate connectivity parameters with rather low bias and uncertainty. However, quality of inferences is highly dependent on some hypotheses which have not been checked in this work; in particular, a bad knowledge of both the spatial distribution and the value of the tag-declaration rate implies a systematic bias in posterior estimates of movement parameters. . Finally, this work suggest to maximize the number of tags (>300) and to enhance communication about the project towards fishermen in order to encourage declaration and then obtain the optimal information to infer connectivity parameters among the three subpopulations.

Mots-clés : Sole en Manche Est, modèle hiérarchique Bayésien, modèle de cycle de vie intégré, connectivité, marquage recapture, taux de declaration

Key Words: Sole in the Eastern Channel, hierarchical Bayesian model, integrated life cycle, connectivity, mark-recapture data, tag-declaration rate